United States
Environmental Protection
Agency

Office of Research and
Development
Washington DC 20460

EPA/600/R-00/006
January 2000

Natural Attenuation of MTBE in the Subsurface under Methanogenic Conditions

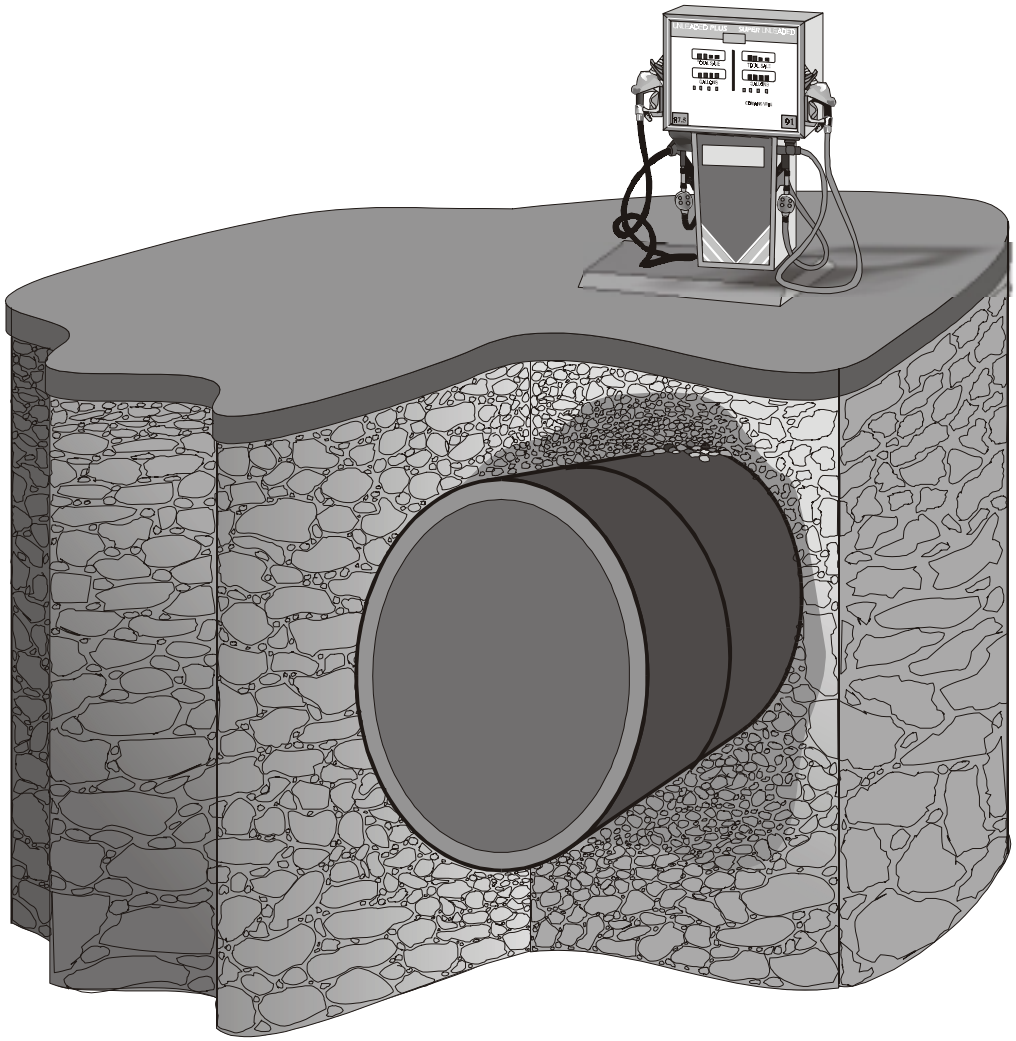

EPA/600/R-00/006
January 2000

Natural Attenuation of MTBE in the Subsurface under Methanogenic Conditions

John T. Wilson
Jong Soo Cho
Barbara H. Wilson
Subsurface Protection and Remediation Division
National Risk Management Research Laboratory
Ada, Oklahoma 74820

James A. Vardy
Civil Engineering Branch
United States Coast Guard
Cleveland, Ohio 41199-2060

Project Officer
John T. Wilson
Subsurface Protection and Remediation Division
National Risk Management Research Laboratory
Ada, Oklahoma 74820

National Risk Management Research Laboratory
Office of Research and Development
U.S. Environmental Protection Agency
Cincinnati, OH 45268

Notice

This work was carried out by staff of the U.S. Environmental Protection Agency (Office of Research and Development, National Risk Management Research Laboratory) and by staff of the U.S. Coast Guard, in a collaboration funded in part under Interagency Agreement # RW-69-937352. It has been subjected to the Agency's peer and administrative review and has been approved for publication as an EPA document. Mention of trade names or commercial products does not constitute endorsement or recommendation for use. Certain samples were collected or analyzed by employees of ManTech Environmental Research Services Corp., an in-house contractor to the U.S. Environmental Protection Agency.

Representations and interpretations of the behavior of methyl-tertiary-butyl-ether (MTBE) or tertiary-butyl alcohol (TBA) apply only to the site of the case study presented in this report. The authors, the U.S. Environmental Protection Agency, and the U.S. Coast Guard make no claim in this report concerning the behavior of methyl-tertiary-butyl-ether (MTBE) or tertiary-butyl alcohol (TBA) at other sites.

All research projects making conclusions or recommendations based on environmentally related measurements and funded by the Environmental Protection Agency are required to participate in the Agency Quality Assurance Program. This project was conducted under an approved Quality Assurance Project Plan. The procedures specified in this plan were used without exception. Information on the plan and documentation of the quality assurance activities and results are available from John T. Wilson.

Foreword

The U.S. Environmental Protection Agency is charged by Congress to protect the Nation's land, air, and water resources. Under a mandate of national environmental laws, the Agency strives to formulate and implement actions leading to a compatible balance between human activities and the ability of natural systems to support and nurture life. To meet these mandates, EPA's research program is providing data and technical support for solving environmental problems of today and building a science knowledge base necessary to manage our ecological resources wisely, understand how pollutants affect our health, and prevent or reduce environmental risks in the future.

The National Risk Management Research Laboratory is the Agency's center for investigation of technological and management approaches for reducing risks from threats to human health and the environment. The focus of the laboratory's research program is on methods for the prevention and control of pollution to air, land, water, and subsurface resources; protection of water quality in public water systems; remediation of contaminated sites and ground water; and prevention and control of indoor air pollution. The goal of this research effort is to catalyze development and implementation of innovative, cost-effective environmental technologies; develop scientific and engineering information needed by EPA to support regulatory and policy decisions; and provide technical support and information transfer to ensure effective implementation of environmental regulations and strategies.

The U.S. Environmental Protection Agency's Office of Underground Storage Tanks uses a risk management approach to protect ground water from contamination with the soluble components of fuels that are accidentally spilled or released from underground storage tanks. Contamination of ground water with MTBE and TBA associated with spills from underground storage tanks is an emerging problem in the United States. Little is known of the prospects for biodegradation of MTBE and TBA in ground water. Consistent with the Agency's goal of sound science as a basis for risk management, the Subsurface Protection and Remediation Division is developing information on the rate and extent of natural attenuation of MTBE and TBA in ground water. This research effort emphasizes natural biodegradation under various geochemical environments. This report describes natural attenuation of MTBE under methanogenic conditions. It is the first in a series of reports; subsequent reports will examine natural attenuation of MTBE under aerobic conditions, and under sulfate-reducing and iron-reducing conditions.

Clinton W. Hall, Director
Subsurface Protection and Remediation Division
National Risk Management Research Laboratory

Abstract

At many fuel spill sites, the spread of contamination from benzene, toluene, ethylbenzene, and the xylenes (BTEX compounds) is limited by natural biodegradation of the petroleum hydrocarbons in the ground water. At present there is much uncertainty about whether MTBE from fuel spills will follow the same pattern as the petroleum-derived hydrocarbons, or whether MTBE is biologically recalcitrant in ground water. If MTBE does not biodegrade in ground water, then dilution and dispersion are the only mechanisms that are available to attenuate MTBE. As a consequence, plumes of MTBE could expand farther than plumes of benzene or the BTEX compounds in the absence of biodegradation.

This case study was conducted at the former Fuel Farm Site at the U.S. Coast Guard Support Center at Elizabeth City, North Carolina. The geochemistry of the site is typical of sites where natural biodegradation limits the spread of BTEX compounds. The plume is undergoing extensive anaerobic oxidation of petroleum hydrocarbons, as well as fermentation of hydrocarbons to methane. The hydrocarbon metabolism through sulfate and iron oxidation is approximately equivalent to the hydrocarbon metabolism through methanogenesis. The amount of hydrocarbon metabolized through anaerobic pathways is about ten times the amount degraded with molecular oxygen.

There are two laboratory studies in the literature that report the biotransformation of MTBE in aquifer material under methanogenic conditions. Neither study included an evaluation of the field-scale performance of natural attenuation. This case study is intended to answer the following questions: Can MTBE be biodegraded under methanogenic conditions in ground water that was contaminated by a fuel spill? Will biodegradation produce concentrations of MTBE that are less than regulatory standards? Is the rate of degradation in the laboratory adequate to explain the distribution of MTBE in the ground water at the field site? What is the relationship between the degradation of MTBE and degradation of the BTEX compounds? What is the rate of natural attenuation of the source area?

The apparent first order rate of removal of MTBE in the field was a sensitive function of ground-water seepage velocity. The rate of removal was calculated for an upper boundary on velocity, an average velocity, and a lower boundary on velocity. The rate was 5.0 per year at the upper boundary; 2.7 per year at the average velocity, and 2.2 per year at the lower boundary. Methane was considered to be a conservative tracer of ground-water flow at the site. The apparent rate of removal of methane was taken as an estimate of attenuation along the flow path due to dilution and dispersion. The apparent first order rate of removal of methane at the average estimate of seepage velocity was 0.50 +/- 0.65 per year.

Biodegradation was evaluated in laboratory microcosms that were constructed with material from the contaminated portion of the aquifer. After 490 days of incubation, the average concentration of MTBE remaining in six replicates of a treatment that was supplemented with BTEX compounds was 81 µg/l, compared to 5680 µg/l at the beginning of incubation. The average concentration remaining in the control treatment after 490 days was 1470 µg/l, compared to 3330 µg/l at the beginning of incubation. MTBE was also removed in microcosms that were not supplemented with alkylbenzenes. After 490 days of incubation, the concentration of MTBE in all six of the replicate microcosms that were sampled was below 40 µg/l, compared to 3110 µg/l at the beginning of incubation. Removal of MTBE in the microcosms did not require the presence of BTEX compounds. The removal of MTBE did not begin until the removal of the BTEX compounds was complete.

The first order rate of removal of MTBE in microcosms supplemented with alkylbenzenes was 3.02 per year +/- 0.52 per year at 95% confidence. Removal in the corresponding controls was 0.39 +/- 0.19 per year at 95% confidence. The removal in the microcosms without added alkylbenzenes was 3.5 per year +/- 0.65 per year at 95% confidence. Removal in the corresponding controls was 0.30 per year +/- 0.14 per year at 95% confidence. The rate of removal of MTBE in the laboratory studies can explain the apparent attenuation of MTBE at field scale.

The rate of natural attenuation of the source area was evaluated by comparing that flux to the total mass of MTBE in the source area. The mass transfer of MTBE from the source LNAPL to the ground water moving underneath was estimated by calculating the flux of MTBE moving away from the source, then dividing the flux into the quantity of MTBE remaining. The flux of MTBE away from the source area in 1996 was 2.76 kg/year. The lower boundary on the total quantity of MTBE in the source area was 46 kg. If the rate of transfer of MTBE to ground water is proportional to the amount of MTBE in the source, the instantaneous rate of transfer is 0.06 per year. The average concentration at the most contaminated location in the transect is 1200 µg/l. At this rate of attenuation of the source, it would require at least sixty years for the concentration to reach 30 µg/l.

Tertiary Butyl Alcohol (TBA) has been documented as a transformation product of MTBE in a number of studies. At the Old Fuel Farm Site, there is no evidence of accumulation of TBA in the ground-water plume as a whole. With two exceptions, the concentration of TBA in ground water downgradient of the source area was less than 200 µg/l. Ground water from a location immediately downgradient of the source area had a higher concentration of TBA, near 2000 µg/l. In this sample there was a corresponding reduction in the concentration of MTBE. At this location the TBA was probably produced from transformation of MTBE.

Contents

Figures

Tables

Acknowledgments

The authors appreciate the excellent technical support extended by Frank Beck and Cherri Adair of the SPRD, by Kelly Hurt while he was a National Research Council associate, by staff of ManTech Environmental Research Services Corp., and by staff of Dynamac, Inc.

SECTION 1
Introduction

MTBE is widely distributed in ground water. The U.S. Geological Survey sampled shallow ambient ground water from eight urban areas in 1993 and 1994. MTBE was detected at concentrations at or above 0.2 μg/l in 27% of the 210 wells and springs that were sampled (Squillace et al.,1996). The U.S. Environmental Protection Agency has tentatively classified MTBE as a possible human carcinogen (U.S. EPA, 1996). There is currently much concern about the occurrence and behavior of MTBE in ground water that might be used for a drinking water supply. Higher concentrations of MTBE in ground water are the result of releases of gasoline containing oxygenates from underground storage tanks (Landmeyer et al., 1998). Fuels also contaminate ground water with benzene and alkylbenzenes including toluene, ethylbenzene, and the xylenes (BTEX compounds). Careful and detailed studies of the transport and fate of the BTEX compounds demonstrated that these compounds were biologically degraded under natural conditions in ground water (summarized in Wiedemeier et al. 1999).

The data supports the theory that the spread of BTEX contamination at many sites was limited by natural biodegradation processes. As a result of our increased understanding of benzene plume behavior, natural attenuation is now being formally recognized as a component of many risk-based remedies at petroleum fuel spill sites.

There is little recognition in the literature that natural biodegradation may control the spread of MTBE contamination in ground water. In his review, Chapelle (1999) noted that "Field studies of MTBE biodegradation relative to BTEX compounds ... indicate that MTBE is biodegraded in shallow aquifers, but that biodegradation is less than for BTEX compounds." Mormile et al. (1994) conclude "the common ether oxygenates resist both anaerobic and aerobic decay and must be considered recalcitrant chemicals." As will be discussed in the next section, there is evidence in the literature that anaerobic degradation of MTBE is possible. There are also many experiments where degradation was not detected.

Evidence for Biodegradation of MTBE under Anaerobic Conditions in Ground Water

There are two reports of MTBE biotransformation in laboratory studies under methanogenic conditions. Yeh and Novak (1994) constructed static soil and water microcosms with material from three sites; a site at a wooded area at the Virginia Polytechnic Institute (VPI) at Blacksburg, Virginia, that is largely unsaturated clay; a site at VPI in a low area that is mainly sandy loam that receives runoff from a feedlot, and a site at Newport News, Virginia, that is mainly silty loam. Ethanol and starch were added as a source of molecular hydrogen. Potassium phosphate and ammonium chloride were added as nutrients. Cysterine and sodium sulfide were added to encourage anaerobic processes. Sodium molybdate was added to inhibit sulfate-reducing microorganisms in the microcosms that were intended to simulate methanogenic conditions. The initial concentration of MTBE in the microcosms was 100 mg/l. The microcosms were incubated at 20°C for times extending from 250 days to 300 days. Removals in microcosms were compared to removals in autoclaved controls prepared for each site.

After 250 days of incubation, there was no removal of MTBE in excess of removal in autoclaved controls in microcosms constructed with material from the sandy loam site downgradient of the feed lot, or the silty loam site. However, in excess of 99 percent of MTBE was removed in a microcosm constructed with clay material collected at a depth of 1.5 meters below land surface, and 80 percent of MTBE was removed in a microcosm constructed from material collected at a depth of 3.0 meters below land surface. The rate of removal in the microcosm constructed with material from a depth of 1.5 meters corresponded to a first-order rate of removal of 3.3 per year, or a half life of eleven weeks. The removal in the microcosm constructed with material from a depth of 3.0 meters corresponded to a first-order rate of removal of 2.0 per year or a half life of eighteen weeks.

In their studies, Yeh and Novak (1994) found no evidence of MTBE biodegradation under anaerobic conditions where nutrients and a hydrogen source were not added, or under denitrifying conditions or sulfate-reducing conditions when nutrients and a hydrogen source were added. The removal of MTBE was only associated with methanogenic conditions.

Mormile et al. (1994) examined material from a sandy water-table aquifer near Empire, Michigan, that had been contaminated with gasoline; sediment from the Ohio River that had been impacted by oil storage and barge loading facilities; and, sediment from Mill Creek in Cincinnati, Ohio, that had been impacted with industrial and municipal sewage sludge. Microcosms were constructed with slurries of sediment and ground water. The slurries were

amended with sodium sulfide, but no additional nutrients or hydrogen sources were added. Some of the microcosms received sodium sulfate or sodium nitrate to stimulate sulfate-reducing and nitrate-reducing conditions. The initial concentration of MTBE was 50 mg/l as carbon.

There was removal of MTBE in one of three replicate microcosms constructed with the sediment from the Ohio River. After 152 days of incubation, the concentration of MTBE was reduced to 22 mg/l carbon from an initial concentration of 48 mg/l carbon. There was no removal of MTBE in an autoclaved control. In the microcosm, the removal of MTBE was associated with the production of tertiary butyl alcohol (TBA).

In contrast to the removal of MTBE in the one microcosm constructed with sediment from the Ohio River, there was no removal in sediment that was contaminated with gasoline after 230 days of incubation, or in the sediment impacted with sewage sludge after 180 days of incubation. In an earlier study, Suflita and Mormile (1993) had examined the degradtion of a variety of oxygenate in material from a sandy water table aquifer at Norman, Oklahoma, that had been contaminated with landfill leachate. After 249 days of incubation, there was no evidence of removal of MTBE.

Consistent with the work of Yeh and Novak (1994), Mormile et al. (1994) found no removal of MTBE under sulfate-reducing conditions or nitrate-reducing conditions in the three materials they examined.

There are two additional reports of MTBE degradation under anaerobic conditions. Landmeyer et al. (1998) examined MTBE degradation at a site on Port Royal Island, South Carolina, in the Lower Coastal Plain of the Atlantic Coastal Plain geophysical province. The aquifer had been contaminated with a gasoline spill. Microcosms were constructed with material from an area with high concentrations of BTEX contamination and MTBE contamination, and a second area with high concentrations of MTBE but much lower concentrations of BTEX. Microcosms were constructed with material from each site with a high or a low concentration of MTBE. Transformation of MTBE was assayed by collecting radio-labeled carbon dioxide produced from the transformation of MTBE that was uniformly labeled with carbon 14 (radio-labeled impurity less than 0.2% of the total label).

The headspace of the microcosms was helium, which resulted in iron-reducing conditions in the microcosms. After 28 weeks of incubation, between 2.0% and 3.0% of the label was transformed to carbon dioxide (mean of triplicate microcosms for all four experimental treatments). Attenuation under iron-reducing conditions was real, but the rate of transformation was slow, corresponding to a first-order rate of attenuation of 0.06 per year. Anaerobic biodegradation did not attenuate the plume of MTBE in ground water before it approached the receptor.

Church et al. (1997) examined the effluent from a column microcosm constructed with core material from a site in Trenton, New Jersey. The influent concentration of MTBE was near 100 µg/l. After 35 days of operation, the effluent concentration of MTBE was 160 µg/l, and there was no detectable concentration of TBA (interpretation of their Figure 2). After 44 days of operation, the effluent concentration of MTBE was 160 µg/l and the concentration of TBA was 20 µg/liter. After 52 days of operation, the effluent concentration of MTBE was reduced to 40 µg/l, and the concentration of TBA increased to 60 mg/l.

Purpose of the Case Study

This case study is intended to answer the following questions. Can MTBE be biodegraded under methanogenic conditions in ground water that was contaminated by a fuel spill? Will biodegradation reach concentrations of MTBE that are less than regulatory standards? Is the rate of degradation in the laboratory adequate to explain the distribution of MTBE in the ground water at the field site? What is the relationship between the degradation of MTBE and degradation of the BTEX compounds? How long can the fuel release continue to contaminate ground water at the site?

The case study was conducted at a former fuel farm that had been operated by the United States Coast Guard at their Support Center at Elizabeth City, North Carolina. Fuel for aircraft was stored at the site until December 31, 1991. The fuel farm had been in use since 1942, and originally consisted of a 50,000-gallon concrete underground storage tank, and two steel underground storage tanks with a volume of 12,000-gallons and 15,000-gallons, respectively (adjacent to location CPT-1 in Figure 1.1). The steel tanks were apparently removed in the mid-1980s.

The United States Coast Guard has conducted extensive free product recovery efforts at the site. Figure 1.1 depicts the location of residual LNAPL, the direction and speed of ground-water flow, and the ground-water sampling locations at the site.

A GeoProbe™ push point sampler was used to acquire water samples at the location in Figure 1.1. At each location the aquifer was sampled in a vertical profile that extended from the water table, through a shallow silty clay layer, into a fine sand unit, and then into a silty clay unit beneath the sand. The GeoProbe™ push points were screened over a vertical interval of 1.5 feet. The GeoProbe™ samples extended from 5 feet below land surface to 30 feet below land surface. The aquifer was confined to an interval between 10 and 25 feet below land surface. At a minimum, every other 1.5 foot vertical interval was sampled.

The hydraulic conductivity of the material sampled was estimated for each GeoProbe™ sample. The measured concentration of MTBE, benzene, and methane were weighted by the hydraulic conductivity of the interval being sampled before the vertical samples were averaged. Because the GeoProbe™ samples are flow-weighted averages, there is no danger that the data could give a false impression of natural attenuation due to hydraulic averaging along the flow path in the aquifer.

The concentration of MTBE in ground water under the spill was high, 1740 µg/L at location CPT-1 in Figure 1.1. However, the only monitoring locations downgradient of

the source area that had concentrations of MTBE that exceeded regulatory standards were monitoring locations ESM-14 and ESM-3, and the concentrations were approximately 20% of the maximum concentration in the source area.

The concentration of MTBE in a permanent monitoring well at location ESM-14 (see Figure 1.1) showed good agreement with the weighted-average concentration from the vertical profile sampling (see Table 1.1). In order to estimate the temporal variability of the plume, data from the permanent monitoring well at location ESM-14 are reported for sampling events extending from August 1996 through September 1999. The August 1996 sampling event was almost five years after the site was no longer used for fuel storage. In the interval from August 1996 to September 1999 there are no recognizable trends in the concentration of MTBE, benzene, or methane. There is no evidence that the concentrations of MTBE leaving the source are decreasing over time.

The site was selected for study for two reasons. The source of the MTBE plume was relatively stable, based on trends in MTBE concentrations in the most contaminated permanent monitoring well at the site (Table 1.1). This made it possible to differentiate attenuation in concentration as water moved downgradient from attenuation of the source area itself. The site was also selected because the concentrations of MTBE were greatly attenuated at monitoring locations that were relatively close to the source area in terms of time of travel of ground water. The time required for ground water to travel from the source area to the most distant sampling location is less than five years. This suggested that the kinetics of natural attenuation at this site should be rapid.

Table 1.1 Temporal variation in the concentrations of MTBE, Benzene, and Methane at the most contaminated permanent sampling location that is downgradient of the LNAPL area.

	Vertical Profile	Permanent Well ESM-14					
	8/1996	8/1996	10/1997	10/1998	12/1998	7/1999	9/1999
	---------(µg/l)---------						
MTBE	383	353	194	154	65	259	609
Benzene	139	631	389	1280	1300	2185	1070
Methane	7,780	11,500	15,400	16,200	10,900	8,400	962

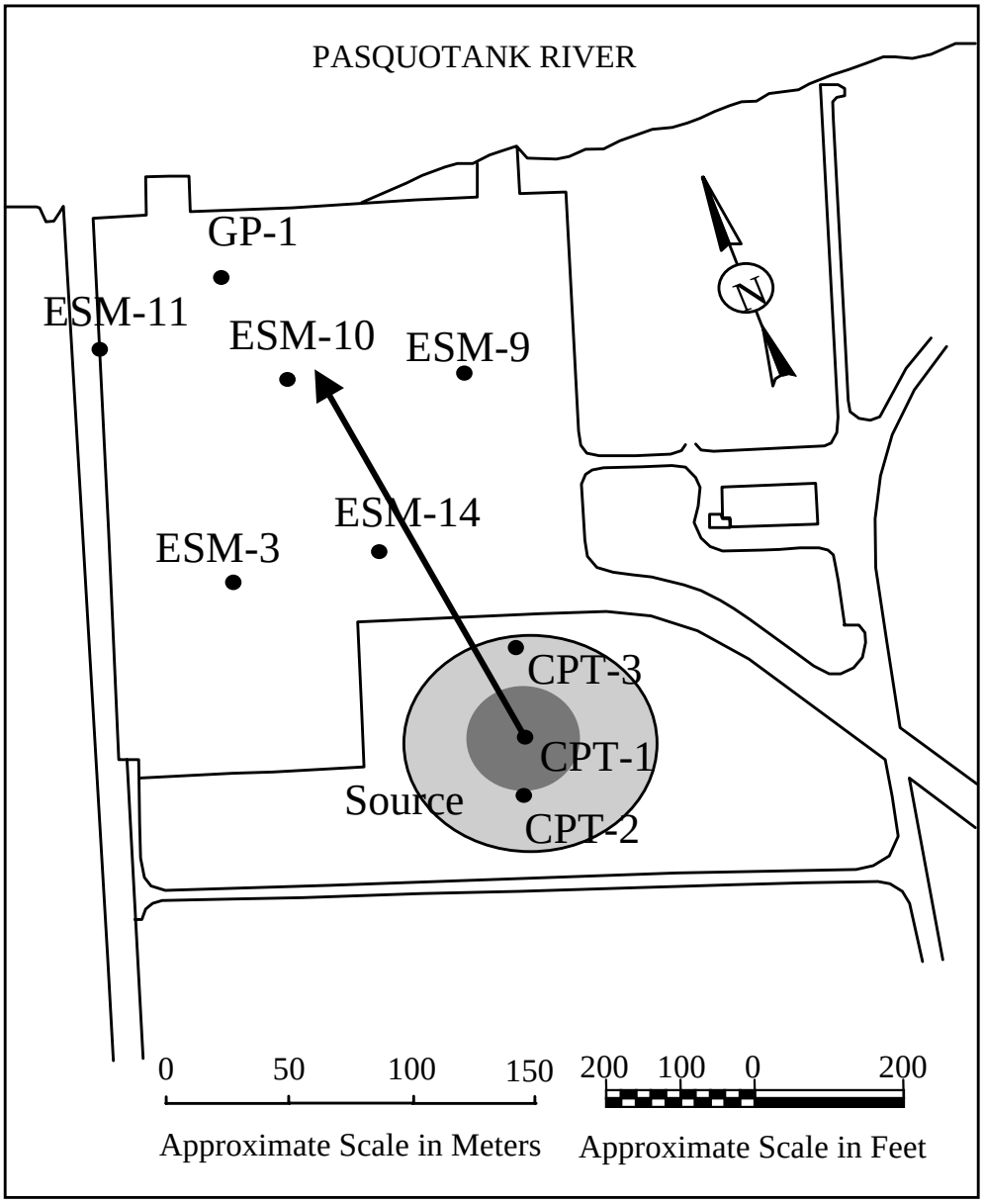

Figure 1.1 Site selected for the case study of natural attenuation of MTBE under methanogenic conditions. The shaded concentric circles represent the residual LNAPL from a fuel spill. The concentration of MTBE at location CPT-1 was 1740 µg/l. The arrow represents the distance traveled by the ground water in three years. The only sampling location with concentrations of MTBE above 20 µg/l was ESM-14.

SECTION 2
Laboratory Studies

Construction, Sampling and Analysis of Microcosms

Microcosms were constructed with aquifer material from location ESM-14. This location had the highest concentration of MTBE in the permanent monitoring wells that were available at the time the samples for the microcosm study were collected. At this location, approximately 10 feet (3 meters) of silty clay overlies 15 feet of silty sand and fine sand. The water table is near 10 feet below land surface. A hollow stem auger was advanced into the earth to a depth of approximately 15 feet (4.6 meters). The auger was maintained at this depth, and was rotated to elevate material on the auger flights. The initial material that was elevated was silty clay; this material was discarded. Approximately 0.3 cubic meters of fine sand was elevated on the auger flights and discarded, then 8 liters of sediment was collected for construction of microcosms. The sediment was collected and stored in 1-quart glass jars. To protect the anaerobic microorganisms that might be present in the samples from oxygen in the atmosphere, the head space above the sediment was replaced with ground water from the borehole immediately after collection. The samples were cooled and shipped to the Robert S. Kerr Environmental Research Center with water ice, and stored at 4 °C until used to construct microcosms.

To protect anaerobic microorganisms from oxygen in the atmosphere, all manipulations to prepare the microcosms were carried out in a glove box with a concentration of oxygen in the atmosphere that was less than 1 ppm (v/v). This corresponds to a concentration of oxygen in water (at equilibrium) of 0.00004 mg/l. Microcosms were prepared in glass serum bottles with a volume of 25 ml. Ground water from the bore hole was added to the sediment to make a thick slurry. This slurry was transferred to the serum bottles with a scoop. Each microcosm received 40 gm wet weight of slurry and 1.0 ml of a dosing solution containing MTBE, or MTBE and alkybenzenes. The remaining volume (3 to 4 ml) was filled with autoclaved ground water from the bore hole. The microcosms were sealed with a grey butyl rubber septum and a crip cap. The microcosms were stored in the same glove box, under an atmosphere that was 2% to 5% hydrogen and contained less than 1 ppm oxygen. Ground-water temperatures from permanent wells at the site varied from 19° to 24°C between sampling dates in December and September. The microcosms were incubated at room temperature (20° to 22°C).

To prepare abiotic controls, a portion of the sediment was autoclaved overnight. Four treatments were prepared; sediment amended with MTBE alone, autoclaved sediment amended with MTBE alone, sediment amended with MTBE and alkylbenzenes, and autoclaved sediment amended with MTBE and alkylbenzenes. The initial concentrations of MTBE and alkylbenzenes that were achieved in the microcosms are listed in Table 2.1.

The microcosms were sampled and analyzed as follows. The contents of the microcosms were vigorously stirred with a vortex mixer. The microcosms were centrifuged to settle the solids. Then the crimp cap and septa were removed, and 1.0 ml of water was transferred to 39 ml of dilution water and sealed in 40 ml VOA bottle with a Teflon™-faced silicone septum and a screw cap. The dilution water was distilled water that had been boiled, each sample received one drop of sulfuric acid to preserve the sample. The concentration of MTBE and alkylbenzenes were determined by purge and trap analysis using gas chromatography with a PID detector. The limit of quantification for MTBE and the alkylbenzenes was 1 µg/l, corresponding to a limit of quantification of 40 µg/l in the pore water of the microcosms.

The sediment selected to construct the microcosms was intended to represent the region in the aquifer where natural attenuation of MTBE was in progress. The microcosms were constructed with material from a location where the apparent natural attenuation of MTBE was extensive, but was not complete. Table 2.1 compares the concentration of MTBE in the source area of the plume to the concentration in a permanent monitoring well at the location that was used to acquire the sediment for the microcosms. At the sample location, the concentration of MTBE was reduced approximately tenfold from the concentration in the LNAPL source area. Another tenfold reduction would approach concentrations that would meet regulatory standards for MTBE.

The microcosms incubated over time were intended to represent the travel of a representative volume of water along the entire flow path, starting with the source and extending to a potential receptor. The sediments in the microcosms were amended with MTBE to simulate the highest concentration in the source area. The travel time of MTBE from the source to a potential receptor is on the order of four years. The microcosm study was designed to last for eighteen months to two years.

Table 2.1 The concentration of MTBE and alkylbenzenes in the most contaminated sample of ground water from the LNAPL source area, in the permanent monitoring well at the location where the sediment used to construct the microcosms was acquired, and the initial concentrations achieved in the microcosms.

Compound	*Most Impacted Ground Water*	*Sample Location Ground Water*	*Microcosms*			
	CPT-1 3.1 m to 3.6 m bls	*Well ESM-14*	*MTBE alone*	*MTBE alone control*	*MTBE plus BTEX*	*MTBE plus BTEX control*
	Single Analysis		*Mean (Sample Standard Deviation, n = 3)*			
			µg/l			
MTBE	*3640*	*353*	*3112 (188)*	*2908 (538)*	*5680 (138)*	*3330 (360)*
Benzene	*7830*	*631*	*<40*	*<40*	*2079 (218)*	*1953 (174)*
Toluene	*383*	*1.8*	*<40*	*<40*	*2183 (233)*	*1996 (176)*
Ethylbenzene	*396*	*1.9*	*<40*	*<40*	*1256 (130)*	*1109 (108)*
o-xylene	*23*	*<1*	*<40*	*<40*	*1911 (170)*	*1697 (146)*
m-Xylene			*<40*	*<40*	*1592 (158)*	*1404 (134)*
p-Xylene			*<40*	*<40*	*1556 (151)*	*1361 (139)*
m+p-Xylene	*1250*	*2.9*				
1,2,3-trimethylbenzene	*286*	*1.2*	*<40*	*<40*	*887 (54)*	*747 (78)*
1,2,4-trimethylbenzene	*430*	*<1*	*<40*	*<40*	*625 (40)*	*521 (62)*
1,3,5-trimethylbenzene	*107*	*<1*	*<40*	*<40*	*664 (45)*	*551 (69)*

To determine whether there was any interaction between the presence of alkylbenzenes and the removal of MTBE, one set of treatments was amended with benzene, toluene, ethylbenzene, the three xylenes, and the three trimethylbenzenes, and one set of treatments was not amended. The initial concentrations of individual alkylbenzenes in the microcosms were higher than their concentration in the source area, with the exception of benzene, where the concentration in the microcosms was approximately one-fourth the maximum concentration in the source area (Table 2.1). Background concentrations of alkylbenzenes were not detected in microcosms that were not amended with alkylbenzenes.

Removal of MTBE

Removal of MTBE in material that was supplemented with alkylbenzenes was extensive (Figure 2.1). There was no evidence of MTBE removal over removal in the controls in the first 175 days of incubation. The concentrations of MTBE in replicate microcosms from both the living and control treatments show relatively little scatter. After 385 days of incubation, there is evidence of removal in the living treatment. The data after 385 days of incubation show a great deal of scatter. The range in concentrations in six replicates is over an order of magnitude wide. After 490 days of incubation, there is consistent removal of MTBE compared to the controls.

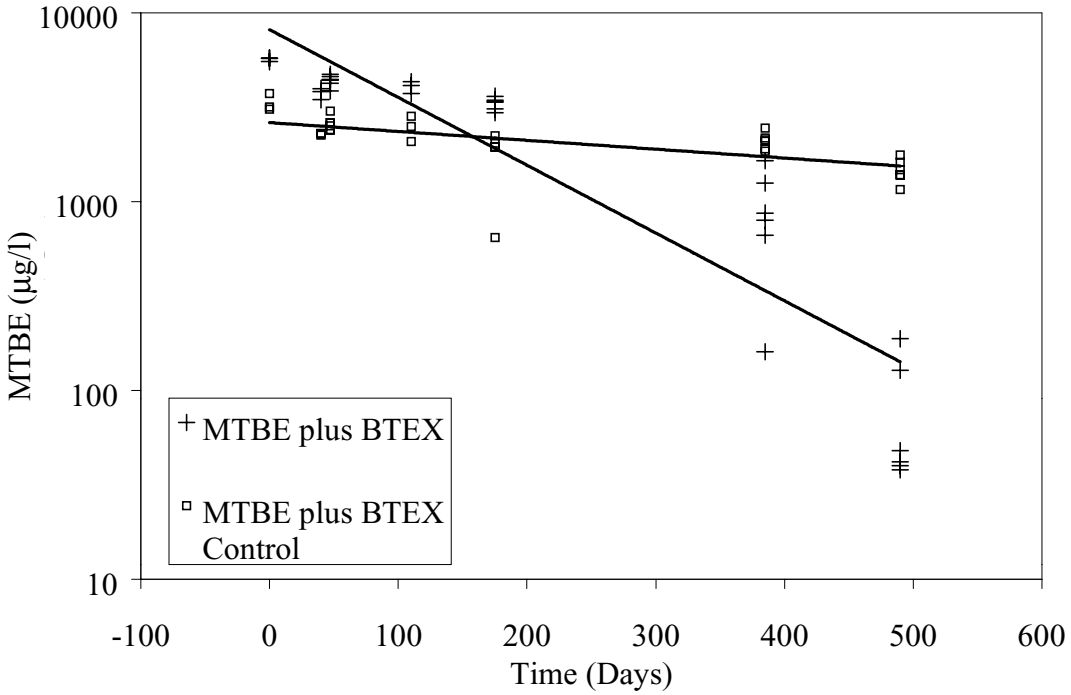

Figure 2.1 Removal of MTBE in microcosms constructed with MTBE and BTEX compounds compared to removal in control microcosms that were autoclaved to prevent biotransformation of MTBE.

The average concentration remaining in six replicates of the living treatment was 81 µg/l, compared to 5680 µg/l at the beginning of incubation. The average concentration remaining in the control treatment after 490 days was 1466 µg/l, compared to 3330 µg/l at the beginning of incubation. The removal in the controls was a little more than twofold, while removal in the living microcosms was 70-fold.

Removal of MTBE in material that was not supplemented with alkybenzenes was also extensive (Figure 2.2). There was little evidence of removal in the first 175 days of incubation. After 385 days, the removal of MTBE in the living microcosms was extensive. After 490 days of incubation, the concentration of MTBE in six replicate microcosms was below 40 µg/l, compared to 3112 µg/l at the beginning of incubation. After 490 days, the average concentration of MTBE in the control microcosms was 1571 µg/l, compared to an initial concentration in the controls of 2908 µg/l.

A first-order rate of removal was fitted to the data by a linear regression of the natural logarithm of the concentration of MTBE on the time of incubation. The rate of removal of MTBE in microcosms supplemented with alkylbenzenes was 3.02 per year ±0.52 per year at 95% confidence. Removal in the corresponding controls was 0.39 +/- 0.19 per year at 95% confidence. The removal in the microcosms without added alkylbenzenes was 3.5 per year +/- 0.65 per year at 95% confidence. Removal in the corresponding controls was 0.30 per year, ±0.14 per year at 95% confidence. The rate constants were fit to the entire data; no correction was made for the apparent lag period.

A container control was not done. There is no way to determine if the removals in the controls are due to kinetically slow sorption to the aquifer solids, or to diffusion out of the microcosm through the septa.

Removal of Benzene, Toluene, and Ethylbenzene

Toluene was removed rapidly and extensively in the microcosms. After only 40 days or 47 days of incubation, toluene removal was extensive in most of the microcosms sampled (Figure 2.3). After 110 days of incubation, the concentration of toluene was less than 40 µg/l in all of the microcosms sampled. Benzene was also rapidly removed from the microcosms. There was no evidence of benzene removal after 40 days or 47 days of incubation (Figure 2.4) although removal of toluene was evident. After 110 days of incubation, the concentration of benzene in all the microcosms sampled was less than 40 µg/l. There is no evidence of a lag for removal of toluene. There may have been a slight lag in the removal of benzene.

The behavior of ethylbenzene (Figure 2.5) is representative of the behavior of the xylenes and trimethylbenzenes as well. Removal was extensive in both living microcosms and controls. There was no difference in removal in living and control microcosms through 110 days of incubation. After 175 days of incubation, the concentration of ethylbenzene in the living microcosms is below the limit of quantification (40 µg/l) but the average concentration in the controls is only 113 µg/l compared to an initial concentration of 1109 µg/l. After 490 days of incubation, the concentration in both living and control microcosms was less than the quantification limit.

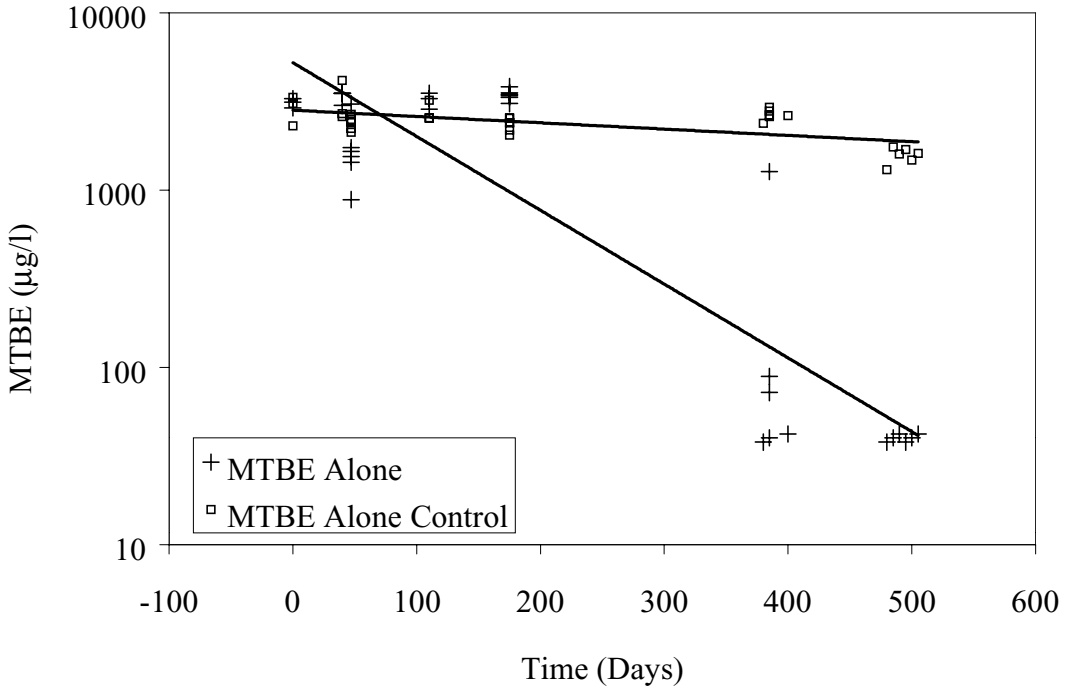

Figure 2.2 Removal of MTBE in microcosms constructed with MTBE but without supplemental concentrations of BTEX compounds compared to removal in control microcosms that were autoclaved to prevent biotransformation of MTBE.

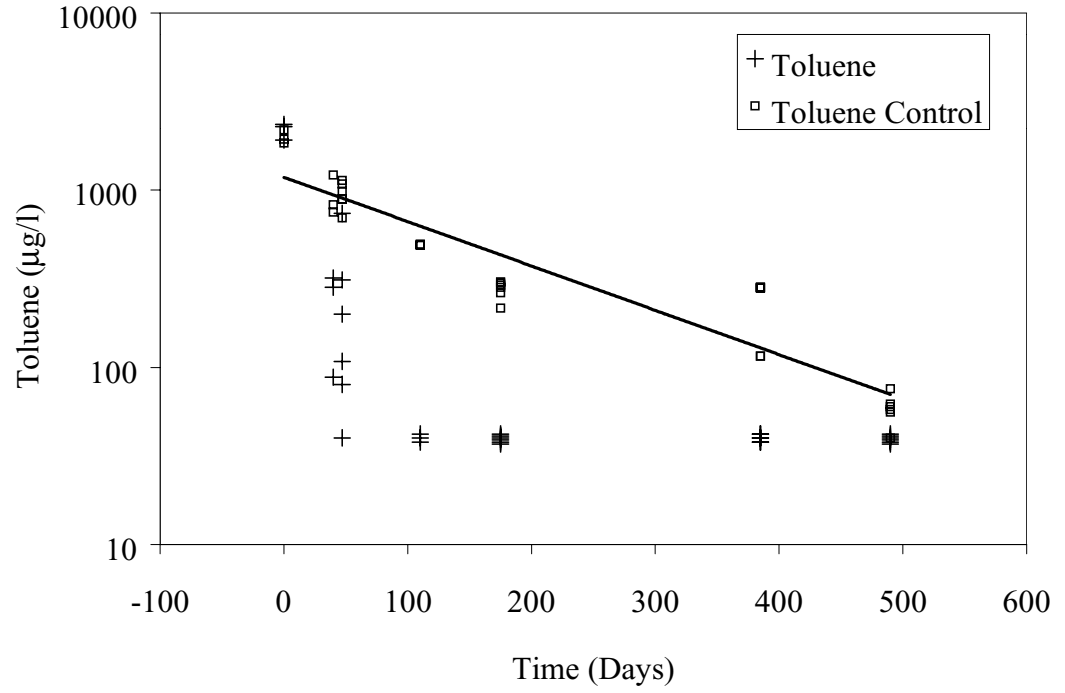

Figure 2.3 Removal of Toluene in microcosms constructed with MTBE and BTEX compounds compared to removal in control microcosms that were autoclaved to prevent biotransformation of toluene. The solid line is fit through the removal in the controls.

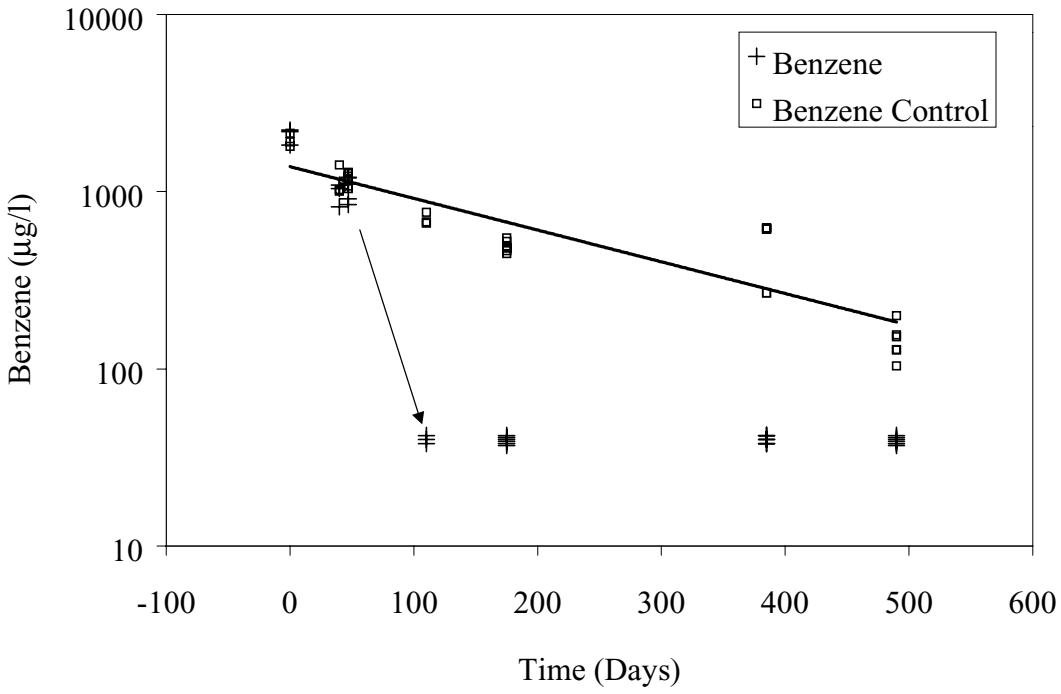

Figure 2.4 Removal of Benzene in microcosms constructed with MTBE and BTEX compounds compared to removal in control microcosms that were autoclaved to prevent biotransformation of benzene. The solid line is fit through the removal in the controls.

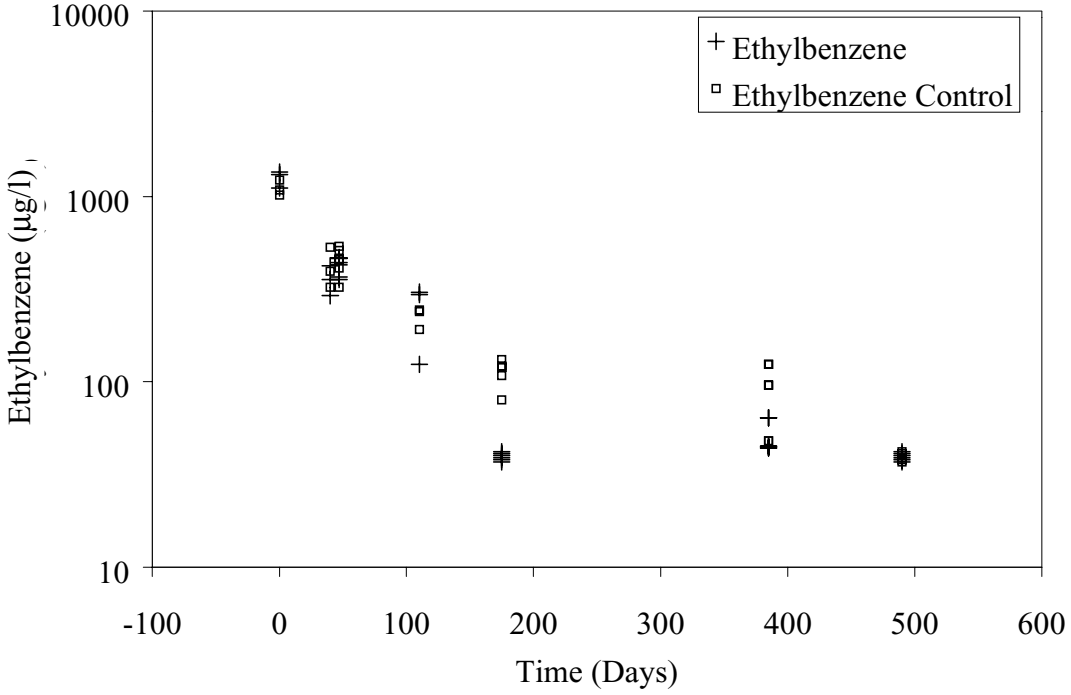

Figure 2.5 Removal of Ethylbenzene in microcosms constructed with MTBE and BTEX compounds compared to removal in control microcosms that were autoclaved to prevent biotransformation of ethylbenzene.

Relationship between removal of BTEX compounds and removal of MTBE

Removal of MTBE did not require the presence of BTEX compounds. Figure 2.6 plots the removal of MTBE, benzene, toluene, and ethylbenzene. Toluene was entirely depleted within 40 to 47 days, benzene was entirely depleted within 110 days, and ethylbenzene was entirely depleted within 175 days. During this time period there was no evidence of removal of MTBE. After 385 days there was evidence of extensive removal of MTBE in one microcosm, limited removal in three microcosms, and no evidence of removal in two microcosms. The removal of MTBE did not begin until the removal of the BTEX compounds was complete.

There is a possibility that removal of MTBE may have been inhibited by the presence of BTEX compounds. However, the lag for removal of MTBE in microcosms without BTEX compounds was also long, at least 175 days (Figure 2.6). Removal of MTBE in microcosms that did not contain detectable concentrations of alkylbenzenes was not detected until 385 days of incubation. There is not enough resolution in the sampling schedule to determine if the presence of BTEX compounds inhibited MTBE removal.

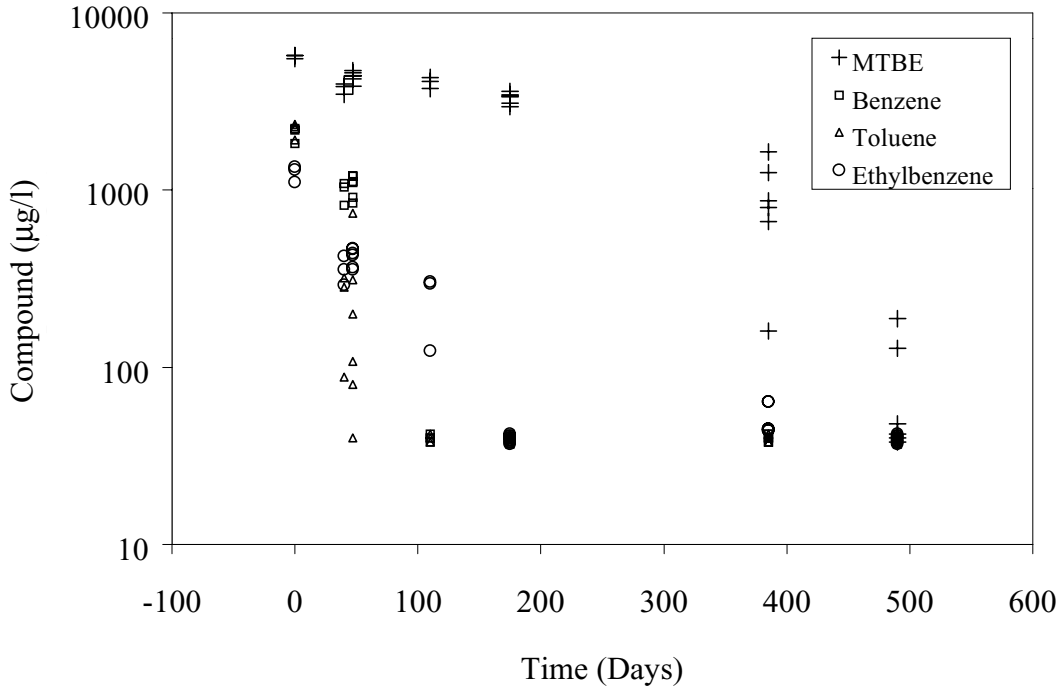

Figure 2.6 Comparison of the time lags for removal of MTBE, and of benzene, toluene, and ethylbenzene in microcosms constructed with all the compounds present together.

SECTION 3
Site Characterization

Site Description and History

The case study was conducted at a former fuel farm located at the U.S. Coast Guard Support Center at Elizabeth City, North Carolina. The following description is excerpted from the Former Fuel Farm Work Plan, a part of the Remediation Feasibility Assessment Work Plan prepared for the U.S. Coast Guard Support Center, Elizabeth City (SCES), North Carolina, by Parsons Engineering Science, 1996.

The Support Center is located on the southern bank of the Pasquotank River. The former fuel farm was located south of a concrete ramp used to recover seaplanes from the Pasquotank River (Figure 3.1). Currently a plume of MTBE and fuel hydrocarbons in ground water emanates from a source area in the location of the former fuel farm, and flows under the concrete ramp toward the Pasquotank River to the north, and toward a drainage canal along the western side of the seaplane ramp. This source area corresponds to the former location of fuel storage tanks on the site (Figure 3.1).

Fuel was stored at the site until December 31, 1991. The fuel farm had been in use since 1942, and originally consisted of a 50,000-gallon concrete underground storage tank (TANK 23 in Figure 3.1), and two steel underground storage tanks with a volume of 12,000-gallons and 15,000-gallons, respectively (adjacent to location CPT-1 in Figure 3.1). The steel tanks were apparently removed in the mid-1980s. In addition to the underground storage tanks, two steel, above-ground storage tanks with a capacity of 50,000 gallons were installed in the mid-1980s. There was evidence of corrosion in the transfer lines from these tanks. They were taken out of service and removed from the site. No evidence of a release from the pipes was discovered.

The U.S. Coast Guard began a free product recovery effort at the site in September 1990. Eight recovery wells were arranged around the source area in a circle. By March 1992, a total of 79,000 gallons of fuel was recovered.

Core Sampling the Source Area

In September 1996, a GeoProbe™ was used to acquire core samples in continuous vertical profiles at seven locations in or near the source area (locations CPT-1 through CPT-7 in Figure 3.1). The water table was 7.0 to 8.0 feet below land surface (2.1 to 2.4 meters below land surface). The cores extended from the surface to a depth 12 to 16 feet (3.7 to 4.9 meters).

The cores were cut into subcores that were 4 inches long (10 cm long). A plug of material approximately 1.0 cm in diameter and 5 cm long was acquired from each subcore with a paste sampler. The plugs were immediately transferred in the field into 40-ml glass vials with 5 ml of methylene chloride and 10 ml of distilled water. The vials were sealed with Teflon™-faced septa and screw caps, then they were shaken to extract organic components into the methylene chloride. The contents were allowed to settle, then the methylene chloride was taken for analysis by gas chromotography using a mass spectrometer as a detector. The limit of quantitation for MTBE and for BTEX compounds was 0.01 mg/kg; the limit of quantitation for Total Petroleum Hydrocarbons was 50 mg/kg.

The cores at each sampling location extended from clean soil above the release, through the release to clean aquifer material below the release. The quantity of Total Petroleum Hydrocarbon (TPH) or MTBE in individual cores was summed to determine the total amount of TPH and MTBE present at each location. The subcores were 10 cm long. The concentration reported in mg/kg was considered representative of a block of soil that was 1.0 meter square and 0.1 meter deep. The dry bulk density of the soil or sediment was assumed to be 1,820 kg/ m^3. Each block of soil would have a weight of 182 kg/m^2. The concentration reported in mg/kg was multiplied by 182 kg/m^2 to determine the quantity in each block. The quantity in each block was summed to determine the total quantity at each location. Results are presented in Table 3.1.

The greatest quantity of TPH was found at locations CPT-2 and CPT-1 (Table 3.1). These locations were near the location of the original steel underground storage tanks (Figure 3.1). These two locations also had the greatest mass of MTBE, and the highest concentration of MTBE in the residual fuel. The quantity of TPH at location CPT-3 was high, but the concentration of MTBE in the TPH was lower than the concentration in locations CPT-1 and CPT-2. MTBE was detected at location CPT-7, but the quantity and concentration in the TPH was much lower than at locations CPT-1 and CPT-2. The fuel release that contains MTBE is centered around locations CPT-1 and CPT-2, and

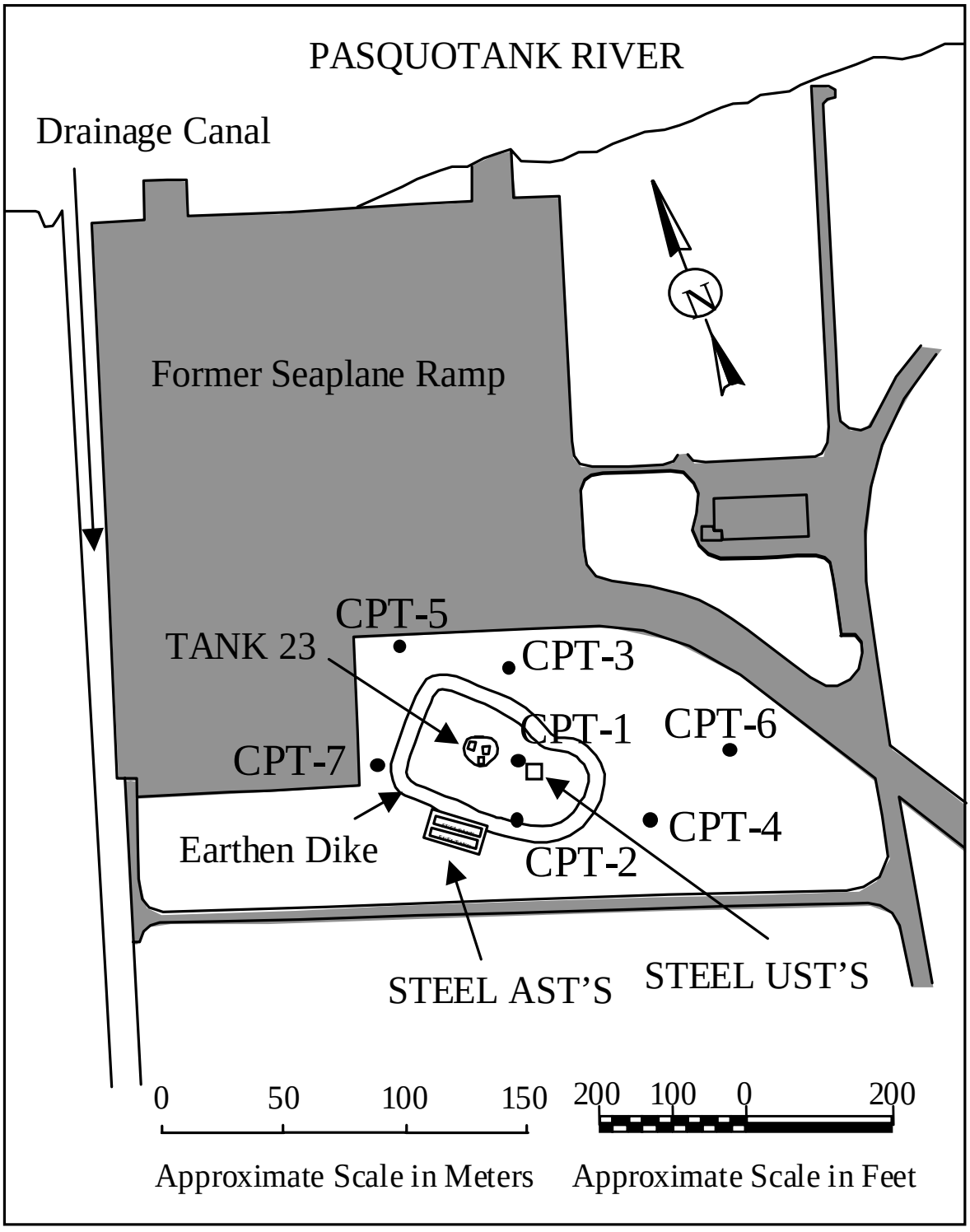

Figure 3.1 Relationship between the sampling locations for characterization of the LNAPL source area (labeled CPT-1 through CPT-5), and the former location of storage tanks for fuels.

Table 3.1. Quantity of Total Petroleum Hydrocarbon and MTBE at seven sampling locations in or near the point of release of fuel.

Location	*Total Petroleum Hydrocarbons (kg/m^2)*	*MTBE (kg/m^2)*	*Mass Fraction MTBE ppm MTBE per TPH*
CPT-7	*9.7*	*0.00017*	*18*
CPT-5	*0.220*	*<0.0001*	
CPT-3	*26*	*0.0015*	*57.7*
CPT-1	*54*	*0.0152*	*282*
CPT-2	*75*	*0.0104*	*139*
CPT-6	*1.3*	*<0.0001*	
CPT-4	*30*	*<0.0001*	

is roughly bound by CPT-7 to the west, by CPT-5 and CPT-3 to the north, and by CPT-6 and by CPT-4 to the east.

Estimation of Total Quantity of TPH and MTBE and the Area Impacted

The former location of the steel underground storage tanks was selected as the location of CPT-1. This location had the highest quantity of MTBE (Table 3.1), and will be taken as the center of the release. Location CPT-1 is 60 meters from CPT-7, 67 meters from CPT-5, 37 meters from CPT-3, 88 meters from CPT-6, and 60 meters from CPT-4 (Figure 3.2). If the source is a circle that fits within the space bounded by CPT-7, CPT-5, and CPT-4, then its radius is 60 meters, and its area is 11,000 m^2. If the concentration of TPH in the source is 46 kg/m^2 (the average of locations CPT-1, CPT-2, CPT-3, and CPT-4 in Table 3.1), the total quantity of fuel hydrocarbons remaining in the source is 500,000 kg. If the density of the fuel is 0.82, this corresponds to 620,000 liters or 180,000 gallons of fuel.

Addendum 2 to the Corrective Action Plan, Former Fuel Farm (SWMU No. 32), U.S. Coast Guard Support Center Elizabeth City, Elizabeth City, North Carolina, Parsons Engineering Science, 1997, provides an independent assessment of the mass of fuel remaining. They estimate that approximately 100,000 gallons (380,000 liters) remain in the soil, and that the impacted area is approximately 150,000 square feet (14,000 m^2). The agreement between their estimate and our estimate is acceptable.

The average quantity of MTBE at locations CPT-1 and CPT-2 was 12.8 g/m^2 (Table 3.1). If the area of the source is 11,000 m^2, this corresponds to a total quantity of 140 kg of MTBE. This would be an upper boundary on the quantity of MTBE in the source.

If the source "hot-spot" is restricted to the interval between CPT-1 and CPT-2 (see Figure 3.2), then the radius of the "hot-spot" is 29 meters, and the area of the hot spot is 2,600 m^2. The average concentration of MTBE at CPT-1 and CPT-2 is 12.8 g/m^2, for a total in the "hot spot" of 33.2 kg of MTBE. If the remaining area of the source (8,400 m^2) has a quantity of MTBE equal to that of location CPT-3 (1.5 g/m^2), the addition quantity is 12.6 kg for a grand total 46 kg in the source area. This would be a lower boundary on the quantity of MTBE in the source.

Vertical Distribution of TPH and MTBE in Core Samples

Figure 3.3 presents the vertical distribution of MTBE and TPH in the continuous core samples from location CPT-1. The majority of TPH was confined to a depth interval between 1.5 and 3.0 meters. The relative proportions of MTBE in the TPH were very consistent over this interval. Below 3 meters TPH disappears, while the concentration of MTBE declines gradually with increase in depth. The MTBE in core samples below a depth of 3 meters can only be dissolved in the ground water. In this interval there is no TPH to partition into, and sorption to aquifer solids should be negligible.

The vertical distribution of TPH and MTBE at location CPT-2 (Figure 3.4) was very similar to the distribution at location CPT-1 (Figure 3.3). The majority of the TPH was confined to an interval between 1.5 and 3 meters below land surface. The relative proportions of MTBE and TPH were consistent across the vertical profile, and it was the same proportion seen at location CPT-1. At the time the cores were collected, the depth to the water table was 7.0 feet (2.13 m). One core sample, located right at the water table, had a TPH concentration of 139,000 mg/kg. This concentration is high enough to represent free product floating on the water table. The concentration of MTBE in this sample was 11.5 mg/kg. At location CPT-2, both TPH and MTBE disappeared below a depth of 3 meters.

At location CPT-3, the TPH was also confined to an interval between 1.5 and 3.0 meters (Figure 3.5). The quantity of MTBE relative to TPH was less than the proportion at locations CPT-1 and CPT-2. As was the case at the other locations, the relative proportion of MTBE to TPH did not change across the vertical profile.

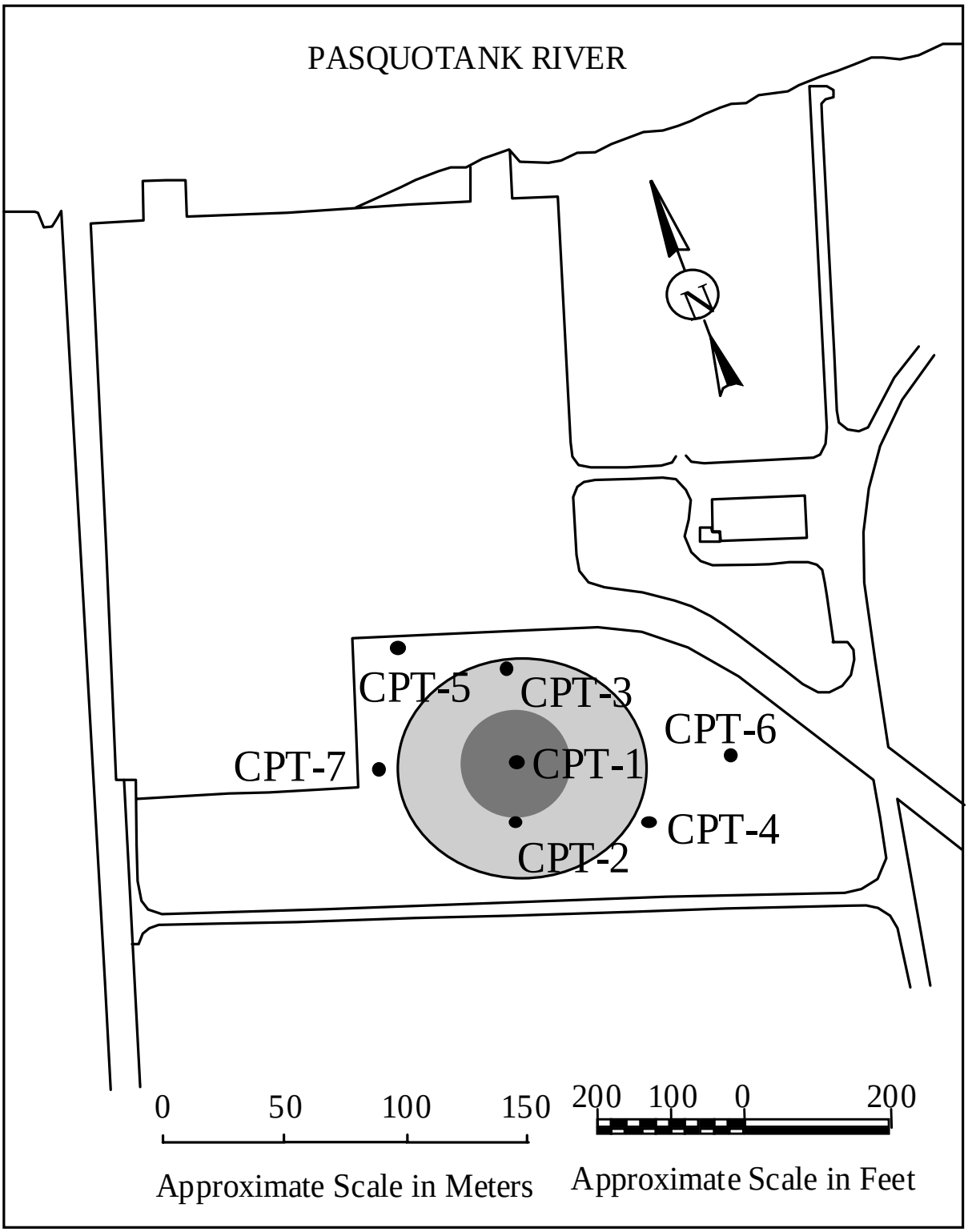

Figure 3.2 Inferred location of the fuel release, based on vertical core samples and the location of the steel underground storage tanks.

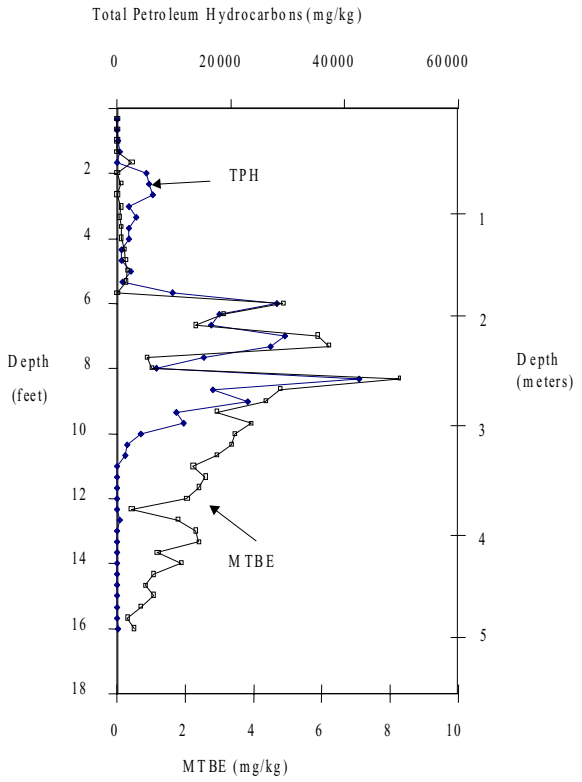

Figure 3.3 Vertical distribution of MTBE and Total Petroleum Hydrocarbon (TPH) in core samples at location CPT-1 (see Figure 3.1 for map).

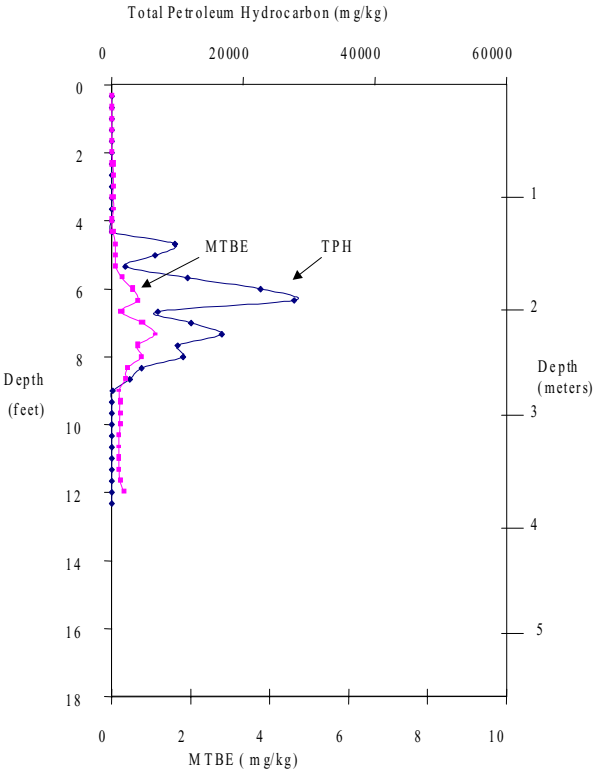

Figure 3.5 Vertical distribution of MTBE and Total Petroleum Hydrocarbon (TPH) in core samples from location CPT-3 (see Figure 3.1 for map).

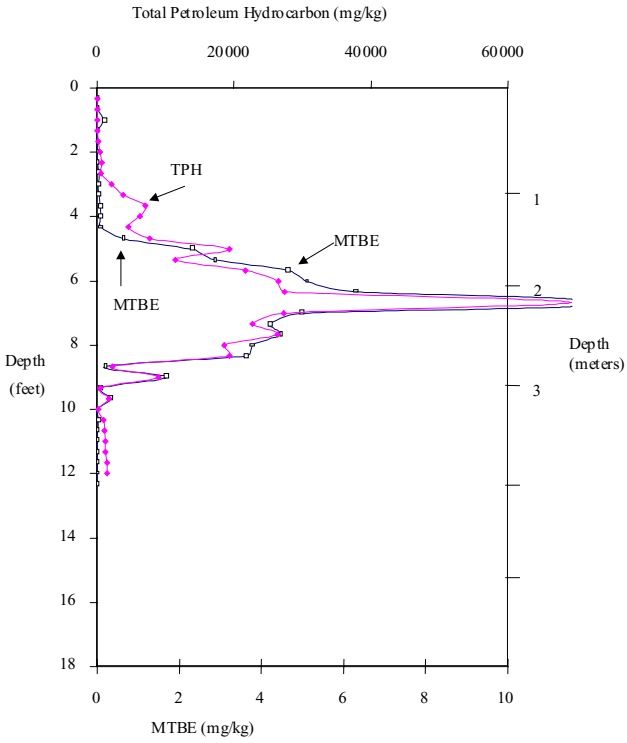

Figure 3.4 Vertical distribution of MTBE and Total Petroleum Hydrocarbon (TPH) in core samples from location CPT-2 (see Figure 3.1 for map).

Distribution of Total Petroleum Hydrocarbons and Hydraulic Conductivity with Depth

Water samples were acquired using GeoProbe™ rods with an outer diameter of 1.0 inch (2.54 cm). The leading rod had 1.5 vertical feet (0.46 meter) of vertical mill slot screens. In addition to collecting samples for analysis of chemical parameters, the hydraulic conductivity was determined at each depth interval using an inverse specific capacity test following the procedure of Wilson et al. (1997).

Figure 3.6 depicts the vertical relationship of Total Petroleum Hydrocarbon (TPH) and Hydraulic Conductivity at location CPT-1 (Figure 3.6). The TPH was confined to an interval extending from 5 to 10 feet below land surface. This may represent a “smear” zone around the water table, which was located 7 feet below land surface when the core and water samples were collected in August 1996. The core material containing significant concentrations of TPH was silty clay to clay with very low hydraulic conductivity.

The depth interval with significant hydraulic conductivity extended from 10 to 27 feet (3 to 8 meters) below land surface (Figure 3.6). The interval containing TPH was just above the interval allowing significant flow of ground water.

Figure 3.7 plots the locations of ground-water samples at the site. At each location, sampling was attempted at depths that extended across the first aquifer, starting in the

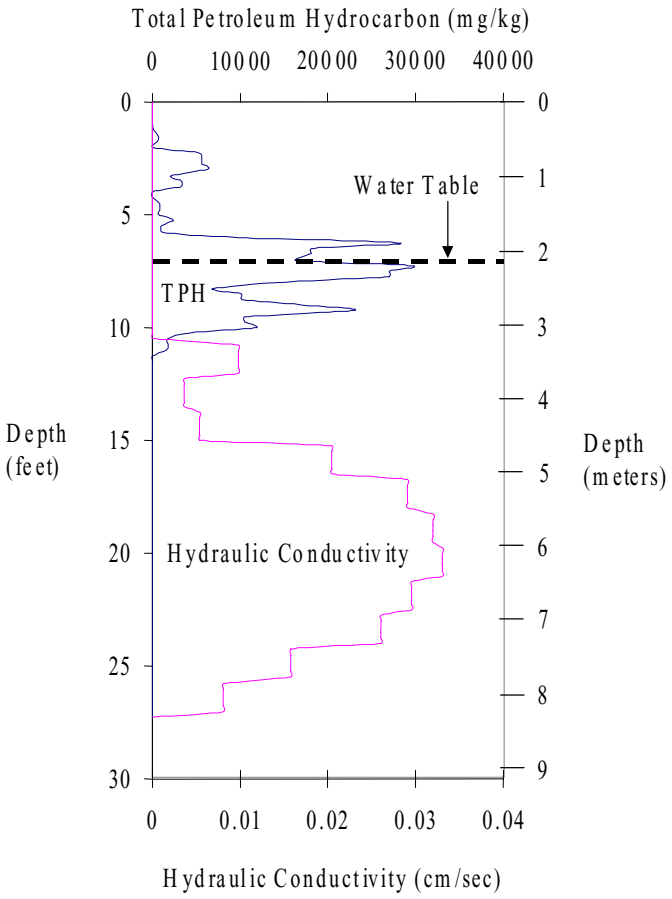

Figure 3.6 Relationship between the vertical extent of Hydraulic Conductivity and the vertical extent of Total Petroleum Hydrocarbon at location CPT-1.

low conductivity material near the surface and extending across the aquifer to the confining zone below the aquifer. The vertical distribution of hydraulic conductivity in Figure 3.6 is representative of the distribution of hydraulic conductivity across the transects depicted in Figure 3.7. At a minimum, the hydraulic conductivity was measured in every other 1.5 foot interval at each location. At many locations, the hydraulic conductivity was measured in every successive 1.5 foot interval. For each location in Figure 3.7, Tables 3.2 and 3.3 compare the average hydraulic conductivity across the aquifer, the highest hydraulic conductivity measured, and the conductivity in the confining layers above and below the aquifer.

In the area that was sampled, hydraulic conductivity in this aquifer was remarkably uniform. The aquifer abruptly pinched out to the southeast (compare GP-21 and GP-22 in Table 3.3), and pinched out to a more limited extent to the northwest. There was no systematic change in hydraulic conductivity moving north toward the Pasquotank River. In general, the highest hydraulic conductivity was twice the average conductivity, as would be expected if the shape of the distribution of hydraulic conductivity with depth was triangular.

Figures 3.8 and 3.9 depict the vertical distribution of the actual sampling locations on transects that are depicted in Figure 3.7, and summarized in Tables 3.2 and 3.3. These figures are offered to provide the reader an indication of the density of the data that are contoured in Figures 3.10 through 3.15.

The depth to the water table was approximately 7 feet in the source area and 6 feet below land surface farther toward the Pasquotank River. Figures 3.10 through 3.15 depict contours as depth below the water table.

Figures 3.10 and 3.11 contour the distribution of hydraulic conductivity. In both transects, the conductive interval starts approximately 5 to 6 feet below the water table and extends to 18 to 20 feet below the water table. In the horizontal plane, there is little indication that flow of ground water is confined to preferential flow channels with markedly higher hydraulic conductivity than surrounding aquifer material.

Distribution of MTBE and BTEX Compounds with Depth

The distribution of MTBE in the north-south transect is depicted in Figure 3.12. The highest concentrations of MTBE are in the shallow ground water underneath the LNAPL at the south end of the transect. As the ground water moves north (to the right in Figure 3.12), the highest concentrations of MTBE are found in the depth intervals with the highest hydraulic conductivity. There is a threefold reduction in the concentration of MTBE at the most contaminated depth interval with each 200 feet north of the source area. All the ground water from the location that was closest to the Pasquotank River had less than 1 µg/l MTBE.

The transect of samples collected in December 1997, runs approximately northwest to southeast. The transect is oriented 50 degrees west of north. As discussed in Appendix A, the average direction of ground-water flow is 8 degrees west of north. The angle between the transect and the direction of flow is 42 degrees. The distribution of MTBE in the northwest to southeast transect reveals a plume that is approximately 350 feet wide. The distance containing MTBE that is perpendicular to ground-water flow is calculated by multiplying the sine of 42 degrees by the contaminated length along the transect. The width of the plume perpendicular to ground-water flow (230 feet, or 90 meters) is slightly less than the diameter of the source area (compare Figure 3.7) . The MTBE plume attenuates abruptly on its northwest side, and attenuates more gradually on its southeastern side.

The distribution of BTEX compounds along the north-south transect is depicted in Figure 3.14. As was the case with MTBE, the highest concentrations are in the shallow ground water underneath the LNAPL. As ground water moves away from the source area, the highest concentrations are found in the most conductive depth intervals. Unlike the pattern seen at other sites, there is no evidence that BTEX compounds are attenuating while MTBE is persistent. There is little practical difference in the pattern of attenuation for MTBE and BTEX compounds.

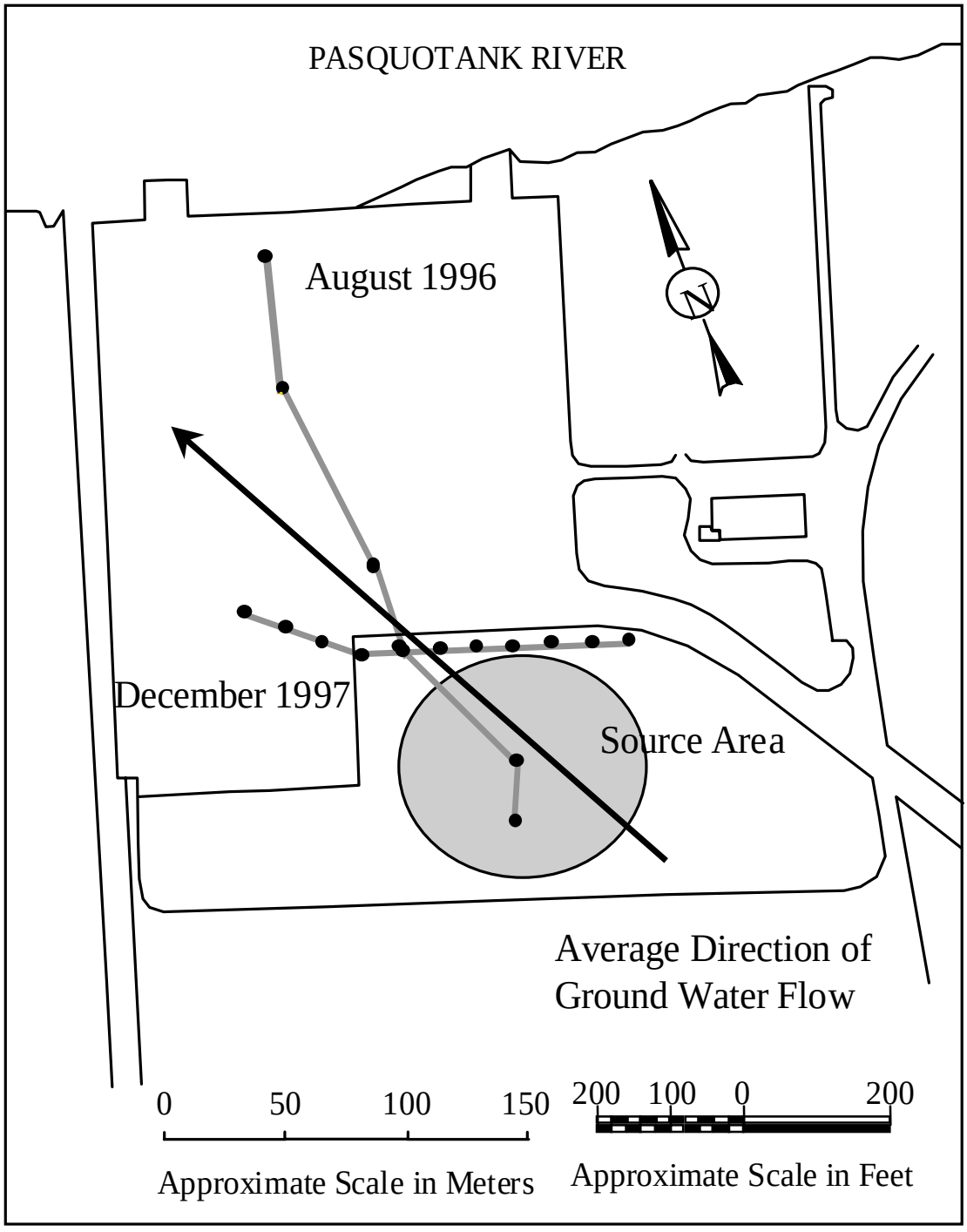

Figure 3.7 Relationship between two transects of ground-water samples and the fuel release. The arrow represents the average direction of ground-water flow.

Table 3.2 Distribution of Hydraulic Conductivity (K) in the north-south transect sampled in August 1996 (Figure 3.7).

South to North	Number of measurements	Average K 10 to 26.5 feet cm/sec	Highest K cm/sec	Lowest K in Higher Interval cm/sec	Lowest K in Lower Interval cm/sec
CPT-2	11	0.015	0.029	0.0004	0.00035
CPT-1	9	0.020	0.033	0.0036	0.016
CPT-3	10	0.026	0.041	0.0014	0.0001
CPT-5	10	0.022	0.042	0.00001	0.012
ESM-14	9	0.025	0.046	0.0003	0.0005
ESM-10	10	0.031	0.060	0.0077	0.0033
GP-1	7	0.024	0.041	0.0015	0.0015

Table 3.3 Distribution of Hydraulic Conductivity (K) in the east-west transect sampled in December 1997 (Figure 3.7).

West to East	Number of measurements	Average K 10 to 26.5 feet cm/sec	Highest K cm/sec	Lowest K in Higher Interval cm/sec	Lowest K in Lower Interval cm/sec
GP-25	4	0.013	0.038		0.0064
GP-24	6	0.019	0.047	0.0007	0.013
GP-23	8	0.025	0.057	0.00015	0.00021
GP-19	7	0.032	0.084	0.00004	0.012
GP-18	8	0.027	0.063	0.00001	0.00004
GP-17	8	0.024	0.052	0.0016	0.00004
GP-16	7	0.017	0.031	0.0003	
GP-15	8	0.024	0.050	0.00024	0.00023
GP-20	6	0.024	0.051	0.0034	0.010
GP-21	7	0.022	0.052	0.00013	0.00004
GP-22	6	0.0001	0.020	0.00003	0.00002

It is important not to interpret the apparent attenuation along this transect as sufficient evidence for natural attenuation along the flow path. The transect may be askew of the flow path, and may sample water at the distal locations that was never in the plume. The north-south transect is oriented 16 degrees east of north (Figure 3.2). This is only 24 degrees from the average direction of ground-water flow, but this difference is large enough to move out of a plume that is 230 feet wide at a distance of 600 feet from the edge of the source area.

To determine whether a particular location along the transects sampled the plume or missed the plume, the concentration of MTBE at each location was compared to a number of geochemical indicators that correlate with biological activity in ground water. The concentrations of methane, iron (II), oxygen, sulfate, and alkalinity at the transect locations were compared to their concentrations in ground water that was not impacted by the plume (see Figures B.1 through B.6 in Appendix B). The geochemistry of the site is discussed in detail in Appendix B. All of the sampling locations on the north-south transect that were downgradient of the source area were depleted of oxygen and sulfate, and had elevated concentrations of methane, iron (II), and alkalinity, indicating that these locations in the north-south transect sampled the plume.

Figure 3.15 reveals that the plume, as sampled by the east-west transect, is heterogeneous with respect to the distribution of MTBE and BTEX compounds. The higher concentrations of MTBE extend from 50 to 350 feet along the transect (Figure 3.13). The higher concentrations of BTEX extend from 200 feet along the transect to 400 feet along the transect (Figure 3.15). The northwestern reach of the transect has MTBE but no BTEX, the central reach has both MTBE and BTEX, and the southeastern reach has BTEX but no MTBE.

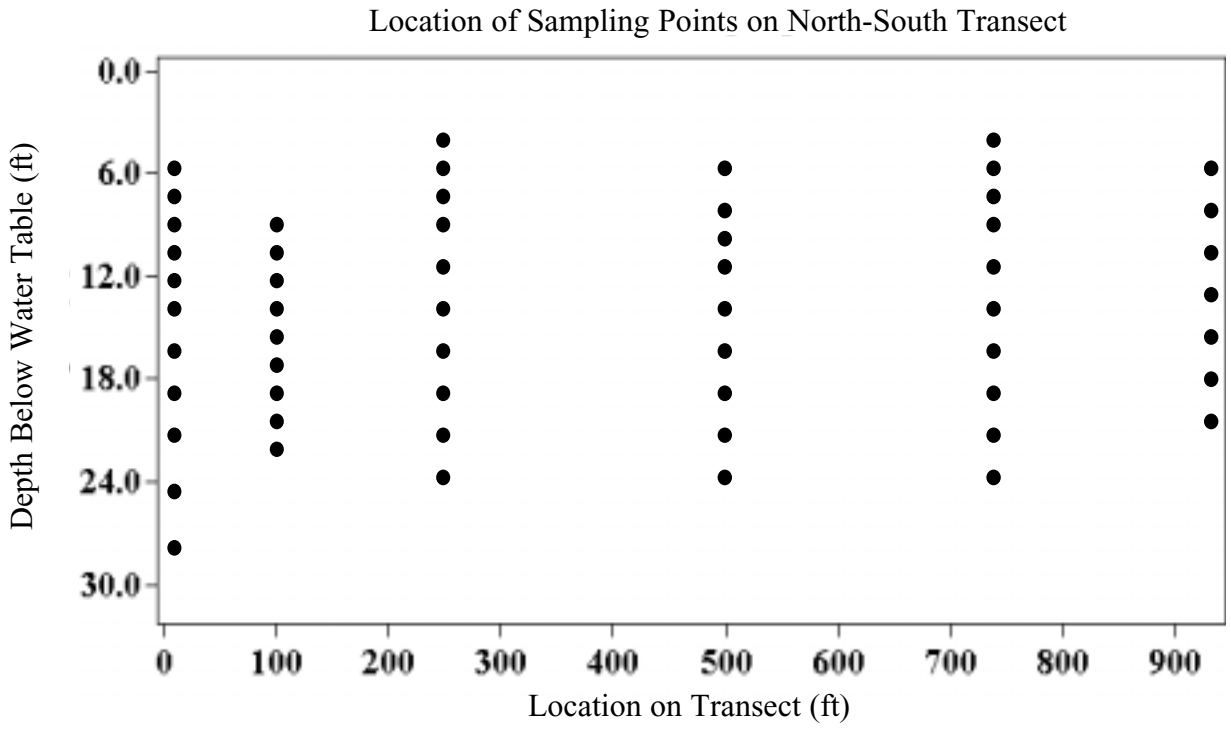

Figure 3.8 Location of vertical sampling points along the north-south transect, collected in August 1996. Distance along the transect extends from south to north (bottom to top in Figure 3.7), in the direction of ground-water flow.

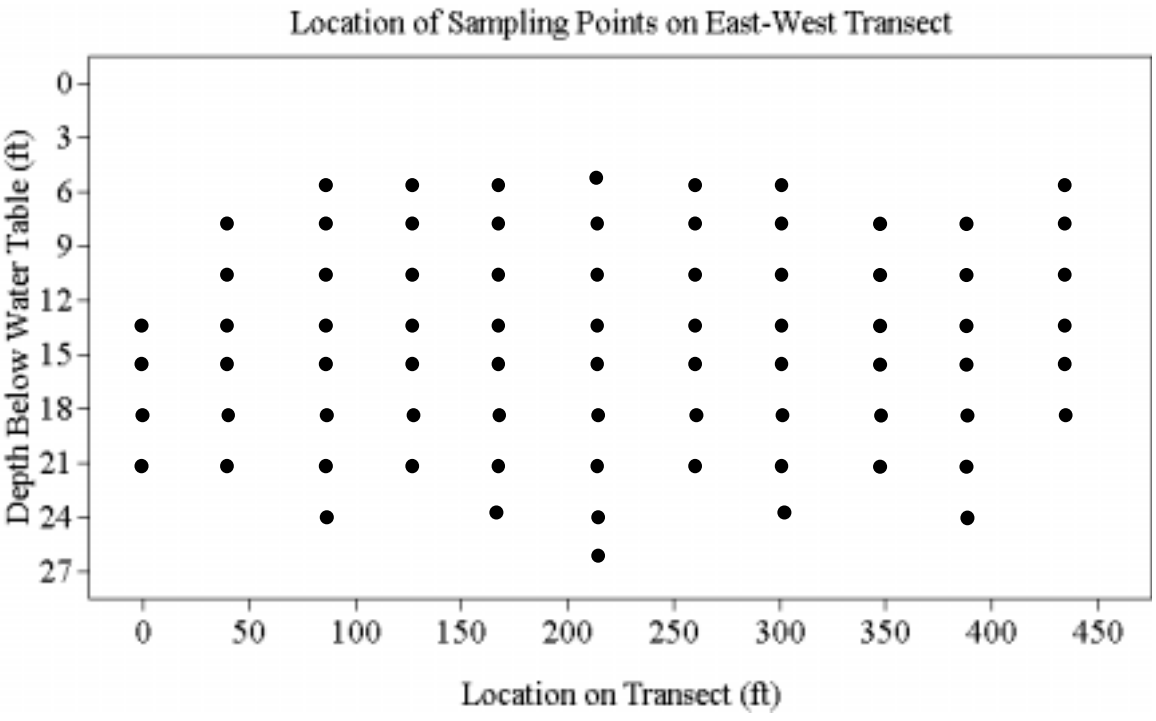

Figure 3.9 Location of vertical sampling points along the east-west transect, collected in December 1997. Distance along the transect extends from west to east (left to right in Figure 3.7), opposite the direction of ground-water flow.

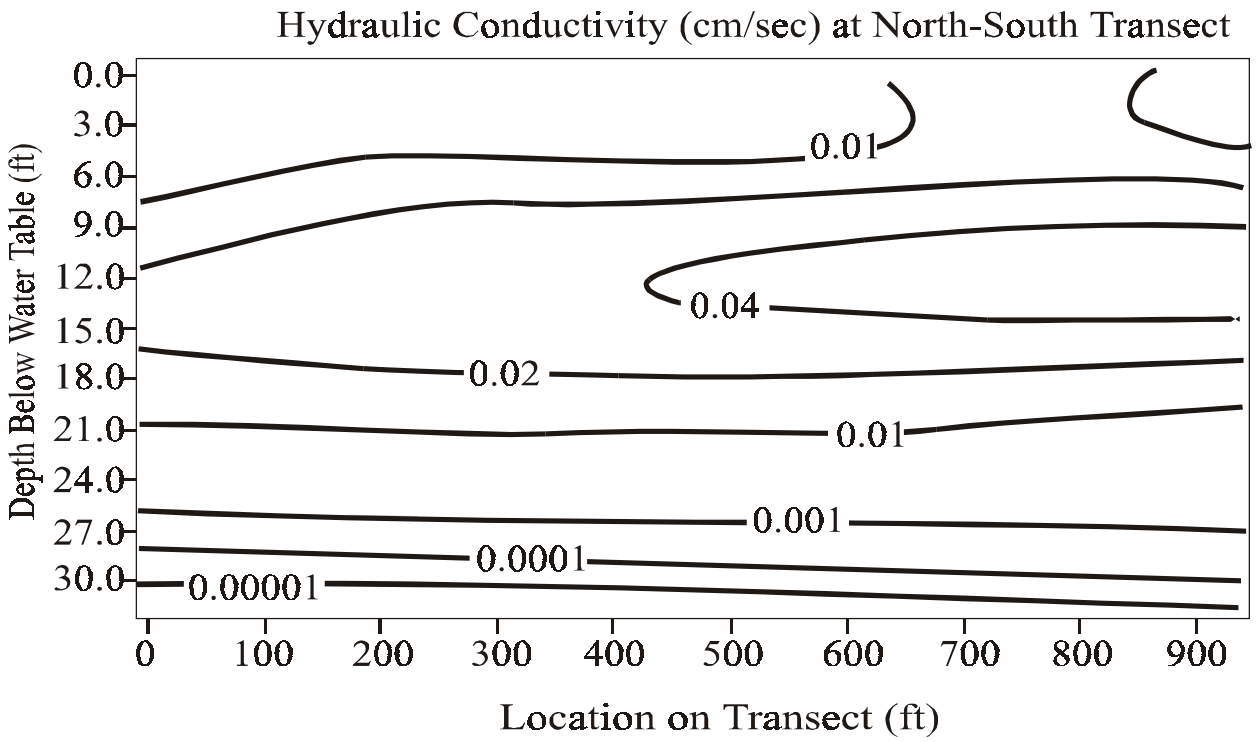

Figure 3.10 Distribution of hydraulic conductivity along the north-south transect, collected in August 1996. Distance along the transect extends from south to north (bottom to top in Figure 3.7), in the direction of ground-water flow.

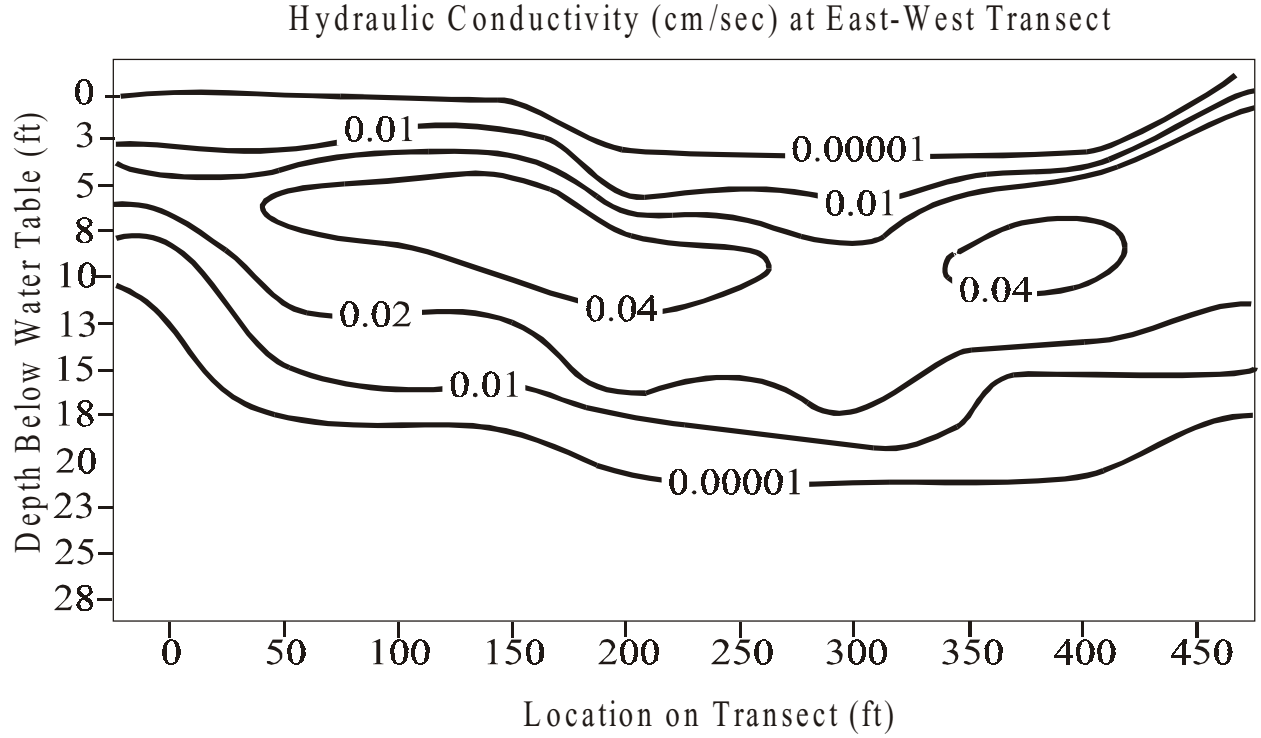

Figure 3.11 Distribution of hydraulic conductivity along the east-west transect, collected in December 1997. Distance along the transect extends from west to east (left to right in Figure 3.7), opposite the direction of ground-water flow.

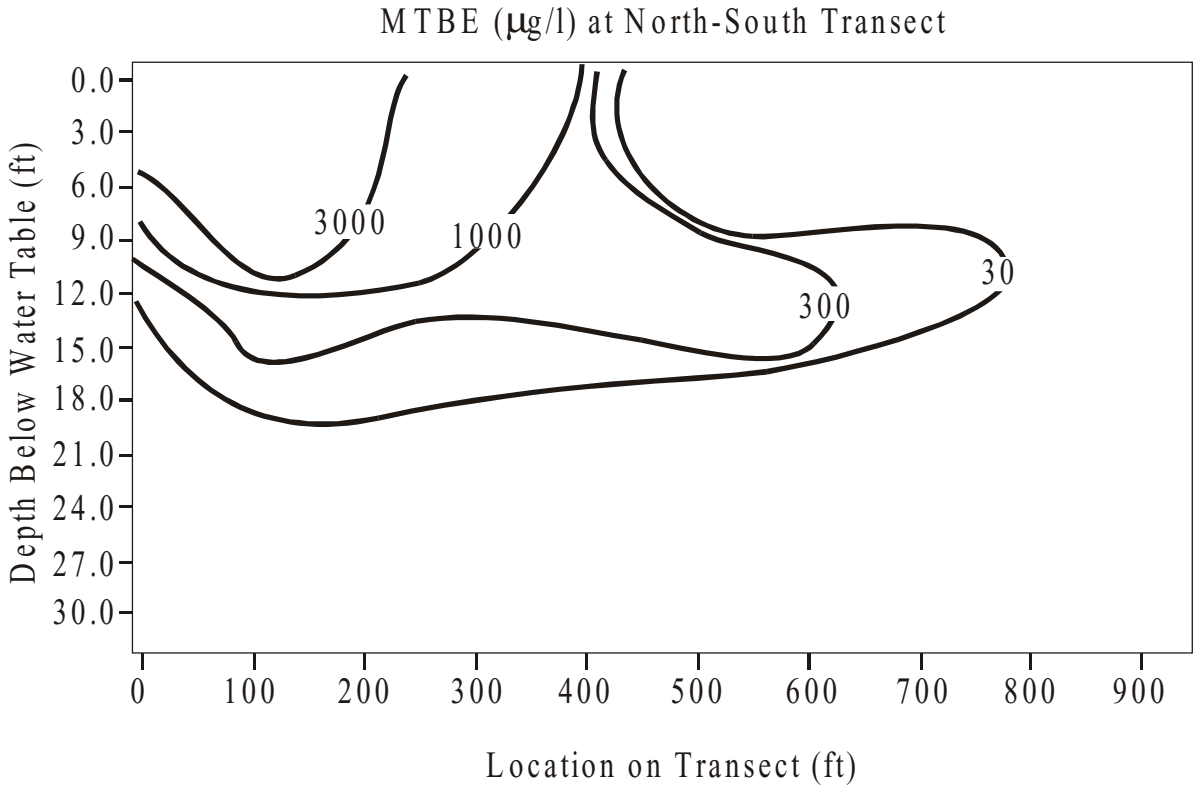

Figure 3.12 Distribution of MTBE along the north-south transect, collected in August 1996. Distance along the transect extends from south to north (bottom to top in Figure 3.7), in the direction of ground-water flow.

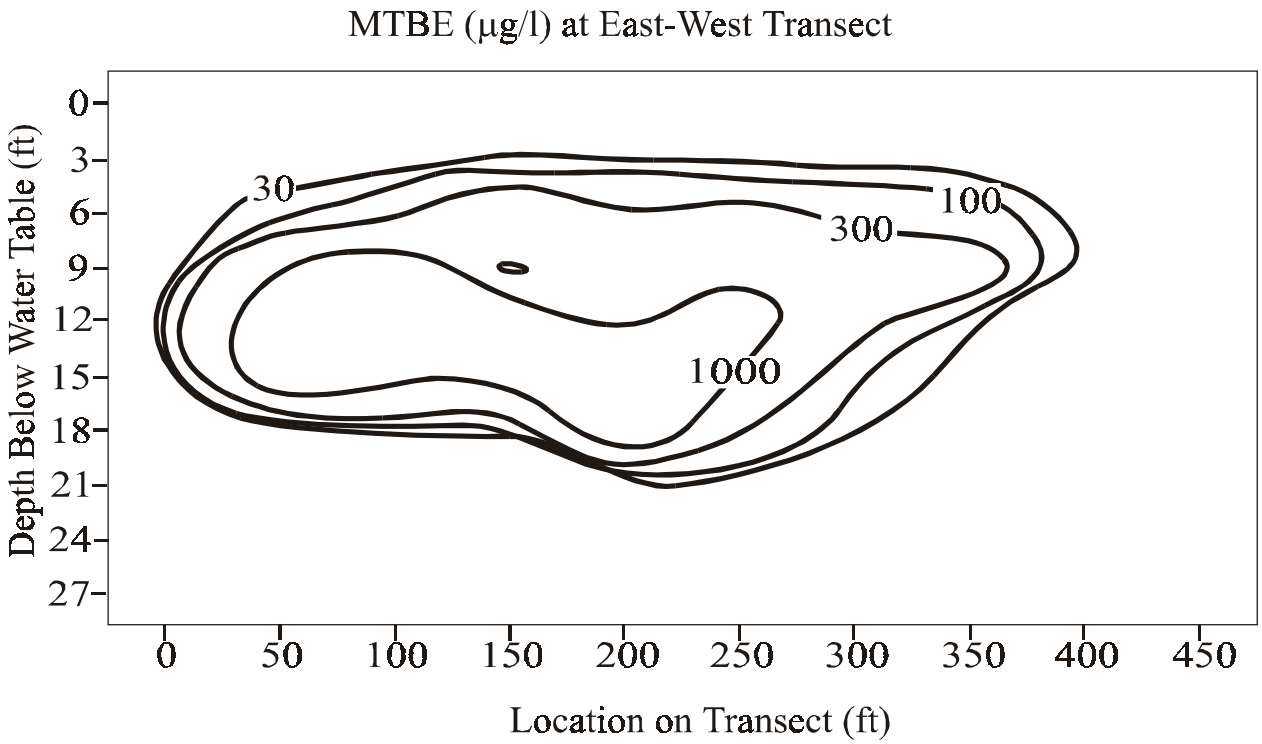

Figure 3.13 Distribution of MTBE along the east-west transect, collected in December 1997. Distance along the transect extends from west to east (left to right in Figure 3.7), opposite the direction of ground-water flow.

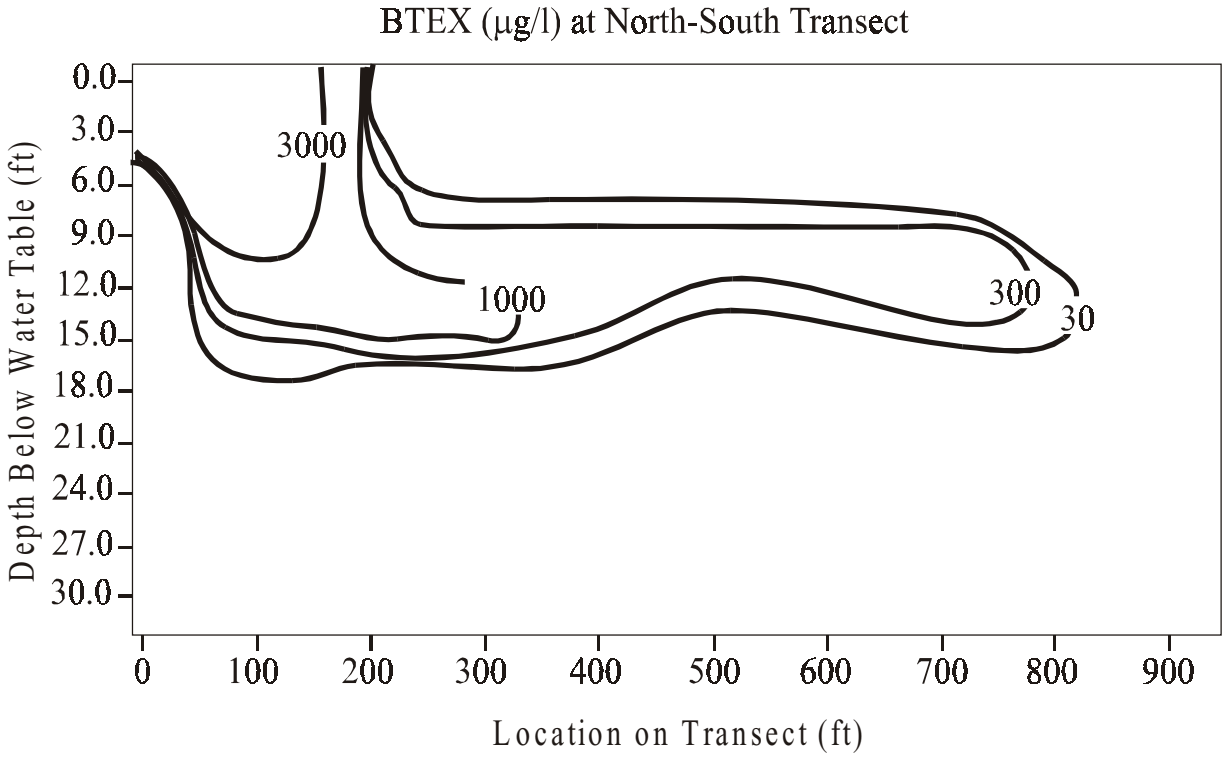

Figure 3.14 Distribution of BTEX along the north-south transect, collected in August 1996. Distance along the transect extends from south to north (bottom to top in Figure 3.7), in the direction of ground-water flow.

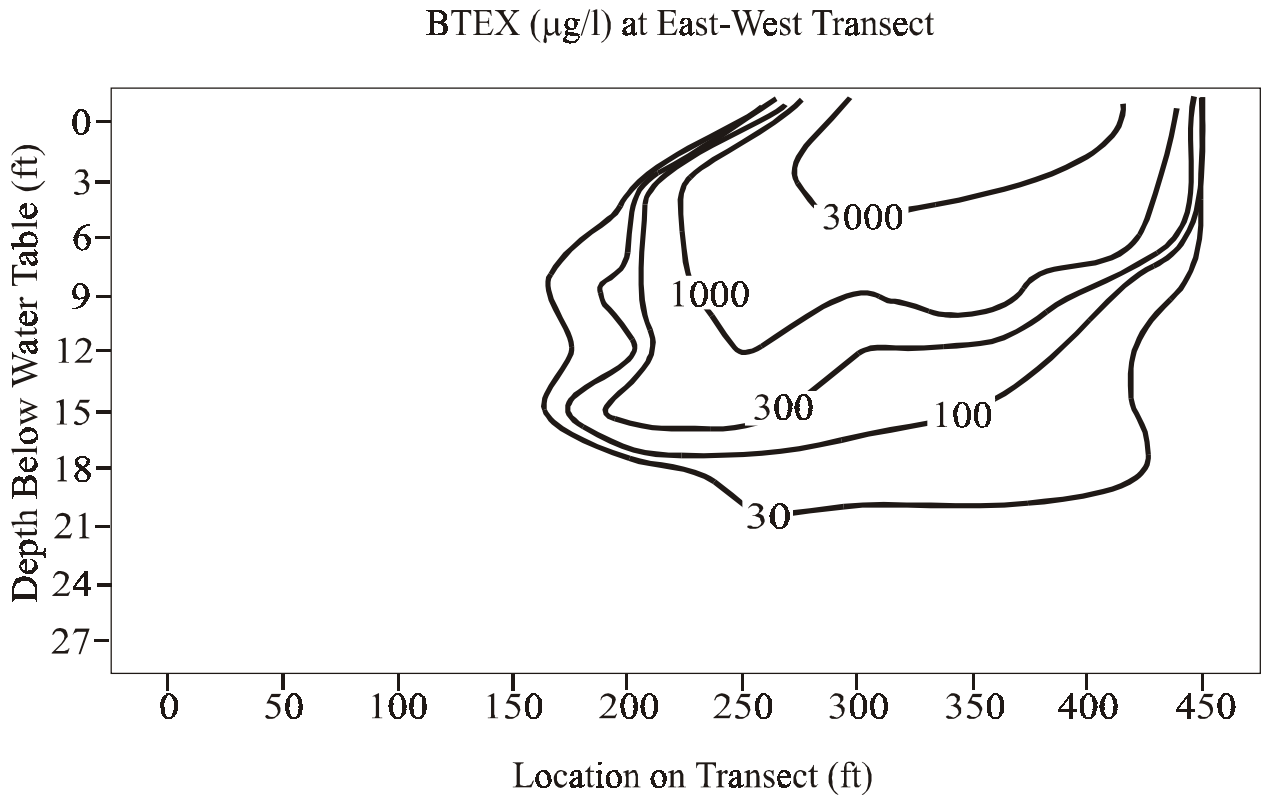

Figure 3.15 Distribution of BTEX along the east-west transect, collected in December 1997. Distance along the transect extends from west to east (left to right in Figure 3.7), opposite the direction of ground-water flow.

SECTION 4
Transport and Fate of MTBE in the Ground Water

Estimated Rate of Attenuation in Ground Water

Ground-water flow carrying the plume of contamination is contained within a semi-confined aquifer. Most of the plume occurs under the concrete of an operational apron at the U.S. Coast Guard Support Center. The bottom of the drainage ditch on the northwest side of the site does not penetrate the upper layer of silty clay, and does not communicate with the sandy layer that carries the plume of contamination. As a result, there is little opportunity for the ground-water flow field to be influenced by local recharge or local discharge. As a simplification, we assume that the shape of the water table is a plane during any particular round of sampling.

The direction of ground-water flow was determined by using a least squares regression technique to fit a plane through the elevation of the water table in eight permanent monitoring wells at the site. A separate regression was performed for each of eighteen rounds of quarterly monitoring starting in September 1994 and extending through December 1998, and each of fourteen rounds of monthly sampling starting in February 1998 and extending to March 1999. Appendix A contains a map showing the location of the permanent monitoring wells used to estimate flow direction, tables showing the water table elevation in the monitoring wells at each round of sampling, and tables showing results of the regression analyses, with estimates of plume direction, hydraulic gradient, and goodness of fit. Appendix A also contains maps that compare the contours of the water table as estimated by the regressions to the measured elevations of the water for the eighteen rounds of quarterly monitoring.

The regional ground-water flow direction is north, directly toward the Pasquotank River; however, the hydraulic gradient at any one time in the study area is strongly influenced by the stage of the Pasquotank River. The direction and magnitude in the flow of ground water as predicted in each round of quarterly sampling is depicted in Figure 4.1. For each round of sampling, an arrow in the figure represents the distance ground water would move in one year under the conditions of gradient and direction that were encountered in that round of sampling. The variation in direction and magnitude in the fourteen rounds of monthly sampling is depicted in Figure 4.2.

The average direction of ground-water flow was calculated by weighting the direction of flow on any particular round of sampling by the hydraulic gradient at that particular round, then taking an average of the weighted flow directions.

For the eighteen rounds of quarterly sampling, the average flow direction was 8.6 degrees west of north, with a standard deviation of 9.1 degrees. For the fourteen rounds of monthly sampling, the average flow direction was 8.7 degrees west of north, with a standard deviation of 23 degrees.

The seepage velocity of the plume was estimated from Darcy's Law. To calculate seepage velocity, the hydraulic conductivity was multiplied by the hydraulic gradient, and divided by the porosity. Table 4.1 summarizes the statistical properties of the parameters used to calculate seepage velocity. There is relatively little variation in hydraulic conductivity; the range of eight samples is only 56% of the mean. There is greater variation in hydraulic gradient from one round of sampling to another. For eighteen rounds of quarterly sampling, the hydraulic gradient varied over an order of magnitude. Nothing is known directly about the range of porosity at the site. The total pore space in core samples was calculated by comparing the wet and dry weight of core samples from five locations. The total porosity was very close to 0.34 to 0.36. A value of 0.35 was taken as an upper boundary on effective porosity. A survey of the literature and professional judgment was used to assign an average effective porosity of 0.3, and lower boundary on effective porosity of 0.25.

The average seepage velocity was calculated by multiplying the average hydraulic conductivity by the average hydraulic gradient, and dividing by an assumed effective porosity of 0.3. The upper boundary on seepage velocity was calculated by multiplying the upper 95% confidence intervals for hydraulic conductivity and hydraulic gradient, then dividing by an assumed effective porosity of 0.25. The lower boundary was calculated by multiplying the lower 95% confidence intervals for hydraulic conductivity and hydraulic gradient, then dividing by an assumed porosity of 0.35. The average calculated seepage velocity at the site was 82 meters per year. The upper boundary was 150 meters per year, and the lower boundary was 67 meters per year. These estimates of seepage velocity

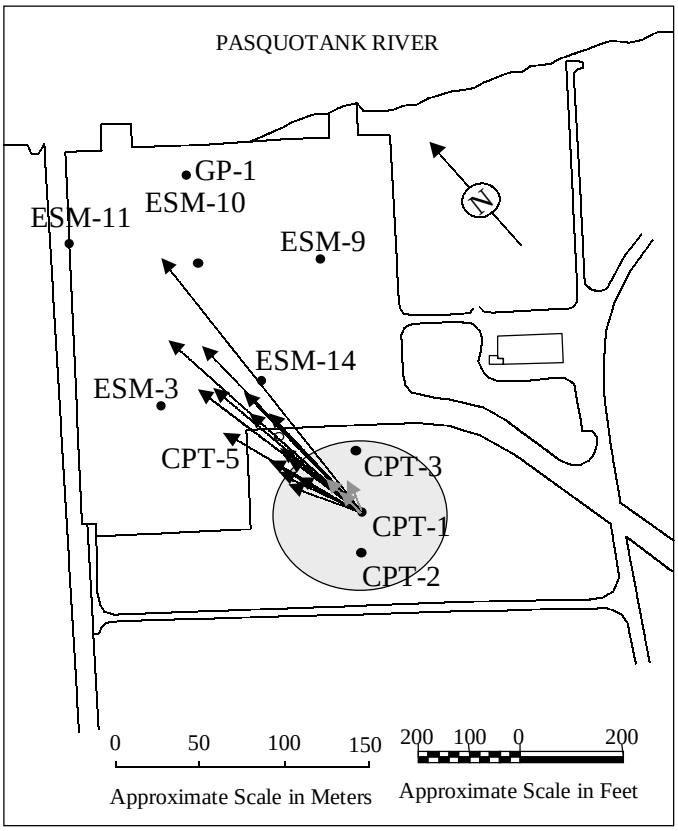

Figure 4.1. Variation in ground-water flow calculated from eighteen rounds of quarterly monitoring. The length of the arrow is the distance that would be traveled by MTBE in one year at that hydraulic gradient.

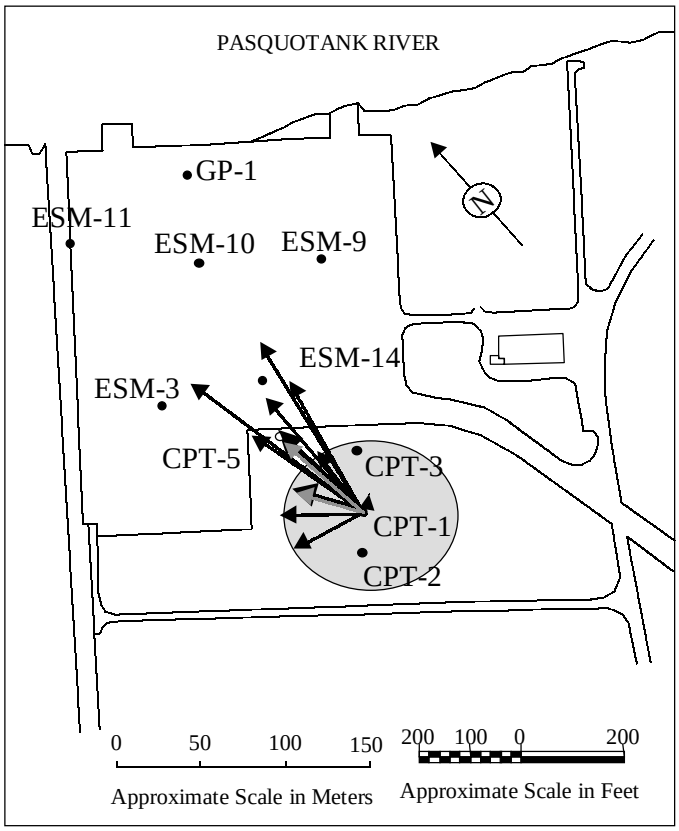

Figue 4.2. Variation in ground-water flow calculated from fourteen rounds of monthly monitoring. The length of the arrow is the distance that would be traveled by MTBE in one year at that hydraulic gradient.

Table 4.1 Sensitivity analysis of the estimates of the seepage velocity of ground water at the site. These estimates were used to calculate a first-order rate of attenuation of MTBE in ground water downgradient of the source area.

Parameter	Hydraulic Conductivity	Hydraulic Gradient	Porosity	Seepage Velocity
Unit	cm per second	meter per meter	Fraction pore space	meter per year
Basis of Boundary	95% Confidence Interval	95% Confidence Interval	Range of Literature	Calculated
Number of Samples	8	18		Calculated
Mean	0.027	0.0029	0.30	82
Maximum	0.036	0.0067		
Minimum	0.020	0.00059		
Upper Boundary	0.031	0.0037	0.25	150
Lower Boundary	0.023	0.0028	0.35	67

Table 4.2. Concentration of MTBE, methane, and iron (II) at monitoring locations used to calculate the rate of attenuation of MTBE, methane, and iron (II) with time of travel downgradient of the location with the highest concentration.

Location	Distance from Source (CPT-1)	Date Sampled	MTBE	Methane	Iron (II)
	meters	Month/Year	µg/l	mg/l	mg/l
Source Area					
CPT-1	0	8/1996	1,740	3.5	34
CPT-3	40	8/1996	823	13.5	96
Downgradient of Source					
CPT-5	70	8/1996	672	5.9	56
ESM-14	104	8/1996	383	7.8	84
ESM-3	134	6/1999	319	1.3	86
ESM-9	180	8/1996	<1	3.24	42
ESM-10	195	8/1996	9.7	4.6	20
ESM-11	238	6/1999	13.5	0.12	33
GP-1	250	8/1996	<1	1.0	59

were used to calculate time of travel of ground water from the most contaminated location (CPT-1) to the downgradient locations.

For various sampling locations presented in Figure 4.1, Table 4.2 compares the distance downgradient to the concentration of MTBE, and the concentrations of methane and iron (II). Methane is expected to be a conservative tracer in ground water once it forms, and iron (II) appears to be conservative at this site as well. Methane and iron (II) will be used as tracers for the plume of contaminated ground water. Monitoring locations CPT-1, CPT-3, CPT-5, ESM-3, ESM-10, ESM-14, and GP-1 have high concentrations of methane and iron (II) indicating that these locations sample the plume. These locations were included in the calculation of the natural biodegradation rate constant.

Although location ESM-11 is directly downgradient of the source area (Figure 4.1), it had low concentrations of methane (Table 4.2). The low concentration of MTBE at location ESM-11 may have resulted from simple dilution; as a result, location ESM-11 was not included in the calculation of the biodegradation rate constant. In contrast, location ESM-9 is not directly downgradient from the source area. However, the geochemical parameters indicate that ground water sampled in this location was in the plume of contamination. As depicted in Figure 4.1, the plume of methane and iron (II) moves more to the east than would be expected from the hydraulic gradient alone. This may reflect anisotrophic flow in the aquifer, rather than error in estimating the direction of the hydraulic gradient. Location ESM-9 was included in the calculation of the biodegradation rate constant.

Figure 4.3 plots the logarithm of concentration of iron (II), methane, and MTBE against the calculated travel time of ground water downgradient of the source. In three years' travel time, there is no attenuation of iron (II), the concentration of methane is attenuated by an order of magnitude, and the concentration of MTBE is attenuated by three orders of magnitude. The attenuation of methane is the best estimate of the effects of attenuation due to dilution and dispersion. The attenuation of MTBE in excess of the attenuation of methane must be due to natural biodegradation.

The first-order rate of attenuation was calculated by a linear regression of the natural logarithm of concentration on time of travel along the flow path. Table 4.3 compares the apparent rate of attenuation, and the 95% confidence interval on that rate, for MTBE, methane, and iron (II). The average total rate of attenuation of MTBE was near 2.7 per year. The attenuation of methane, which may be taken as

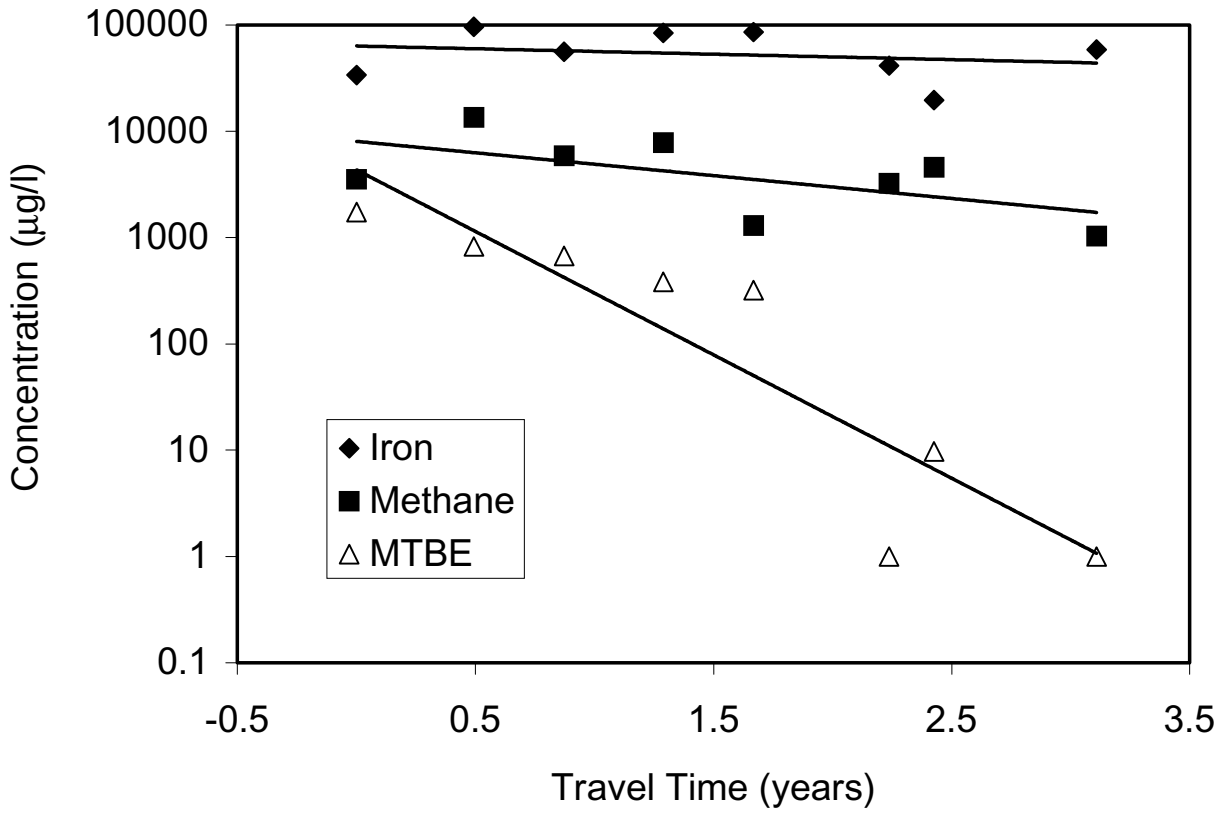

Figure 4.3 Attenuation in concentrations of MTBE, methane, and iron (II) with travel time downgradient from the location with the highest concentration of MTBE.

Table 4.3 The apparent first-order rate of attenuation of MTBE, methane, and iron (II) with time of travel downgradient from the location with the highest concentration of MTBE.

Analyte	Estimate of Plume Velocity	Apparent Rate of Attenuation	Upper 95% Confidence Interval	Lower 95% Confidence Interval
		per year		
MTBE	Upper Boundary	5.0	7.21	2.69
MTBE	Average	2.7	3.89	1.45
MTBE	Lower Boundary	2.2	3.26	1.22
Methane	Average	0.5	1.15	-0.160
Iron (II)	Average	0.12	0.619	-0.384

a surrogate for attenuation of MTBE due to dilution and dispersion, was 0.5 per year. The lower 95% confidence interval for attenuation of MTBE does not overlap the upper 95% confidence interval for methane attenuation. The rates are different at 95% confidence. There was no appreciable attenuation in concentrations of iron (II).

The rate of attenuation in the field compares well with the rate of attenuation in the laboratory microcosm study. The average rate of attenuation in the field was 2.7 per year. The average rate of attenuation in the laboratory was 3.02 ± 0.52 per year at 95% confidence.

Transfer from the Entire Source Area to the Plume

The mass transfer of MTBE from the source LNAPL to the ground water moving underneath was estimated by calculating the flux of MTBE moving away from the source across the east-west transect, then comparing that flux to the total mass of MTBE in the source area.

Figure 4.5 depicts the relationship between the locations on the east-west transect, the direction of ground-water flow, and the source area.

The flow-weighted average concentration of MTBE in ground water at each location along the east-west transect was calculated by multiplying the concentration of each vertical sample by the hydraulic conductivity at that point, dividing each product by the average hydraulic conductivity to produce a weighted concentration, then taking the simple arithmetic average of the weighted concentrations. The results are presented in Figure 4.6. The highest concentrations of MTBE were directly downgradient of the "hot-spot" at CPT-1.

Each location was considered to represent a length along the transect equal to the distance to the mid points between the neighboring locations. The linear distance between the transect locations was 50 feet. For locations 18, 17, 16, 15, 20, 21, and 22, the length that was perpendicular to ground-water flow was 34 feet. For locations 25,

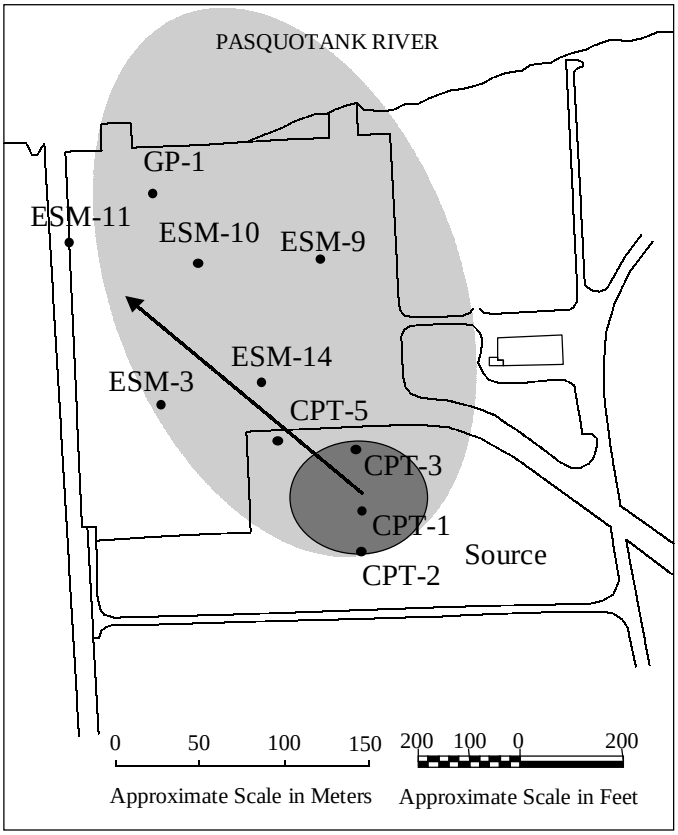

Figure 4.4 Locations of ground-water samples included in the calculation of the rate of natural attenuation. The arrow represents the average direction of ground-water flow. The dark shaded area is the area with LNAPL. The larger lightly shaded area is the area downgradient where the ground water contains high concentrations of methane and iron (II). Only wells in the shaded area were included in the calculation of the rate of natural attenuation.

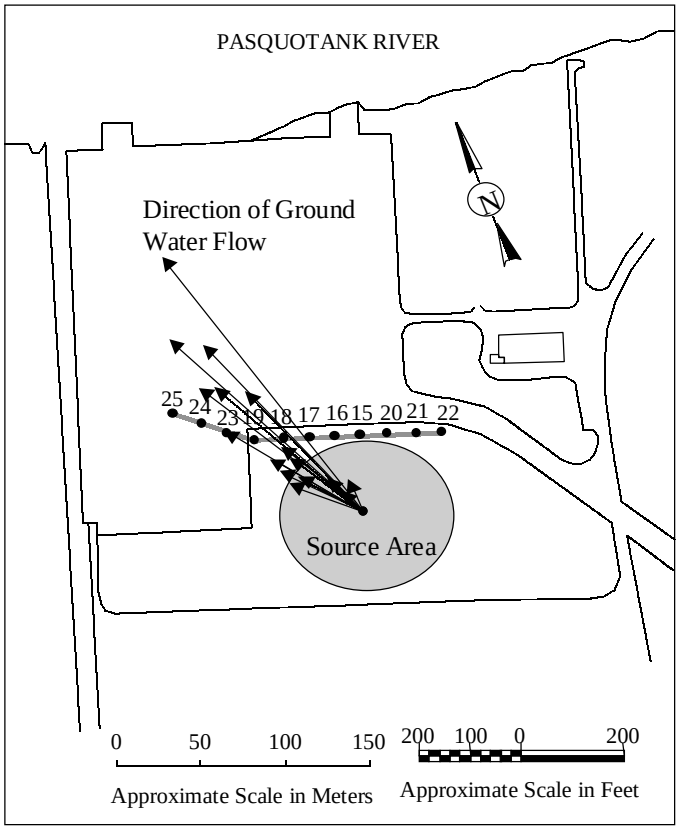

Figure 4.5 Relationship between the direction of ground-water flow and the ground-water sampling locations in the transect sampled in December 1997. Ground-water flow vectors were calculated from the gradients in water table elevation in eighteen different rounds of monitoring The length of arrow is the distance that would be traveled by MTBE in one year of flow at that gradient.

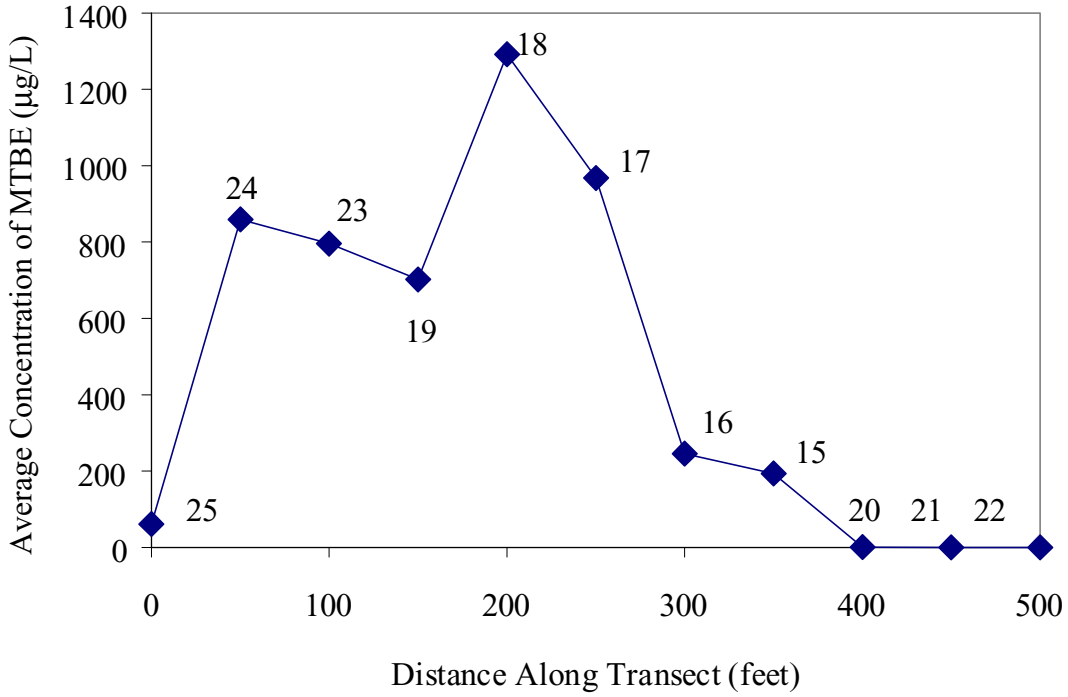

Figure 4.6 Concentrations of MTBE in a transect that extends across the plume in a direction that is roughly perpendicular to ground-water flow. See Figure 4.5 for the positions of the sampling locations identified as 15 through 25 in both Figures. Depicted at each location are the flow-weighted average concentrations of MTBE in ground-water samples from a vertical profile extending across the aquifer at each location.

24, and 23 the distance perpendicular to ground-water flow was 17.1 feet. For location 19, the length was 26 feet.

For each location, the vertical interval that was averaged to get the average concentration (25.5 feet) was multiplied by the length perpendicular to flow to get the cross section, then by the Darcy velocity to get the flux of water. The flux at all the locations was summed. Approximately 5,300 cubic meters of water crosses the transect per year. The flux of water at each location was multiplied by the average concentration at each location, then summed. The flux of MTBE from the source area across the transect was 2.8 kg/year.

The lower boundary on the total quantity of MTBE in the source area was 46 kg (Section 3). If this flux did not change over time, it would take seventeen years to remove the MTBE from the source.

When the MTBE diffuses out of the LNAPL to be swept away by flow in the aquifer, the less soluble petroleum hydrocarbons are left behind. As a result, the concentration of MTBE in the fuel decreases over time. It is not likely that the mass transfer rate of MTBE from the LNAPL remains the same, regardless of the concentration of MTBE remaining in the LNAPL. Diffusion is the mechanism that drives the mass transfer process. The diffusive flux is proportional to concentration gradients, and the gradients of MTBE are proportional to the remaining concentration of MTBE in the LNAPL. The mass transfer of MTBE would be directly proportional to the concentration of MTBE remaining in the LNAPL. If the rate of transfer of MTBE to ground water is proportional to the amount of MTBE in the source, the instantaneous rate of transfer is 0.06 per year. The average concentration at the most contaminated location in the transect is 1200 µg/year. At this rate of attenuation of the source, it would require approximately sixty years for the concentration to reach 30 µg/liter.

Transformation of MTBE to TBA

Tertiary Butyl Alcohol (TBA) has been documented as a transformation product of MTBE in a number of studies (Mormile et al., 1994; Squillace et al., 1996; Church et al., 1997). In the water samples collected in the transect across the plume in December 1997, the concentration of TBA was measured using solid phase micro-extraction. The limit of quantitation was 1 µg/l. Figure 4.7 compares the concentration of TBA to the concentration of MTBE in all the water samples from the transect. With two exceptions, the concentration of TBA was less than 200 µg/l. There is no evidence of accumulation of TBA in the transect as a whole.

In general, it is difficult to determine whether TBA in ground water was a component of the original spill, or if it was produced from biological transformation of MTBE (Church et al., 1997; Landmeyer et al., 1998). Two groundwater samples had higher concentrations of TBA. In one

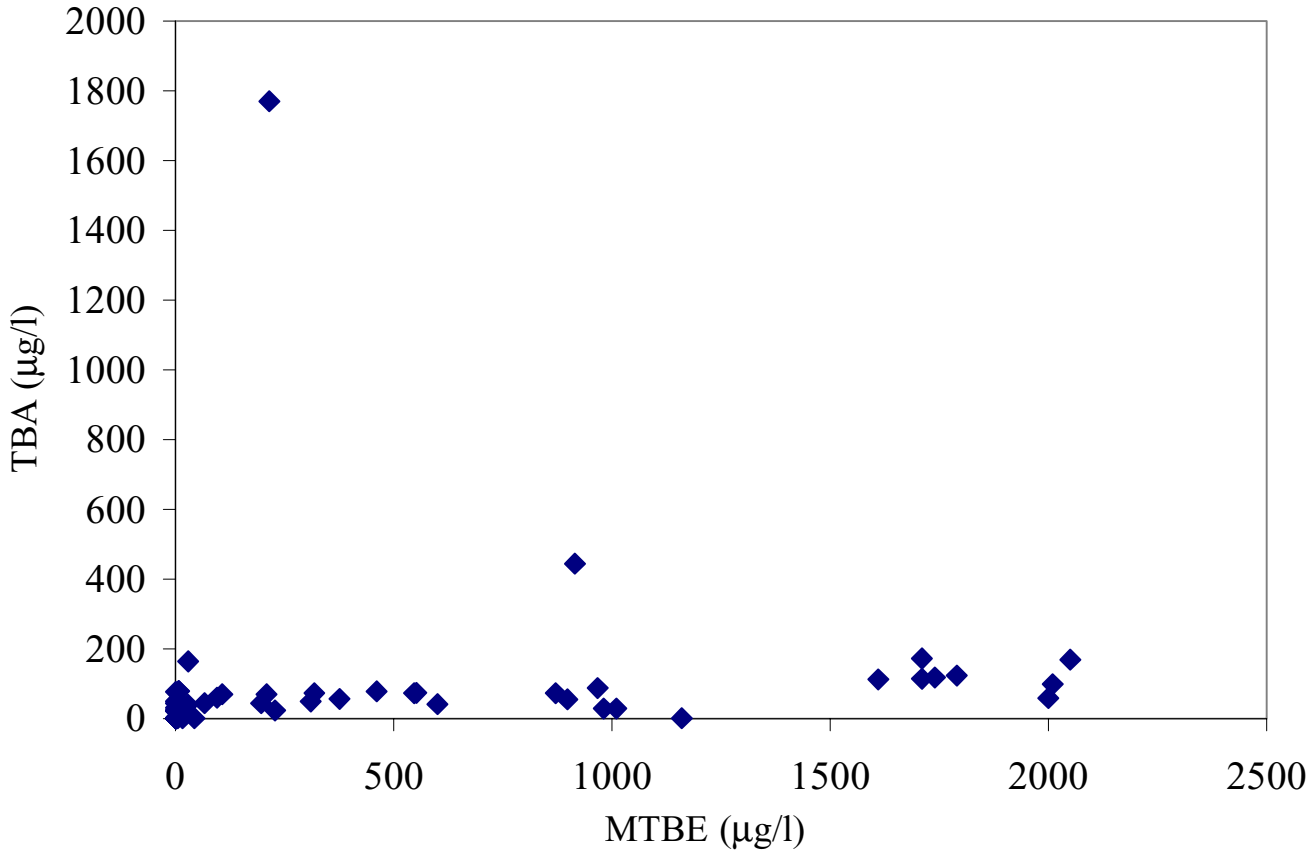

Figure 4.7 Relationship between the concentration of TBA in ground water and the concentration of MTBE in water samples collected in a transect across the plume in December 1997.

of these samples there was a corresponding reduction in the concentration of MTBE. At these locations the TBA was probably produced from transformation of MTBE. Figure 4.8 depicts the distribution of MTBE with depth at three locations immediately downgradient of the source area. Location 19 is between locations 18 and 23. Locations 18 and 23 have a peak in MTBE concentration near 2000 µg/l at a depth of 6 meters. At location 19, at a depth of 6 meters there is a decline in the concentration of MTBE, with higher concentrations at depths of 5 and 7 meters. Figure 4.9 depicts the distribution of TBA with depth at the same locations. There is little accumulation of TBA at locations 18 and 23. However, there is a large accumulation of TBA at a depth of 6 meters at location 19, at the same location where MTBE was depleted.

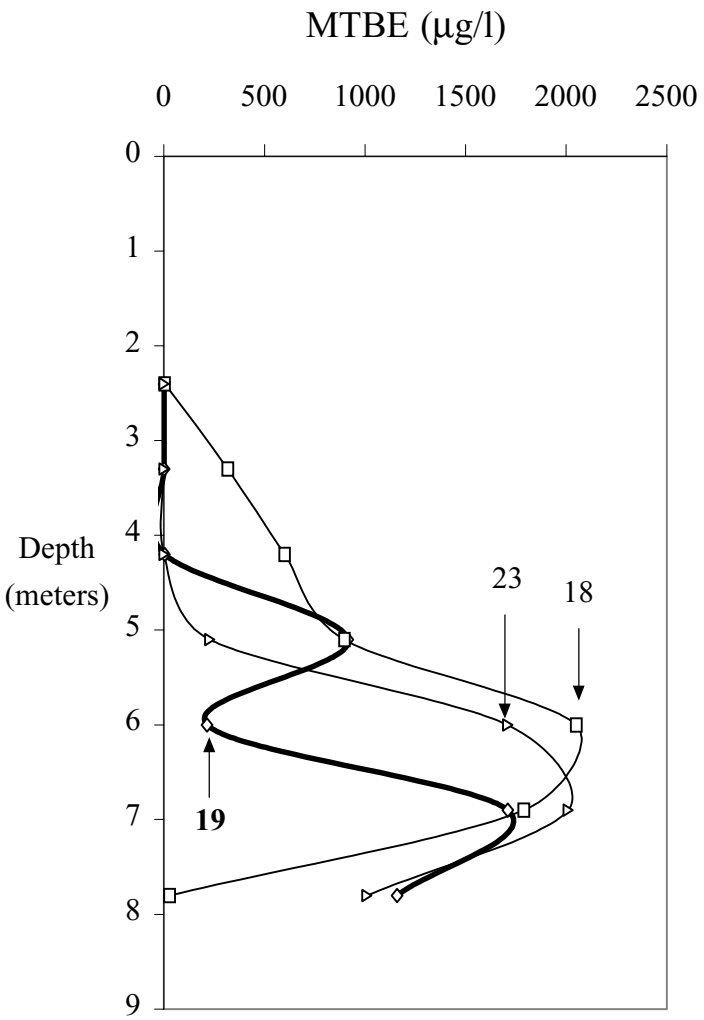

Figure 4.8 Depth distribution of MTBE in three locations downgradient of the LNAPL source area. See Figure 4.5 for position of the locations on a map. Compare location 19 to location 19 in Figure 4.9.

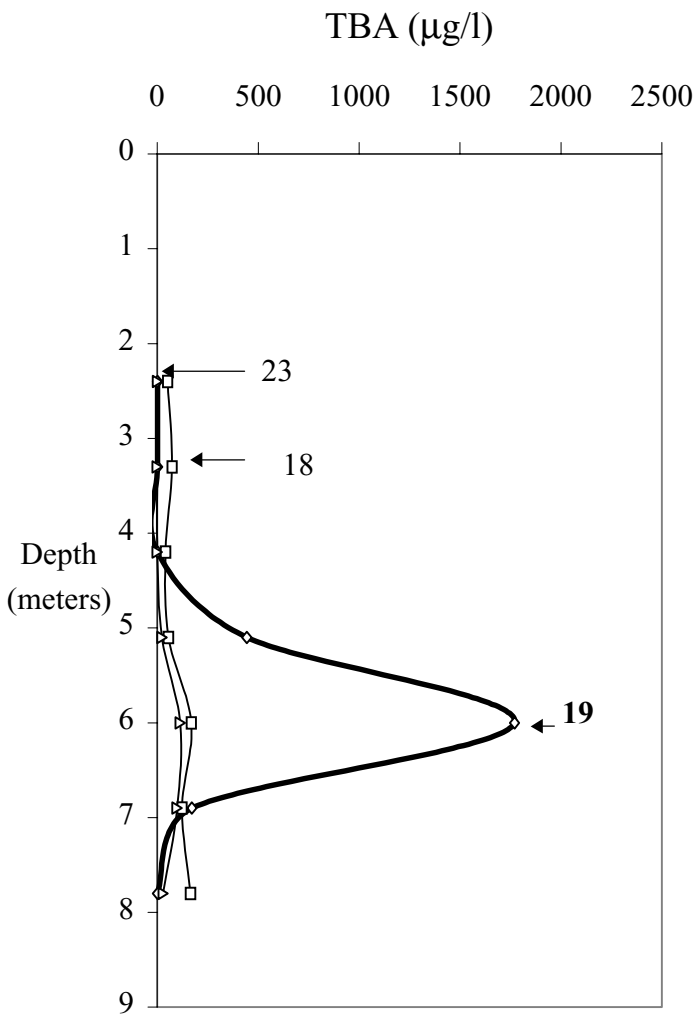

Figure 4.9 Depth distribution of TBA in locations downgradient of the source area. See Figure 4.5 for position of the locations on a map. Compare location 19 to location 19 in Figure 4.8.

SECTION 5
Summary and Conclusions

Extent of Biodegradation of MTBE

Removal of MTBE in microcosms that were supplemented with alkylbenzenes was extensive. There was no evidence of MTBE removal over removal in the controls in the first 175 days of incubation. After 385 days of incubation, there is strong evidence of removal in the living treatment. After 490 days of incubation, there was very extensive removal of MTBE compared to the controls. The average concentration remaining in six replicates of the living treatment was 81 µg/l, compared to 5680 µg/l at the beginning of incubation. The average concentration remaining in the control treatment after 490 days was 1470 µg/l, compared to 3330 µg/l at the beginning of incubation. The removal in the controls was a little more than twofold, while removal in the living microcosms was 70-fold.

Removal of MTBE in microcosms that were not supplemented with alkybenzenes was also extensive. There was little evidence of removal in the first 175 days of incubation. After 385 days, the removal of MTBE in the living microcosms was extensive. After 490 days of incubation, the concentration of MTBE in all six of the replicate microcosms that were sampled was below 40 µg/l, compared to 3110 µg/l at the beginning of incubation.

Role of BTEX Compounds

Removal of MTBE in the microcosms did not require the presence of BTEX compounds. Toluene was entirely depleted within 40 to 47 days, benzene was entirely depleted within 110 days, and ethylbenzene was entirely depleted within 175 days. During this time period there was no evidence of removal of MTBE. The removal of MTBE did not begin until the removal of the BTEX compounds was complete.

Rate of Removal of MTBE

The first order rate of removal of MTBE in microcosms supplemented with alkylbenzenes was 3.02 per year ±0.52 per year at 95% confidence. Removal in the corresponding controls was 0.39 per year ±0.19 per year at 95% confidence. The removal in the microcosms without added alkylbenzenes was 3.5 per year ±0.65 per year at 95% confidence. Removal in the corresponding controls was 0.30 per year ±0.14 per year at 95% confidence.

The apparent first order rate of removal of MTBE in the field was a sensitive function of ground-water seepage velocity. The rate of removal was calculated for an upper boundary on velocity, an average velocity, and a lower boundary on velocity. The rate was 5.0 per year at the upper boundary, 2.7 per year at the average velocity, and 2.2 per year at the lower boundary. Methane was considered to be a conservative tracer of ground-water flow at the site. The apparent rate of removal of methane was taken as an estimate of attenuation along the flow path due to dilution and dispersion. The apparent first order rate of removal of methane at the average estimate of seepage velocity was 0.50 ±0.65 per year.

The rate of removal of MTBE in the laboratory studies can explain the apparent attenuation of MTBE at field scale.

Expected Persistence of the Source of Ground-water Contamination

The mass transfer of MTBE from the source LNAPL to the ground water moving underneath was estimated by calculating the flux of MTBE moving away from the source, then comparing that flux to the total mass of MTBE in the source area. The flux of MTBE away from the source area in 1996 was 2.76 kg/year. The lower boundary on the total quantity of MTBE in the source area was 46 kg. If this flux did not change over time, it would take seventeen years to remove the MTBE from the source. If the rate of transfer of MTBE to ground water is proportional to the amount of MTBE in the source, the instantaneous rate of transfer is 0.06 per year. The average concentration at the most contaminated location in the transect is 1200 µg/l. At this rate of attenuation of the source, it would require approximately sixty years for the concentration to reach 30 µg/l.

Production and Depletion of TBA

Tertiary Butyl Alcohol (TBA) has been documented as a transformation product of MTBE in a number of studies. At the Old Fuel Farm Site, there is no evidence of accumulation of TBA in the ground-water plume as a whole. With two exceptions, the concentration of TBA in ground water downgradient of the source area was less than 200 µg/l. Ground water from a location immediately downgradient of the source area had a higher concentration of TBA, near 2000 µg/l. In this sample there was a corresponding reduction in the concentration of MTBE. At this location the TBA was probably produced from transformation of MTBE.

Geochemical Context of the Plume that Biodegraded MTBE

The entire MTBE plume is contained within a plume of methane. Methane concentrations generally exceed 3.0 mg/l, and often exceed 10 mg/l . Concentrations of methane average 7 mg/l, which corresponds to 9 mg/l of hydrocarbon originally metabolized.

Ground water in the region of the aquifer that contains MTBE and BTEX compounds is also depleted of sulfate. Sulfate concentrations are reduced from a background of near 28 mg/l to less than 4 mg/l; many regions have less than 1 mg/l. A depletion of 24 mg/l of sulfate would oxidize 5 mg/l of fuel hydrocarbons. The same regions that are depleted in molecular oxygen and sulfate have significant accumulations of iron (II) . Background concentrations of iron (II) are less than 0.1 mg/l. Many regions of the aquifer with MTBE and BTEX compounds have iron (II) concentrations greater than 50 mg/l. This accumulation of iron (II) would be capable of oxidizing 3 mg/l of hydrocarbons.

The plume is also undergoing extensive anaerobic oxidation of petroleum hydrocarbons, as well as fermentation of hydrocarbons to methane. The hydrocarbon metabolism through sulfate and iron oxidation is approximately equivalent to the hydrocarbon metabolism through methanogenesis. The amount of hydrocarbon metabolized through anaerobic pathways is about ten times the amount degraded with molecular oxygen.

References

Chapelle, F.H., 1999, Bioremediation of petroleum hyrocarbon-contaminated ground water: the perspectives of history and hydrology, Ground Water 37(1):122-132.

Church, C.D., Isabelle, L.M., Pankow, J.M., Rose, D.L., and Tratnyek, P.G., 1997, Method for determination of methyl *tert*-butyl ether and its degradation products in water, Environ. Sci. Technol. 31(12):3723-3726.

Landmeyer, J.E., Chapelle, F.H., Bradley, P.M.., Pankow, J.F., Church, C.D., and Tratnyek, P.G., 1998, Fate of MTBE relative to benzene in a gasoline-contaminated aquifer (1993-98), Ground Water Monitoring and Remediation, Fall, 1998, pp. 93-102.

Mormile, M.R., Liu, S, and Suflita, J.M., 1994, Anaerobic biodegradation of gasoline oxygenates:extrapolation of information to multiple sites and redox conditions, Environ. Sci. Technol. 28(9):1727-1732.

Squillace, P.J., Zogorski,J.S., Wilber,W.G., and Price, C.V., 1996, Preliminary assessment of the occurrence and possible sources of MTBE in ground water in the United States, 1993-1994, Environ. Sci. Technol. 30:1721-1730.

Suflita, J.M., and Mormile, M.R., 1993, Anaerobic biodegradation of known and potential gasoline oxygenates in the terrestrial subsurface, Environ. Sci. Technol. 27(5):976-978.

U.S. Environmental Protection Agency. 1996. Drinking Water Regulations and Health Advisories. Washington, D.C.

Wiedemeier, T.H., Rifai, H.S., Newell, C.J., and Wilson, J.T., 1999, Natural Attenuation of Fuels and Chlorinated Solvents in the Subsurface, John Wiley & Sons, New York, ISBN 0-471-19749-1.

Wilson, J.T., Cho,J.S., Beck, F.P., and Vardy,J.A., 1997, Field Estimation of Hydraulic Conductivity for Assessments of Natural Attenuation. In Proceedings of the Fourth International In-Situ and On-site Bioremediation Symposium, New Orleans, LA, pp. 309-314.

Yeh, C.K., and Novak, J.T., 1994, Anaerobic biodegradation of gasoline oxygenates in soils, Water Environ. Res., 66(5):744-752.

Appendix A. Temporal Variation in the Hydraulic Gradient and the Direction of Ground-water Flow

Ground-water flow at the site is strongly influenced by the elevation of the Pasquotank River. At Elizabeth City, North Carolina, the Pasquotank River makes a transition from a conventional river to a large estuary. At Elizabeth City, the Pasquotank River is a few hundred feet wide. At the U.S. Coast Guard Air Station, only a few miles farther down river, the Pasquotank is more than two miles wide. The average elevation of the Pasquotank River at the fuel farm site is near sea level. The elevation of the river is not controlled by recent precipitation and runoff, as is usually expected for a river. The strongest influence on the elevation of the river is the recent direction of the wind, producing a phenomenon known as a wind seiche. The trend of the valley is from northwest to southeast. Friction from strong winds coming from the north will drive water out of the river valley, and lower the elevation of the river. Winds from the south drive water into the valley, and raise the water table.

This effect is illustrated in the data in Figure A.1. A pressure transducer was used to record the elevation of the Pasquotank River every fifteen minutes over a time interval extending from September 5, 1996 to October 30, 1996. To minimize the confounding effects of wave action on the measurement of water table elevation, the transducer was located in a drainage ditch in close communication with the river. Over this two-month interval, the elevation of the Pasquotank River varied from 1.5 feet above sea level to 1.5 feet below sea level. The most rapid changes in elevation were drops in elevation on the order of 1.5 feet within one or two days that were associated with cold fronts that came through in the first week of September, and the first week of October. There was also a diurnal cycle that varied from 0.1 to 0.5 feet.

These changes in elevation of the receptor of the ground-water plume are large, compared to the change in elevation of ground water across the fuel farm site. As an illustration, examine Figure A.2 and identify Well ESM-14 located in the center of the study area. The average elevation of ground water in Well ESM-14 over 27 rounds of quarterly or monthly sampling was 1.25 feet above sea level. As a consequence of the temporal variation in the elevation of the Pasquotank River, the hydraulic gradient and the ground-water flow velocity across the site vary widely from one sampling event to another.

Figure A.3 plots the elevation of the water table against time for four representative monitoring wells extending across the site (see Figure A.2 for the location of the wells). Over the period from March 1994 to December 1998, the elevation of the water table in individual wells changed from 1.5 to 2.0 feet. The elevation of the water table in all the wells tended to track each other over time. In some time intervals the elevations of ground water in all the wells are nearly the same. At other intervals, the hydraulic gradient is more strongly expressed. There is no obvious correlation of the hydraulic gradient to seasons of the year, or to the average elevation of ground water across the site.

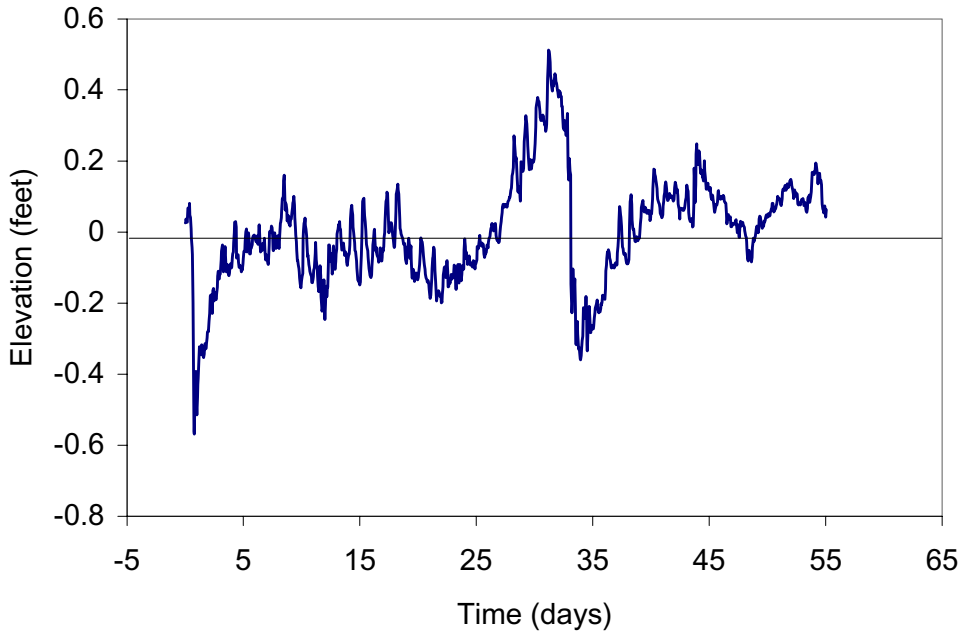

Figure A.1 Variation in elevation of water in the Pasquotank River over a time interval extending from September 5, 1996 to October 30, 1996.

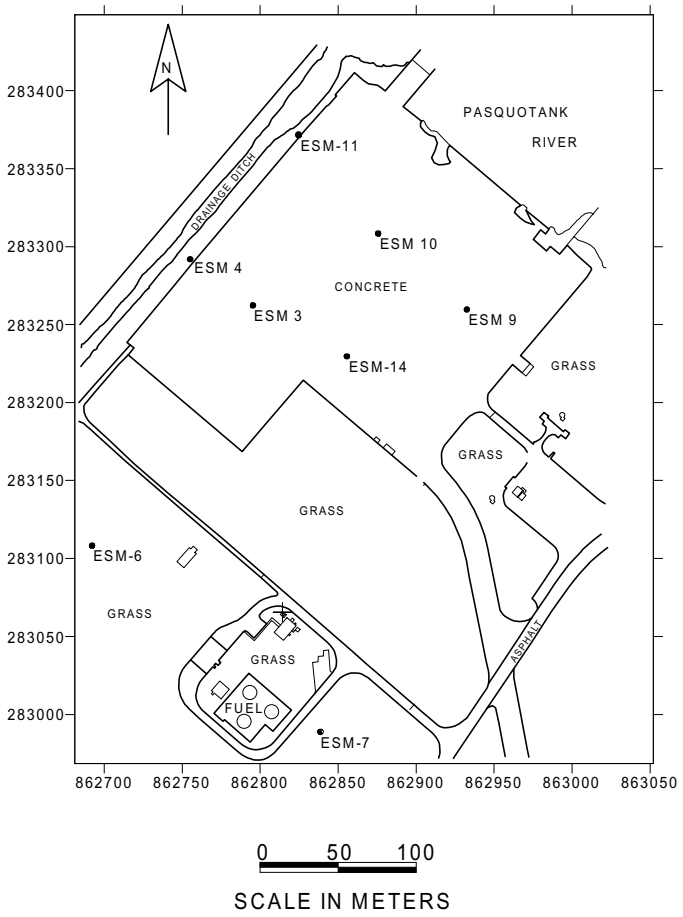

Figure A.2 Location of the permanent monitoring wells used to estimate the hydraulic gradient and direction during each round of monitoring.

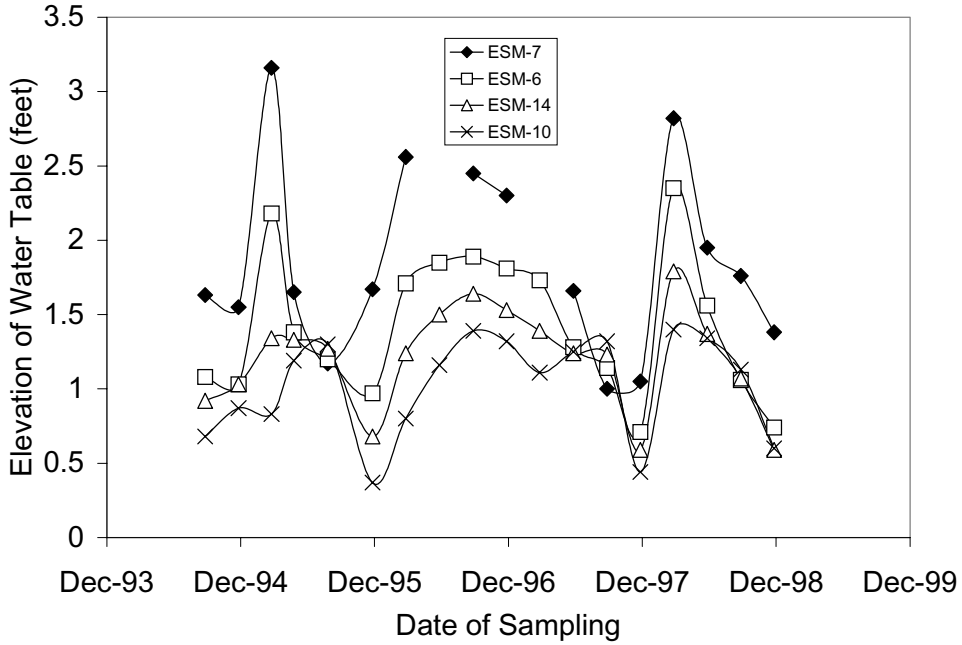

Figure A.3 Variation in elevation of the water table at the fuel farm site over time. Consult Figure A.1 for the location of the monitoring wells. Well ESM-10 is closest to the Pasquotank River, the point of ground-water discharge. Wells ESM-14, ESM-6, and ESM-7 are farther inland.

Water table elevations were available from eighteen rounds of quarterly monitoring and for fourteen rounds of monthly monitoring. The elevations of ground water in wells depicted in Figure A.2 are presented in Table A.1 for eighteen rounds of sequential quarterly sampling, and Table A.2 for fourteen rounds of sequential monthly sampling. There are four sampling dates common to the quarterly monitoring data and the monthly monitoring data. Rather than take one or a few rounds of sampling and use professional judgment to construct ground-water elevation contours that would be representative of the site, a simple statistical approach was used to give equal weight to each round of sampling.

The aquifer containing the plume of contamination is semi-confined across the entire site. The superficial layer of silty clay, and the concrete operational apron prevent recharge of precipitation in the study area. Recharge occurs far inland from the Pasquotank River. The superficial confining layer extends out into the bed of the river. Discharge occurs some distance into the river, not at its bank. As a result, ground-water flow at the site is controlled by regional flow in the aquifer. As an approximation, the ground-water elevation at any round of sampling will be considered to be a linear plane in three-dimensional space. The slope of the plane is the hydraulic gradient and flow direction of ground water.

Table A.3 provides a summary of the regression on the eighteen rounds of quarterly monitoring. The table provides the equation of the regression, the number of wells involved in the regression at each date, the coefficient of correlation r^2, the variance of the estimate of elevations, and the fitted hydraulic gradient and direction for each round of sampling. The seepage velocity of the ground water was calculated from Darcy's Law using an average estimate of hydraulic conductivity of 0.27 cm/sec and an assumed effective porosity of 0.3. In general, the assumption that the water table was a plane was reasonable. The coefficient of correlation exceeded 0.8 for fifteen of the eighteen rounds of sampling. Table A.4 provides the summary of the regression of the fourteen rounds of monthly monitoring. The coefficient of correlation exceeded 0.8 for nine of the fourteen rounds of sampling.

The results of the individual regressions are presented in graphical form in Figures 4.1 and 4.2.

The average direction of ground-water flow was calculated by weighting the direction of flow on any particular round of sampling by the hydraulic gradient at that particular round, then taking an average of the weighted flow directions. For the eighteen rounds of quarterly sampling, the average flow direction was 8.6 degrees west of north, with a standard deviation of 9.1 degrees. The mean of the hydraulic gradient was 0.00252 with a 95% confidence interval of 0.0010. For the fourteen rounds of monthly sampling, the average flow direction was 8.7 degrees west of north, with a standard deviation of 23 degrees. The mean of the hydraulic gradient was 0.00252 with a 95% confidence interval of 0.00070. The results of the regressions for each of the eighteen rounds of quarterly monitoring are presented in Figures A.4 through A.18. The measured elevations submitted to the regressions are listed in the figures to allow a well-by-well evaluation of the fit of the regression.

Table A.1 Elevation of the water table in permanent monitoring wells during eighteen rounds of quarterly monitoring extending from September 1994 through December 1998. The elevations are reported in feet above mean sea level. Compare Figure A.1 for the location of the monitoring wells.

Well	9/94	12/94	3/95	5/95	8/95	12/95	3/96	6/96	9/96	12/96	3/97	6/97	9//97	12/97	3/98	6/98	9/98	12/98
ESM-3	0.74	0.86	1.08	1.23	1.35	0.49	0.97	1.32	1.5	1.4	1.16	1.31	1.29	0.5	1.56	1.27	1.03	0.58
ESM-4	0.44	0.89	0.89	1.11	1.36	0.17	0.65	1.05	1.45	1.18	0.84	1.53	1.37	0.29	1.18	1.19	1.21	0.83
ESM-6	1.08	1.03	2.18	1.38	1.2	0.97	1.71	1.85	1.89	1.81	1.73	1.28	1.14	0.71	2.35	1.56	1.06	0.74
ESM-7	1.63	1.55	3.16	1.65	1.17	1.67	2.56		2.45	2.3		1.66	1	1.05	2.82	1.95	1.76	1.38
ESM-9	0.73	0.92	0.95	1.23	1.33	0.42	0.89	1.25	1.45	1.34	1.09	1.23	1.31	0.52	1.47	1.25	1.08	0.67
ESM-10	0.68	0.87	0.83	1.19	1.3	0.37	0.8	1.16	1.39	1.32	1.11	1.25	1.32	0.44	1.4	1.34	1.13	0.6
ESM-11	0.4	0.9	0.8	1.09	1.38	0.09	0.61	1.02	1.45	1.13	0.78	1.34	1.34	0.26	1.06	1.15	1.17	0.59
ESM-14	0.92	1.03	1.34	1.33	1.27	0.68	1.24	1.5	1.64	1.53	1.39	1.24	1.23	0.59	1.79	1.37	1.07	0.59

Table A.2. Elevation of the water table in permanent monitoring wells during fourteen rounds of monthly monitoring extending from September 1994 through December 1998. The elevations are reported in feet above mean sea level. Compare Figure A.1 for the location of the monitoring wells.

Well	2/11/98	3/10/98	4/7/98	5/13/98	6/16/98	7/9/98	8/6/98	9/2/98	10/1/98	11/14/98	12/7/98	1/6/99	2/1/99	3/5/99
ESM-3	2.34	2.22	1.53	1.06	1.41	1.16	0.52	1.36	1.03	0.85	0.58		0.94	1.05
ESM-4	2.15	1.98	1.29	0.45	1.43	1.4	0.32	1.37	1.21	1.07	0.83	0.78	0.69	0.73
ESM-6	3.14	2.75	1.98	1.59	1.49	1.17	0.82	1.78	1.06	0.88	0.74	1.15	1.42	1.36
ESM-7	3.6	3.13	1.54	2.16		1.73	1.38	2.26	1.76	1.63	1.38	1.62	1.79	1.64
ESM-9	2.17	2.11	1.37	0.91	1.39	1.06	0.47	1.46	1.08	0.91	0.67	0.86	0.66	0.94A
ESM-10	2.12	2.09	1.32	0.85	1.4	0.95	0.47	1.33	1.13	0.99	0.6	0.77	0.68	0.9
ESM-11	2.1	1.94	2.07	0.35	1.44	0.91	0.29	1.36	1.17	1.02	0.59	0.79	0.62	0.69
ESM-14	2.5	2.37	1.61	1.21	1.45	1.19	0.65	1.39	1.07	0.9	0.59		0.98	1.06

Table A.3 Equation of a linear plane that was fit using a least-squares regression through the elevation of the water table in permanent monitoring wells during each of eighteen rounds of quarterly sampling. The plane is in an x,y,z coordinate system where x increases toward the east, y increases toward the north, and z increases with elevation above mean sea level. The equation is in the form Ax+By+C+z where x and y are the grid location in UTM meters and z is the elevation of the water table in feet.

Date	n number of wells	A x coefficient	B y coefficient	C constant	r^2	z Variance	Hydraulic Gradient	Direction (degrees east from north)	Velocity meters /year	Velocity feet/year
Sept. 1994	8	1.03334E-03	-3.25785E-03	31.950	0.96785	0.00700	0.0034	-18	97	318
Dec. 1994	8	7.04719E-04	-1.76193E-03	-108.013	0.83375	0.01227	0.0019	-22	54	177
Mar. 1995	8	-3.91751E-04	-6.66909E-03	2228.290	0.95519	0.04445	0.0067	3	190	622
May 1995	8	4.80194E-04	-1.49026E-03	9.037	0.96893	0.00141	0.0016	-18	44	146
Aug. 1995	8	-1.66687E-05	5.84579E-04	-149.892	0.86551	0.00110	0.0006	-2	17	54
Dec. 1995	8	8.39634E-04	-4.21060E-03	468.710	0.97192	0.01028	0.0043	-11	122	400
Mar 1996	8	5.81895E-04	-5.39052E-03	1025.850	0.96560	0.02110	0.0054	-6	154	505
June 1996	7	1.50708E-04	-3.49088E-03	860.107	0.91667	0.01053	0.0035	-2	99	325
Sept. 1996	8	1.07050E-04	-2.82168E-03	708.465	0.90858	0.01660	0.0028	-2	80	263
Dec. 1996	8	4.21094E-04	-3.16140E-03	533.568	0.97066	0.00613	0.0032	-8	91	297
Mar. 1997	7	5.70420E-04	-4.02255E-03	648.421	0.89316	0.01688	0.0041	-8	115	378
June 1997	8	-2.55409E-04	-6.23482E-04	398.315	0.27942	0.02470	0.0007	22	19	63
Sept. 1997	8	-9.29013E-05	9.90993E-04	-199.269	0.93309	0.00144	0.0010	-5	28	93
Dec 1997	8	7.32342E-04	-2.09248E-03	-38.689	0.97696	0.00205	0.0022	-19	63	206
Mar. 1998	8	1.01025E-04	-4.85332E-03	1289.130	0.96975	0.01529	0.0049	-1	138	452
June 1998	8	3.93228E-04	-2.09999E-03	256.873	0.92957	0.00672	0.0021	-11	61	199
Sept. 1998	8	7.92146E-04	-1.41290E-03	-282.118	0.50305	0.03959	0.0016	-29	46	151
Dec. 1998	8	4.00185E-04	-1.85079E-03	179.655	0.66928	0.03389	0.0019	-12	54	176

Table A.4 Equation of a linear plane that was fit using a least-squares regression through the elevation of the water table in permanent monitoring wells during each of fourteen rounds of monthly sampling. The plane is in an x,y,z coordinate system where x increases toward the east, y increases toward the north, and z increases with elevation above mean sea level. The equation is in the form Ax+By+C+z where x and y are the grid location in UTM meters and z is the elevation of the water table in feet.

Date	n number of wells	A x coefficient	B y coefficient	C constant	r^2	z Variance	Hydraulic Gradient	Direction (degrees east from north)	Velocity meters /year	Velocity feet/year
11-Feb-98	8	-8.05822E-04	-4.33641E-03	1925.990	0.96171	0.01669	0.00441	11	125	411
10-Mar-98	8	-7.31494E-05	-3.33136E-03	1008.970	0.96560	0.00833	0.00333	1	95	310
7-Apr-98	8	-1.75445E-03	9.29881E-05	1489.030	0.19250	0.09695	0.00176	-87	50	164
13-May-98	8	9.33425E-04	-4.79741E-03	554.451	0.94123	0.02886	0.00489	-11	139	455
16-Jun-98	7	-2.64965E-04	-1.24188E-04	265.225	0.65632	0.00006	0.00029	65	8	27
9-Jul-98	8	-1.28825E-04	-1.67917E-03	587.936	0.61699	0.03750	0.00168	4	48	157
6-Aug-98	8	7.07976E-04	-2.89156E-03	208.726	0.95649	0.00759	0.00298	-14	84	277
2-Sep-98	8	2.28660E-04	-2.54803E-03	525.917	0.89449	0.01567	0.00256	-5	73	238
1-Oct-98	8	7.92146E-04	-1.41290E-03	-282.118	0.50305	0.03959	0.00162	-29	46	151
14-Nov-98	8	8.51723E-04	-1.43532E-03	-327.332	0.46232	0.04834	0.00167	-31	47	155
7-Dec-98	8	4.00185E-04	-1.85079E-03	179.655	0.89316	0.03389	0.00189	-12	54	176
6-Jan-99	6	3.50042E-04	-2.31329E-03	354.144	0.93028	0.01330	0.00234	-9	66	218
1-Feb-99	8	-7.16128E-04	-3.26365E-03	1543.220	0.95728	0.01074	0.00334	12	95	311
5-Mar-99	8	2.01839E-04	-2.56719E-03	553.994	0.95110	0.00695	0.00258	-4	73	240

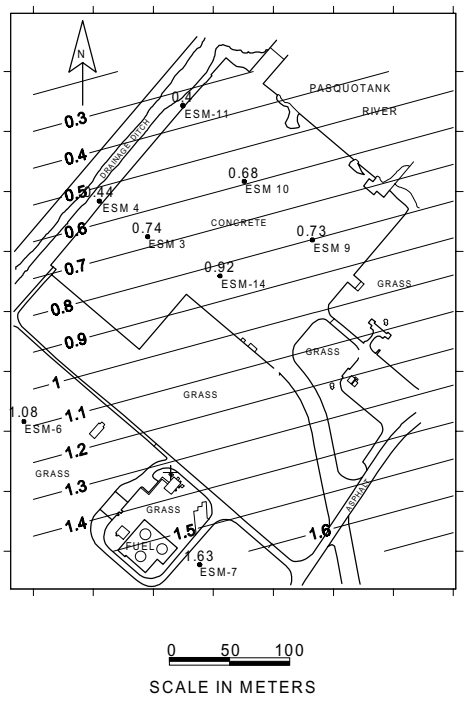

Figure A.4 Direction and gradient of ground-water flow on a sample date in September 1994.

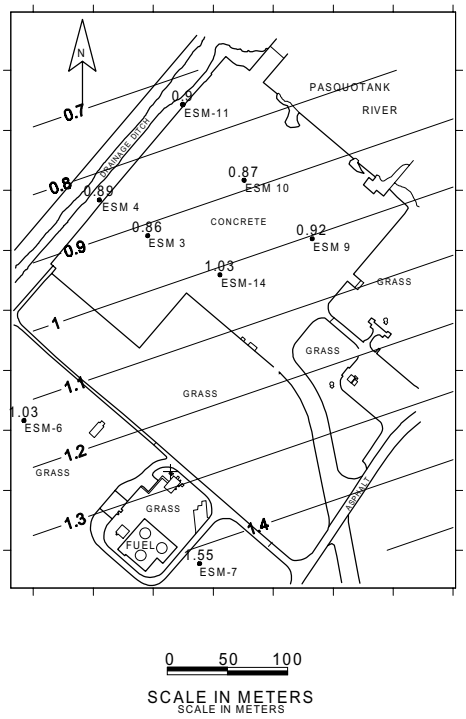

Figure A.5 Direction and gradient of ground-water flow on a sample date in December 1994.

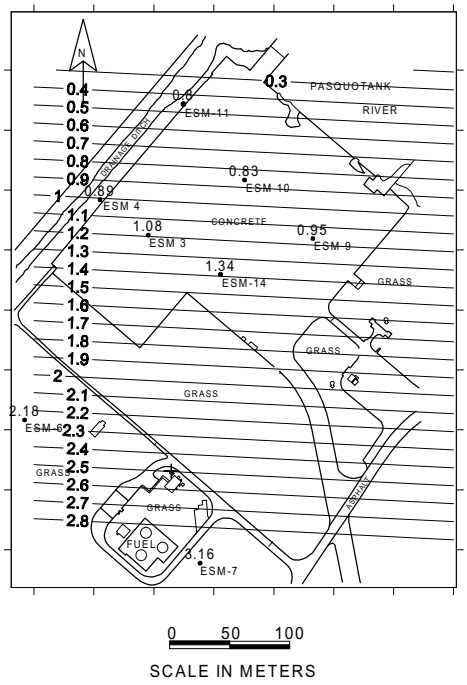

Figure A.6 Direction and gradient of ground-water flow on a sample date in March 1995.

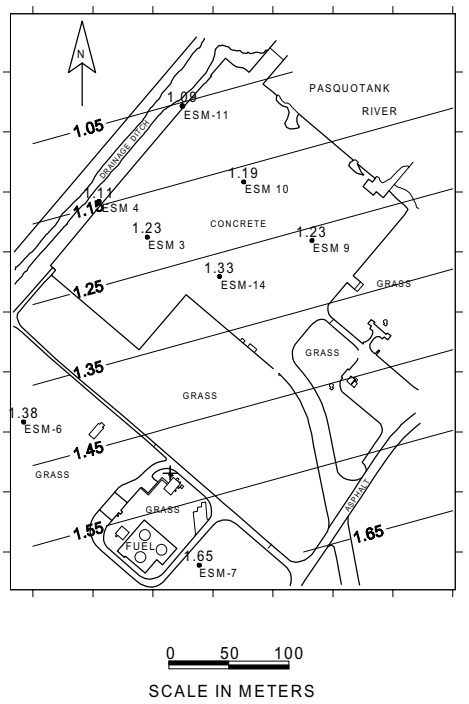

Figure A.7 Direction and gradient of ground-water flow on a sample date in May 1995.

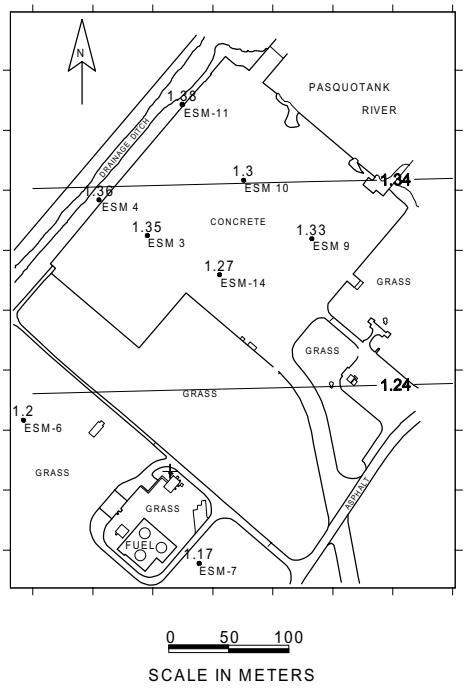

Figure A.8 Direction and gradient of ground-water flow on a sample date in August 1995.

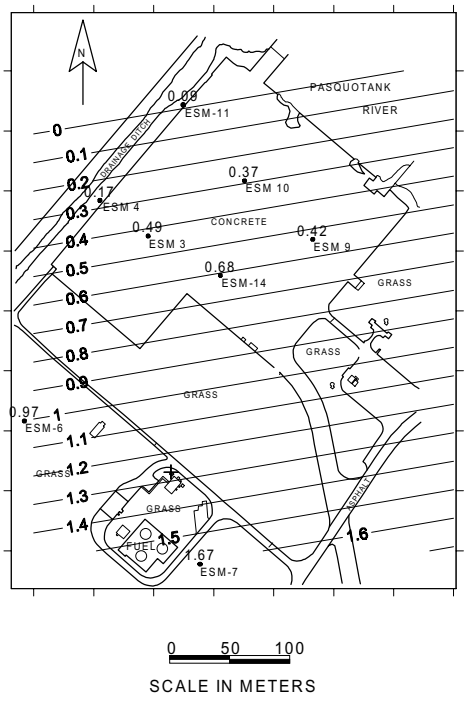

Figure A.9 Direction and gradient of ground-water flow on a sample date in December 1995.

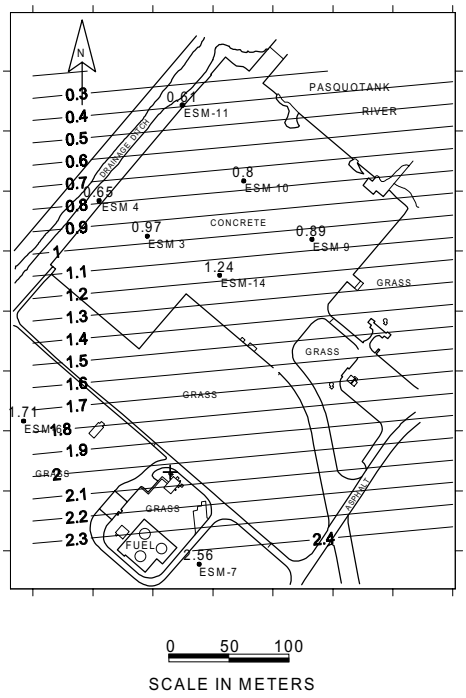

Figure A.10 Direction and gradient of ground-water flow on a sample date in March 1996.

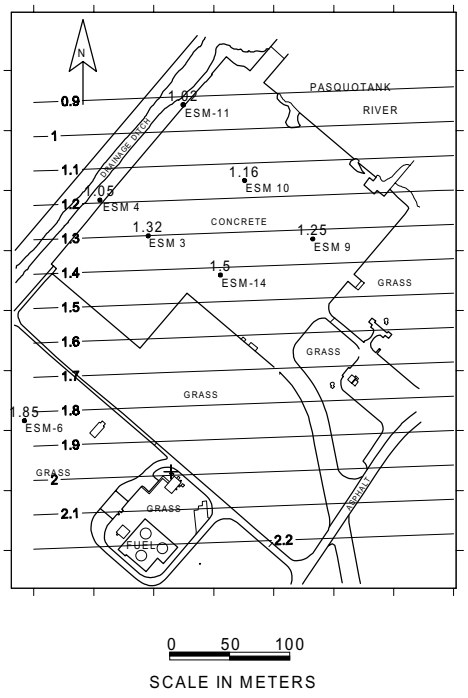

Figure A.11 Direction and gradient of ground-water flow on a sample date in June 1996.

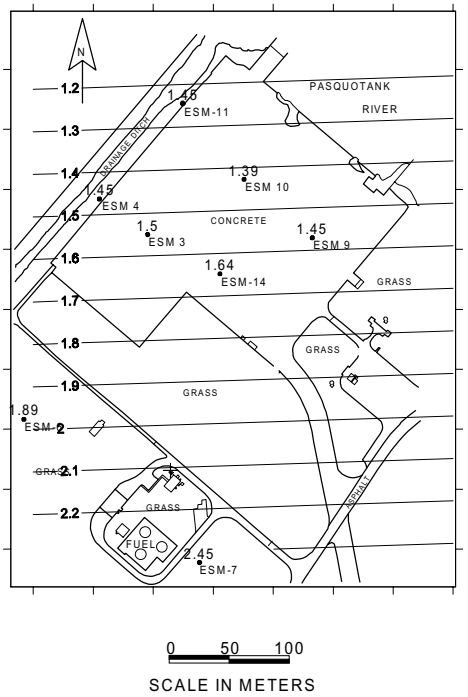

Figure A.12 Direction and gradient of ground-water flow on a sample date in September 1996.

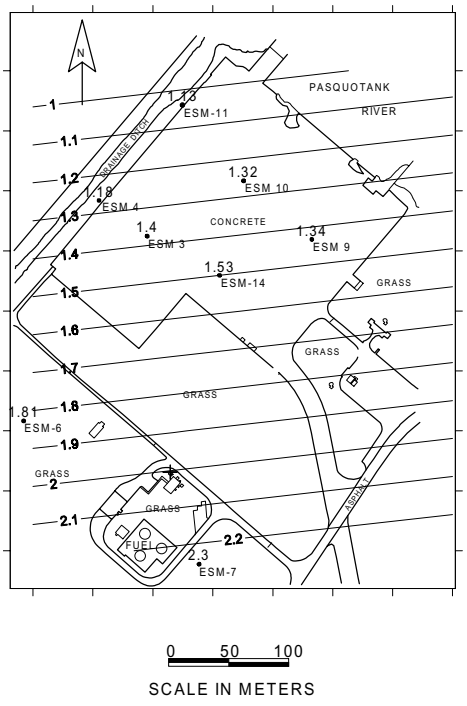

Figure A.13 Direction and gradient of ground-water flow on a sample date in December 1996.

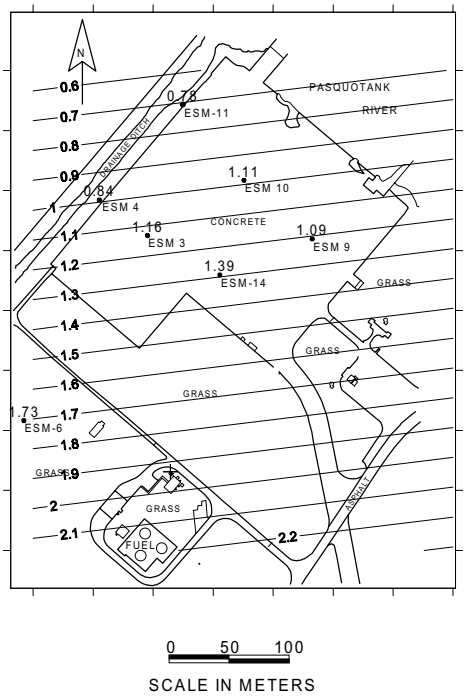

Figure A.14 Direction and gradient of ground-water flow on a sample date in March 1997.

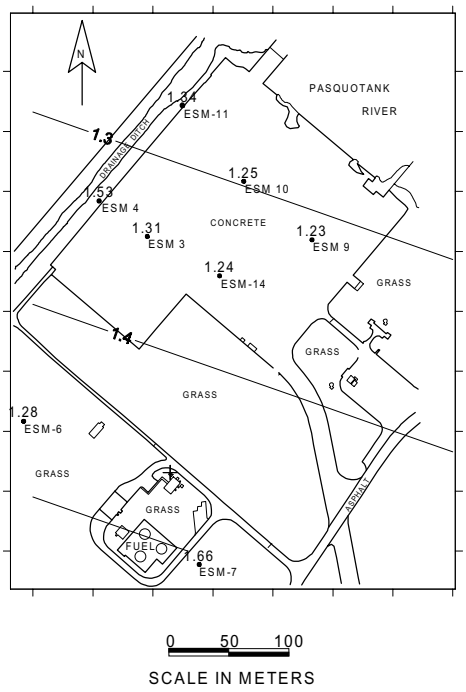

Figure A.15 Direction and gradient of ground-water flow on a sample date in June 1997.

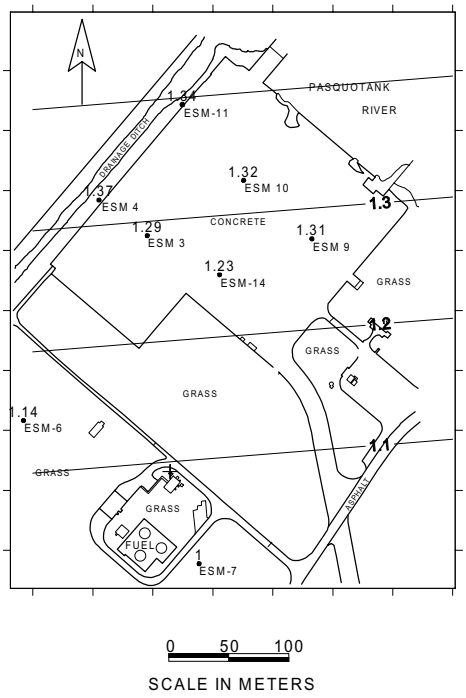

Figure A.16 Direction and gradient of ground-water flow on a sample date in September 1997.

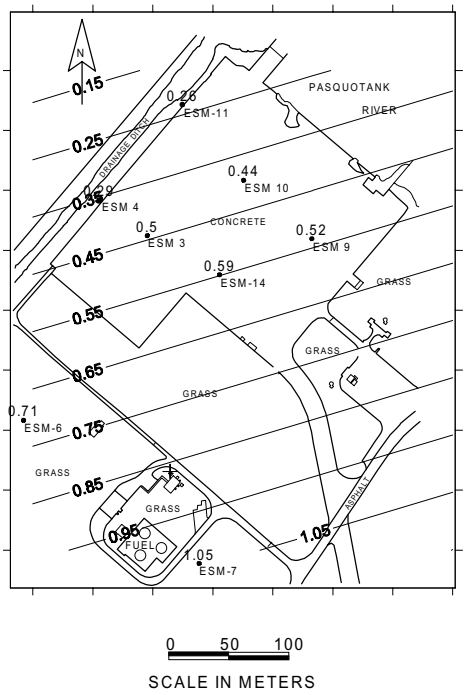

Figure A.17 Direction and gradient of ground-water flow on a sample date in December 1997.

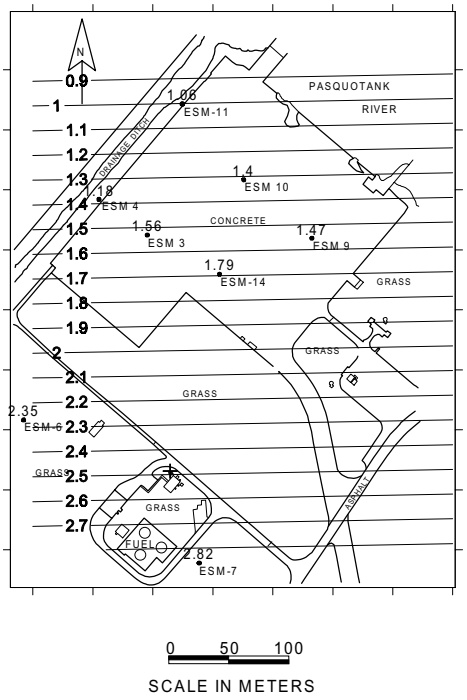

Figure A.18 Direction and gradient of ground-water flow on a sample date in March 1998.

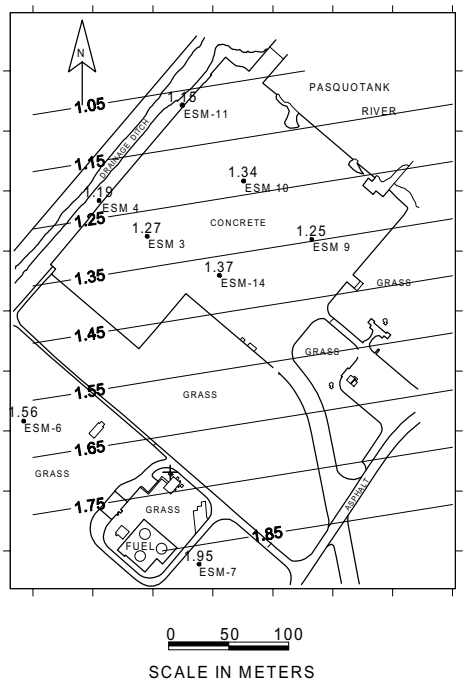

Figure A.19 Direction and gradient of ground-water flow on a sample date in June 1998.

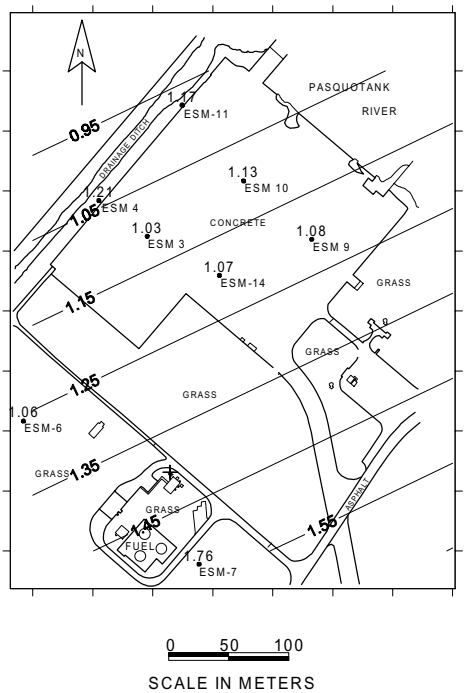

Figure A.20 Direction and gradient of ground-water flow on a sample date in September 1998.

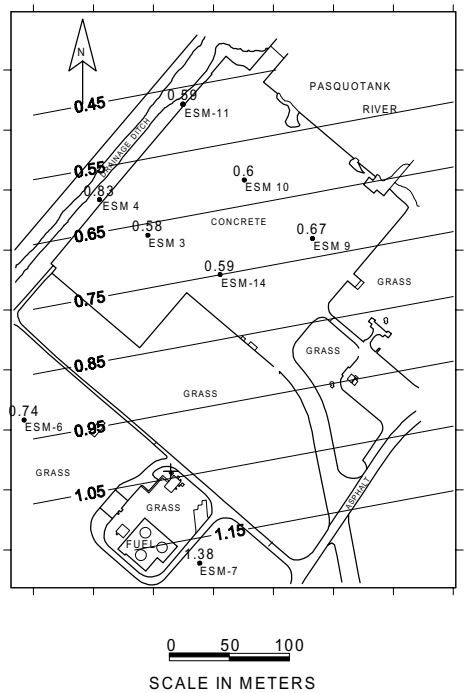

Figure A.21 Direction and gradient of ground-water flow on a sample date in December 1998.

Appendix B: Geochemical Context of the MTBE Plume

Figures B.1 and B.2 compare the distribution of methane and MTBE in the north-south transect (see Figure 3.7). Figures B.3 and B.4 compare the distribution of methane and MTBE in the east-west transect. The entire MTBE plume is contained within a plume of methane. Methane concentrations generally exceeded 3.0 mg/l, and often exceeded 10 mg/l. In general, the distribution of MTBE was contained within the distribution of methane. However, along the east-west transect, at the sampling locations 50, 100, and 150 feet along the transect, the highest concentrations of MTBE extended about three feet deeper into the aquifer than the higher concentrations of methane. In general, this aquifer is strongly methanogenic. Concentrations of methane averaged 7 mg/l, which corresponds to 9 mg/l of hydrocarbon originally metabolized. (Wiedemeier et al., 1999, table 5.3, page 214).

Figures B.5 through B.8 compare the other geochemical parameters in the ground water along the north-south transect. Figure B.5 shows that the MTBE plume is contained within a region of the aquifer that is depleted of molecular oxygen. Many regions of the aquifer have less than 0.1 mg/l oxygen. Background concentrations of oxygen in regions of the aquifer that are not impacted by the fuel spill are near 3.6 mg/l. The depletion in oxygen would account for 1 mg/l of petroleum hydrocarbon.

Ground water in the region of the aquifer that contains MTBE and BTEX compounds is also depleted of sulfate (Figure B.6). Sulfate concentrations are reduced from a background of near 28 mg/l to less than 4 mg/l. Many regions have less than 1 mg/l. A depletion of 24 mg/l of sulfate would oxidize 5 mg/l of fuel hydrocarbons.

The same regions that are depleted in molecular oxygen and sulfate have significant accumulations of iron (II) (Figure B.7). Background concentrations of iron (II) are less than 0.1 mg/l. Many regions of the aquifer with MTBE and BTEX compounds have iron (II) concentrations greater than 50 mg/l. This accumulation of iron (II) would be capable of oxidizing 3 mg/l of hydocarbons.

The plume is undergoing extensive anaerobic oxidation of petroleum hydrocarbons, as well as fermentation of hydrocarbons to methane. The hydrocarbon metabolized through sulfate and iron reduction is approximately equivalent to the hydrocarbon metabolized through methanogenesis. The amount of hydrocarbon metabolized through anaerobic pathways is about seventeen times the amount degraded with molecular oxygen.

The pH of the plume is generally near 6.5 and is below 6.0 only in the ground water that is in direct contact with the LNAPL. Under these conditions, carbon dioxide produced through oxidation of petroleum hydrocarbons will react with carbonate minerals in the aquifer matrix to produce bicarbonate alkalinity in the ground water. Figure B.8 shows that as much as 200 mg/l of alkalinity was produced by oxidation of petroleum hydrocarbons. This corresponds to 88 mg/l of carbon dioxide produced or 28 mg/l of TPH consumed. There is more than enough carbon dioxide production to account for the depletion of oxygen and sulfate, and production of iron (II) and methane.

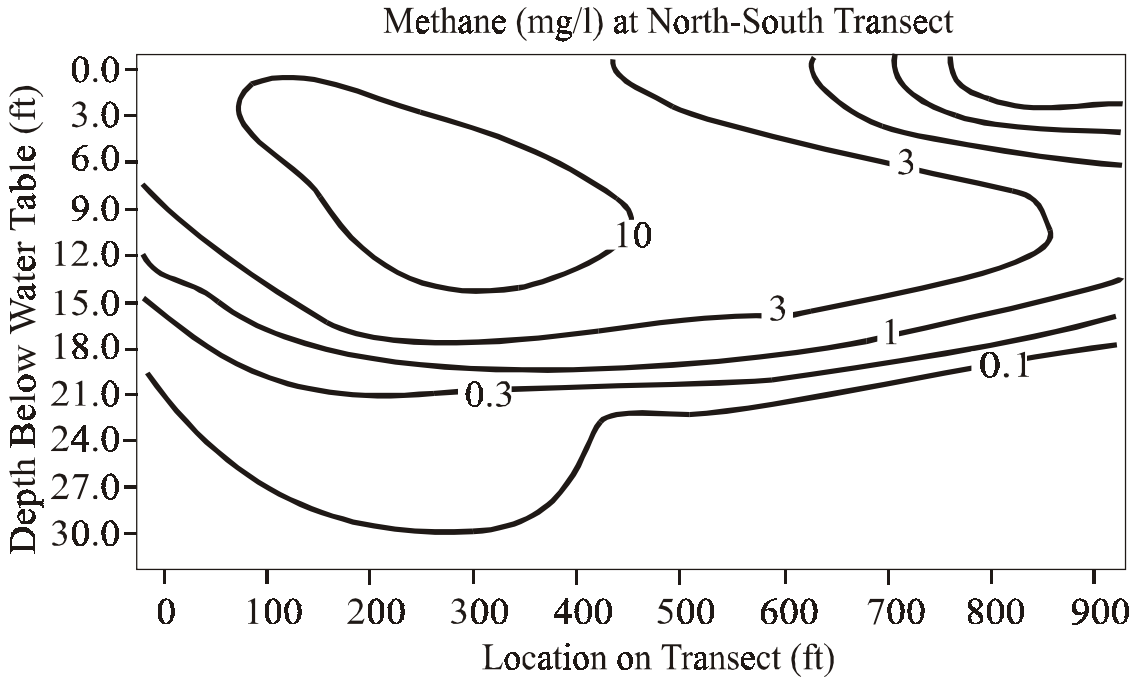

Figure B.1 Distribution of methane along the north-south transect, collected in August 1996. Distance along the transect extends from south to north (bottom to top in Figure 3.7), in the direction of ground-water flow.

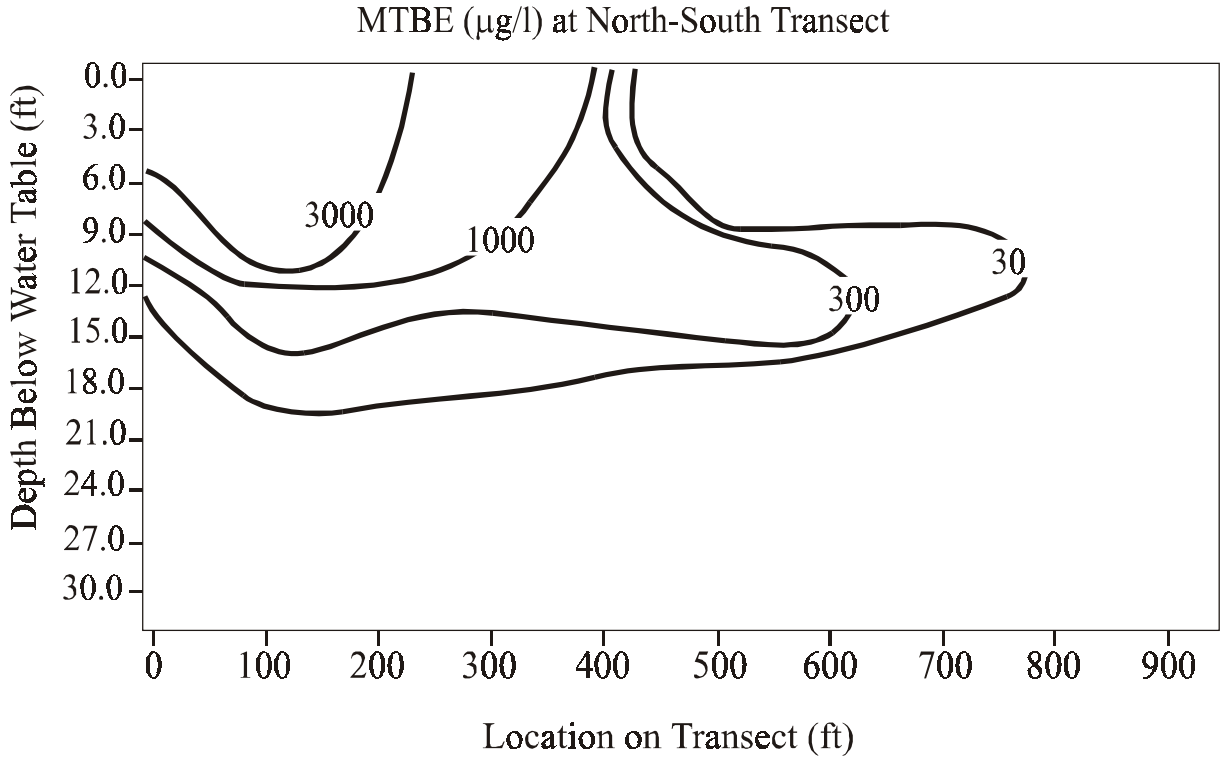

Figure B.2 Distribution of MTBE along the north-south transect, collected in August 1996. Distance along the transect extends from south to north (bottom to top in Figure 3.7), in the direction of ground-water flow.

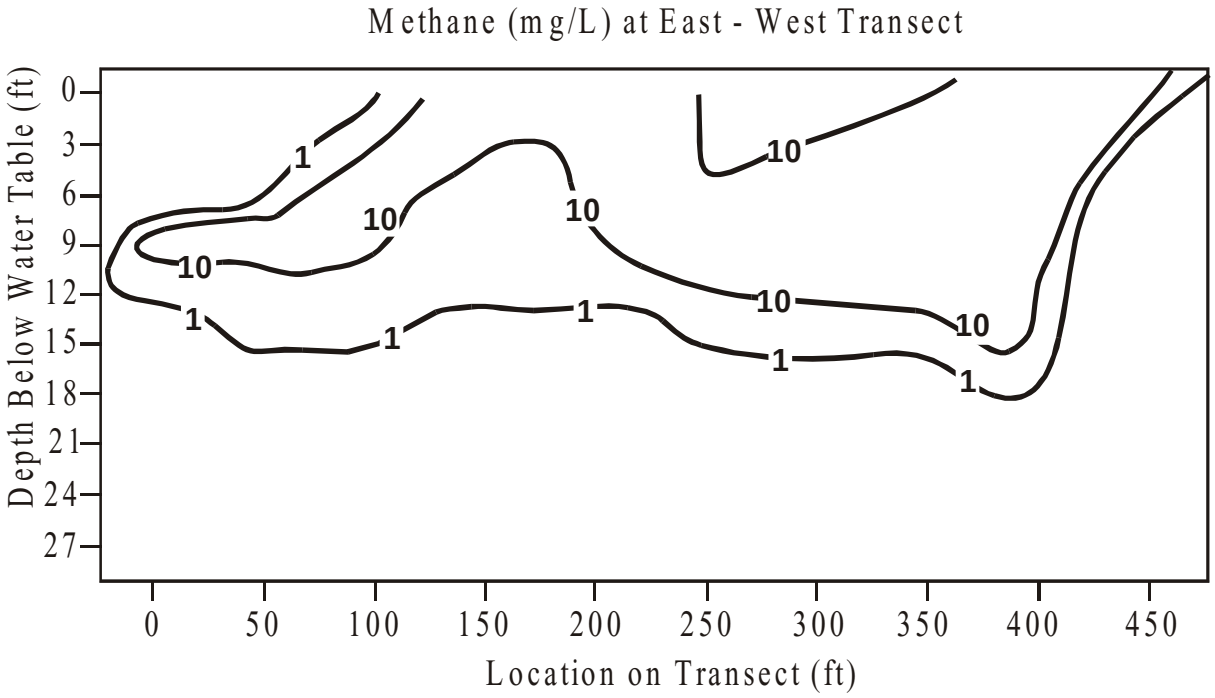

Figure B.3 Distribution of methane along the east-west transect, collected in December 1997. Distance along the transect extends from west to east (left to right in Figure 3.7), opposite the direction of ground-water flow.

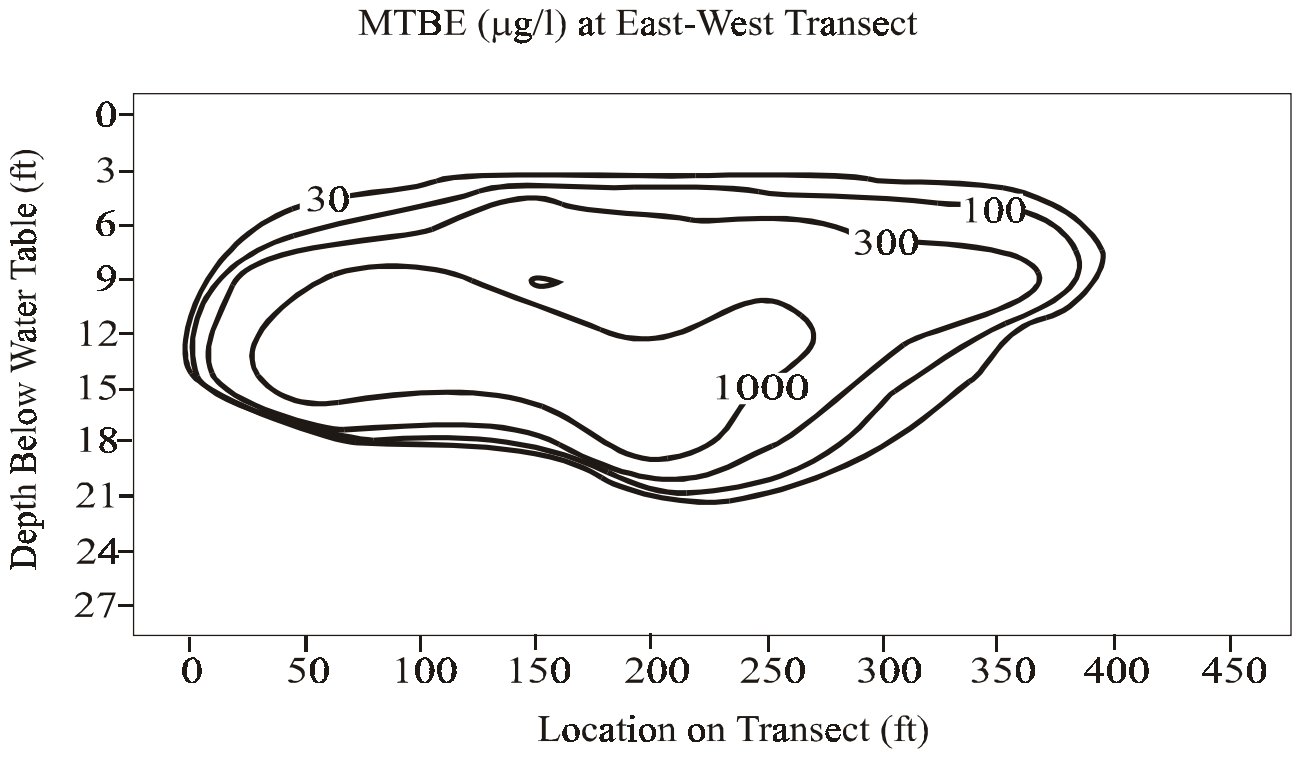

Figure B.4 Distribution of MTBE along the east-west transect, collected in December 1997. Distance along the transect extends from west to east (left to right in Figure 3.7), opposite the direction of ground-water flow.

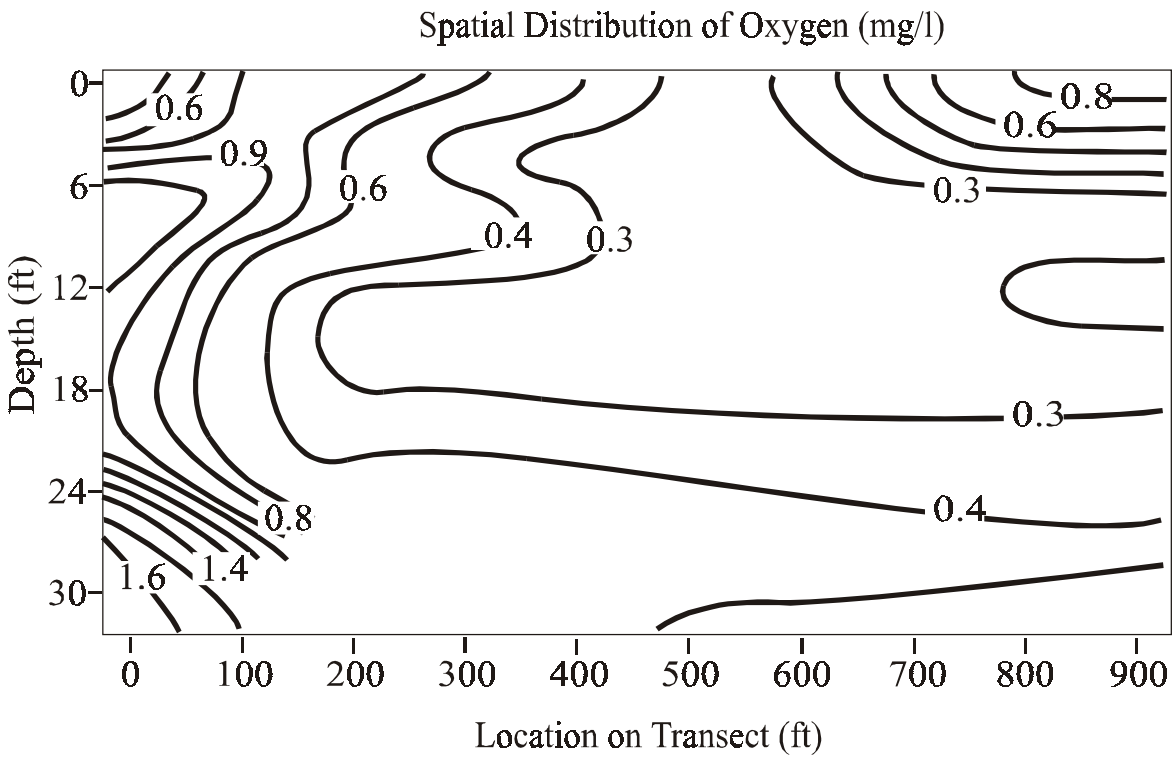

Figure B.5 Distribution of oxygen along the north-south transect, collected in August 1996. Distance along the transect extends from south to north (bottom to top in Figure 3.7), in the direction of ground-water flow.

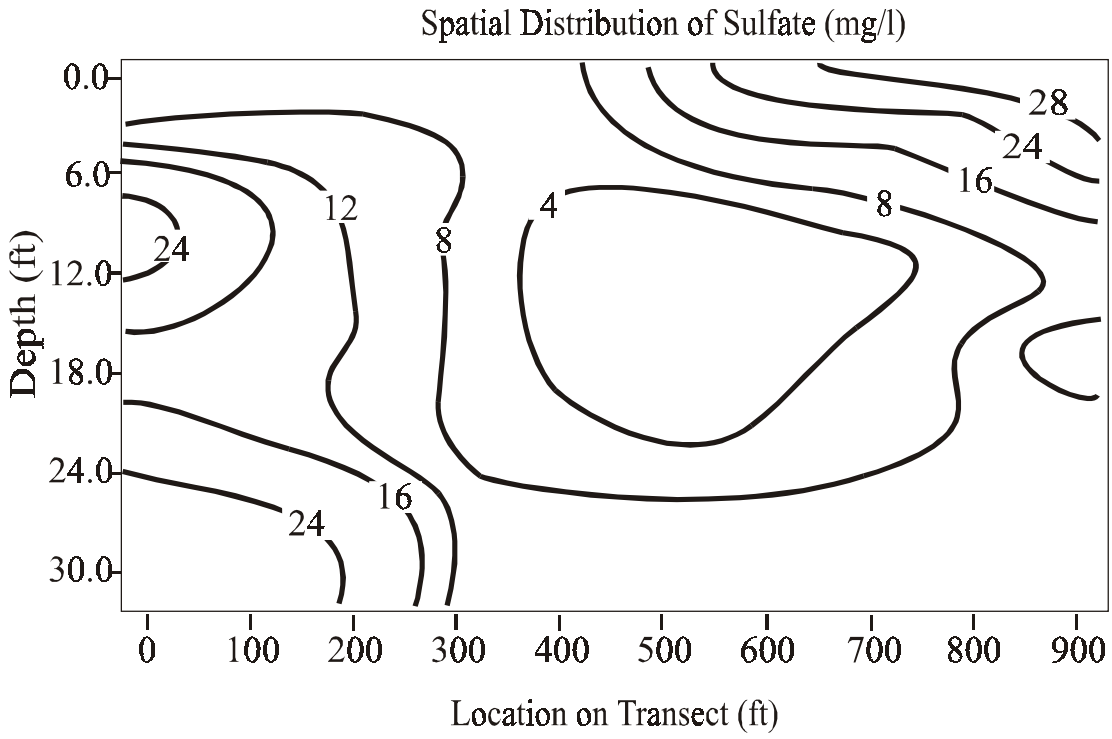

Figure B.6 Distribution of sulfate along the north-south transect, collected in August 1996. Distance along the transect extends from south to north (bottom to top in Figure 3.7), in the direction of ground-water flow.

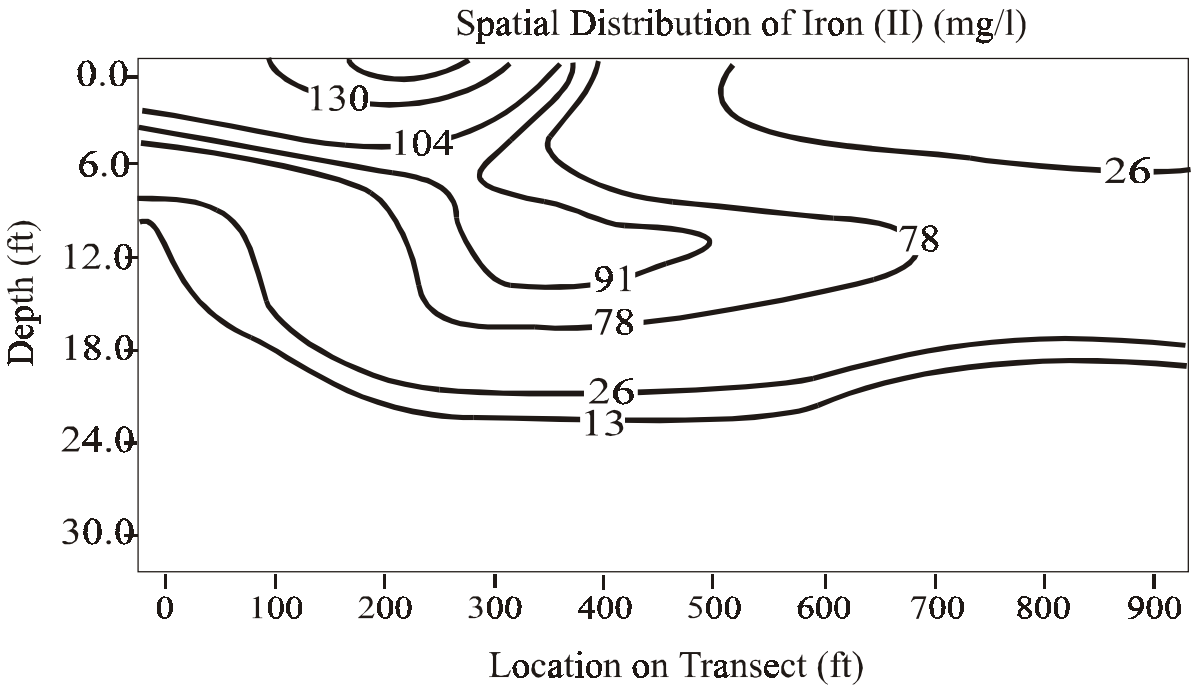

Figure B.7 Distribution of iron (II) along the north-south transect, collected in August 1996. Distance along the transect extends from south to north (bottom to top in Figure 3.7), in the direction of ground-water flow.

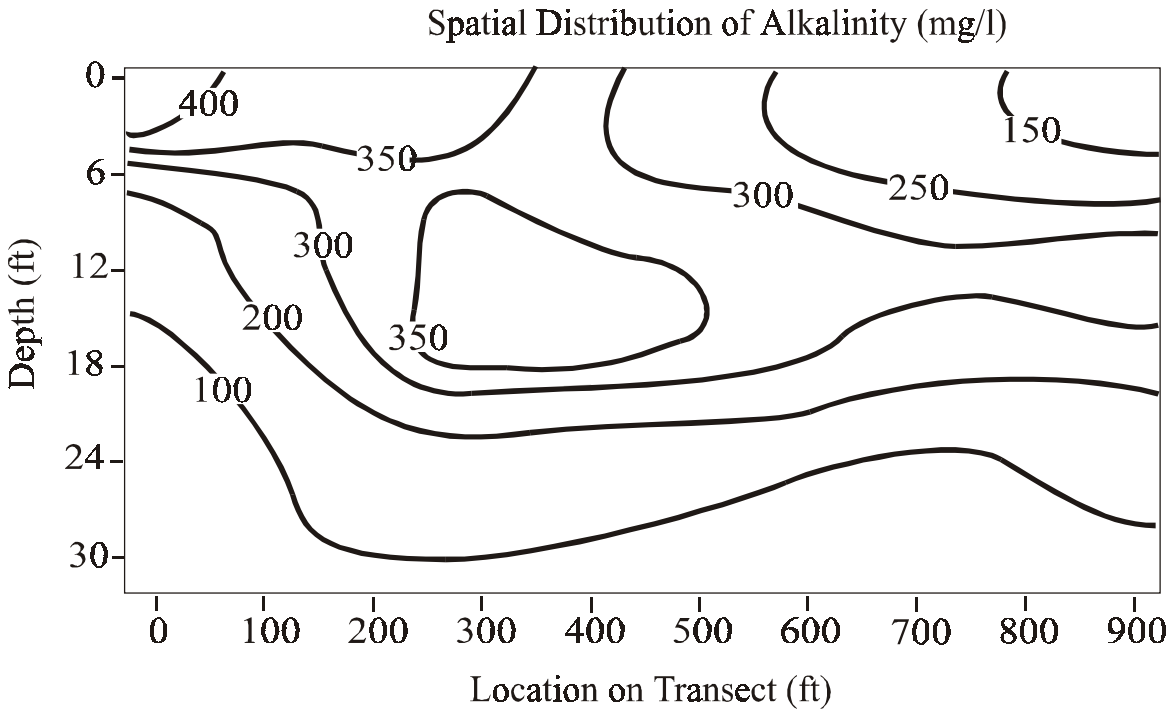

Figure B.8 Distribution of alkalinity along the north-south transect, collected in August 1996. Distance along the transect extends from south to north (bottom to top in Figure 3.7), in the direction of ground-water flow.